NONLINEAR VIBRATION OF MISTUNED BLADED DISK ASSEMBLIES

A THESIS SUBMITTED TO
THE GRADUATE SCHOOL OF NATURAL AND APPLIED SCIENCES
OF
MIDDLE EAST TECHNICAL UNIVERSITY

BY

GÜNAY ORBAY

IN PARTIAL FULFILLMENT OF THE REQUIREMENTS
FOR
THE DEGREE OF MASTER OF SCIENCE
IN
MECHANICAL ENGINEERING

JULY 2008

Approval of the thesis:

NONLINEAR VIBRATION OF MISTUNED BLADED DISK ASSEMBLIES

submitted by **GÜNAY ORBAY** in partial fulfillment of the requirements for the degree of **Master of Science in Mechanical Engineering Department, Middle East Technical University** by,

Prof. Dr. Canan Özgen _____
Dean, Graduate School of **Natural and Applied Sciences**

Prof. Dr. S.Kemal İder _____
Head of Department, **Mechanical Engineering**

Prof. Dr. H. Nevzat Özgüven _____
Supervisor, **Mechanical Engineering Dept., METU**

Examining Committee Members:

Prof. Dr. Kemal Özgören _____
Mechanical Engineering Dept., METU

Prof. Dr. H. Nevzat Özgüven _____
Mechanical Engineering Dept., METU

Assist. Prof. Dr. Yiğit Yazıcıoğlu _____
Mechanical Engineering Dept., METU

Dr. Ender Ciğeroğlu _____
Mechanical Engineering Dept., METU

Dr. Güçlü Seber _____
Aerospace Engineering Dept.,METU

Date: 28 – 07 – 2008

I hereby declare that all information in this document has been obtained and presented in accordance with academic rules and ethical conduct. I also declare that, as required by these rules and conduct, I have fully cited and referenced all material and results that are not original to this work.

Name, Last name : Günay ORBAY

Signature :

ABSTRACT

NONLINEAR VIBRATION OF MISTUNED BLADED DISK ASSEMBLIES

Orbay, Günay
M.S., Department of Mechanical Engineering
Supervisor: Prof. Dr. H. Nevzat Özgüven

July 2008, 138 pages

High cycle fatigue (HCF) failure has been studied extensively over the last two decades. Its impact on jet engines is severe enough that may result in engine losses and even life losses. The main requirement for fatigue life predictions is the stress caused by mechanical vibrations. One of the factors which have major impact on the vibratory stresses of bladed disk assemblies is a phenomenon called "mistuning" which is defined as the vibration localization caused by the loss of cyclic periodicity which is a consequence of inter-blade variations in structural properties. In this thesis, component mode synthesis method (CMSM) is combined with nonlinear forced response analysis in modal domain. Newton-Raphson and arc length continuation procedures are implemented for the solution. The component mode synthesis method introduces the capability of imposing mistuning on the modal properties of each blade in the assembly. Forced response analysis in modal domain reduces the problem size via mode truncation. The main advantage of the proposed method is that it is capable of calculating nonlinear forced response for all the degrees-of-freedom at each blade with less computational effort. This makes it possible to make a

stress analysis at resonance conditions. The case studies presented in this thesis emphasize the importance of number of modes retained in the reduced order model for both CMSM and nonlinear forced response analysis. Furthermore, the results of the case studies have shown that both nonlinearity and mistuning can cause shifts in resonance frequencies and changes in resonance amplitudes. Despite the changes in resonance conditions, the shape of the blade motion may not be affected.

Keywords: Blade Vibrations, Bladed Disk Vibrations, Mistuning in Bladed Disk Assemblies, Nonlinear Vibrations, Component Mode Synthesis Method.

ÖZ

DÜZENSİZ KANATÇIKLARA SAHİP DİSKLERDE DOĞRUSAL OLMAYAN TİTREŞİMLER

Orbay, Günay
Yüksek Lisans, Makine Mühendisliği Bölümü
Tez yöneticisi: Prof. Dr. H. Nevzat Özgüven

Temmuz 2008, 138 sayfa

Yüksek çevrim nedeniyle oluşan yorulma son yirmi yıldır üzerinde yoğun bir şekilde çalışılan bir konudur. Jet motorları üzerindeki etkisi, motor kayıplarına hatta can kayıplarına sebep olacak kadar fazladır. Yorulma ömrünün hesaplanması için mekanik titreşimler sonucu oluşan gerilmelerin bulunması gerekmektedir. Disk-kanatçık sistemlerinde titreşim kaynaklı gerilmeleri en çok etkileyen faktörlerden biri de, kanatçıkların yapısal özellik farklılıklarından ötürü çevrimsel periyodiklik kaybolması ve buna bağlı olarak titreşimin belli bölgelerde yoğunlaşması olarak tanımlanan "düzensizlik"tir. Bu tezde, bileşen biçim sentez metodu, biçim koordinatları kullanarak, doğrusal olmayan system cevabı analizi ile birleştirilmiştir. Sayısal çözümler için Newton-Raphson ve yay uzunluğu süreklilik metodu kullanılmıştır. Bileşen biçim sentez metodu, düzensizliğin kanatçıkların herbirinin biçim matrislerine uygulanabilmesini sağlamaktadır. Buna ek olarak, doğrusal olmayan sistem cevabının biçim koordinatlarında hesaplanması, biçim sayısının azaltılmasıyla problem boyutunu azaltmaktadır. Önerilen yöntemin birinci avantajı, daha az

hesaplamayla bütün kanatçık serbestlik derecelerinde kuvvet cevabının bulunabilmesidir. Bu, rezonans durumunda, kanatçık boyunca gerilmenin hesaplanmasını mümkün kılmaktadır. Yapılan vaka analizleri, mertebesi düşürülmüş modellerin elde edilmesinde kullanılan biçim sayılarının, hem bileşen biçim sentez metodunda hem de doğrusal olmayan sistem cevabı analizinde önemli olduğunu göstermektedir. Ayrıca, vaka analizi sonuçları; düzensizlik ve doğrusal olmayan etkilerin rezonans frekanslarını ve titreşim genliklerini önemli ölçüde değiştirdiğini, ancak, kanatçıkların titreşim şekillerini fazla etkilemediğini göstermiştir.

Anahtar kelimeler: Kanatçık Titreşimleri, Disk-Kanatçık Titreşimleri, Dik-Kanatçık Sistemlerinde Düzensiklik, Doğrusal Olmayan Titreşimler, Bileşen Biçim Sentez Metodu.

To my beloved family.

ACKNOWLEDGEMENTS

I would like to express my dearest appreciation to Prof. Dr. H. Nevzat Özgüven for his guidance and support that made this study possible. Also, I would like to thank Prof. Dr. Kemal Özgören, Assist. Prof. Dr. Yiğit Yazıcıoğlu, Dr. Güçlü Seber and Dr. Ender Ciğeroğlu for their comments.

I deeply owe my father Taşer Orbay, my mother Şükran Orbay and my sister Özge Orbay for everything they have done to encourage and support me to be where and who I am now.

I would like to thank my colleagues, Bekir Bediz, Zekai Murat Kılıç, Orkun Özşahin and Murat Barışık for their friendship and technical support during the thesis period. I also would like to express my dearest appreciation for Nihan Akın for her support and patience.

TABLE OF CONTENTS

LIST OF FIGURES

FIGURES

LIST OF TABLES

TABLES

LIST OF SYMBOLS

SYMBOLS

f : Force

F : Force amplitude

ω : Frequency

$[Z]$: Impedance matrix

γ : Loss factor

$[M]$: Mass matrix

η : Modal coordinate

$[\phi]$: Modal matrix

$[\Delta]$: Nonlinearity matrix

x : Physical coordinate

X, Y : Physical displacement amplitude

$[\alpha]$: Receptance matrix

λ : Relaxation parameter

R : Residual

s : Step length

v, k : Stiffness

$[K]$: Stiffness matrix

$[H]$: Structural damping matrix

$[C]$: Viscous damping matrix

CHAPTER 1

INTRODUCTION

1.1 On Mistuning and High Cycle Fatigue

High cycle fatigue (HCF) failure has been studied extensively over the last two decades. Nicholas [1] personally defines HCF as failures occurred under a fatigue condition which "generally involves high frequencies, low amplitudes, nominally elastic behavior, and large number of cycles". Its impact on jet engines is severe enough that may result in engine losses and even life losses. The United States Air Forces (USAF) statistics showed that nearly half of the engine failures are related to HCF. Consortiums have been established to raise and invest funding on research and the results are promising. The percentage of HCF related failures are decreasing.

On the commercial side, jet engine manufacturers tend to make the engines lighter and more powerful to deliver high power to weight ratios. This, on the other hand, requires limit safety values. Under these circumstances, failure related to HCF is the main focus. Therefore, mechanical vibrations of critical parts, such as compressor and turbine blades, should be predicted with high confidence.

One of the factors which have major impact on vibration amplitudes on bladed disk assemblies is a phenomenon called "mistuning", "disorder" or

"vibration localization". It is defined as the localization of strain energy of a vibration mode to a single or a number of blades throughout the bladed disk assembly due to the imperfections in materials and random variations in manufacturing processes. Since it can also occur due to changes related to operational wear, mistuning is inevitable in its nature.

On the other hand, some suggestions were made on benefits of mistuning. Whitehead [2] showed that mistuning can be used in favor of integrity when flutter is considered. There are ongoing debates on how mistuning could be exploited to increase the integrity of bladed disk assemblies. Either way, mistuning has to be studied extensively. In Chapter 2 mistuning will be explained in detail.

1.2 Literature Review

The studies in the literature related to nonlinear dynamic response analysis of mistuned bladed disk assemblies will be discussed in the upcoming sections. These can be grouped as, studies regarding mistuning modeling and studies regarding nonlinear dynamic response of bladed disk assemblies although some of them include both aspects. Mistuning modeling will be discussed in only considering modal domain methods for which the intention is going to be explained in "the objective of the thesis section." On the other hand, among the myriad of studies about nonlinear vibration of bladed disk assemblies only the most recent and most commonly implemented works will be discussed.

1.2.1 Mistuning Modeling

Mistuning phenomenon has been studied extensively for over half a century, especially for bladed disk assemblies. It is one of the main parameters that affect vibration amplitudes, thus stress levels of rotating turbomachinery components. Due to their cyclic symmetric property, slight imperfections in structural properties and slight deviation on geometries of blades will result in significant increase in vibration amplitudes. This weakens the robustness, integrity and durability of the bladed disk assemblies by increasing the probability of HCF related malfunction. On these reasons, mistuning phenomenon has been the main focus for over a half century.

The early models were based on dynamic analysis of continuous systems of basic elements, namely beams and disks [2, 3]. Although the geometries used in these models did not belong to real bladed disk assemblies, they had sufficient resemblance and thus revealed important information on the phenomenon itself. Ewins [3] formulated a bladed disk assembly by coupling beam-like blades with an axisymmetric disc via receptance coupling. He also developed an alternative method which yields the normal modes of the assembly by constructing element matrices from energy and Lagrange equations. He also demonstrated that the double modes splitting phenomenon due to mistuning. Meanwhile, Whitehead [2] developed a formulation in which the single degree-of-freedom blades in the assembly are coupled aerodynamically. He came up with a simple formula for the worst case of mistuning in terms of amplification factor which is defined as the ratio of the mistuned vibration amplitude to the

tuned vibration amplitude. This formula suggests that the maximum possible amplification factor is a function of the number of blades in the assembly only. Later, he corrected his simple formula for mechanical coupling of the blades through the rotor [4] and then he "amended" his own formula for mechanical coupling and declared the validity of his first formula [2] whilst introducing mode shapes for the worst case of mistuning [5]. The formula he had developed is still used as a theoretical benchmark. Lim et al. [6] used energy formulations to predict the amplification factor bounds and came up with the same formula as Whitehead did using a single degree-of-freedom per sector model. He analyzed 2 degrees-of-freedom per sector and multiple degrees-of-freedom per sector models. He also introduced a stress indicator factor and verified the maximum amplification formula via Monte-Carlo simulations. In addition Feiner et al. [7] developed a method which uses a single degree-of-freedom per sector model. In this study, "the mistuned mode is represented as a sum of the tuned modes, where the coefficients of the tuned modes in the modal summation represent the amount of distortion present in the mode".

With the developments in finite element (FE) methods, realistic geometries have been analyzed to calculate forced responses. As the complexity of the model increases the computational time needed increases too. Therefore researchers aimed to exploit the cyclic symmetric property of bladed disk assemblies. The element matrices of a cyclic symmetric structure can be block diagonalized using Fourier matrix transformation [8]. This divides the problem into a number of smaller subproblems. Solving them reduces the computational time required significantly. Although these analyses gave a good insight on the vibration of bladed disk assemblies, cyclic

symmetry analysis could not be used to look into mistuning. In order to predict forced responses of mistuned bladed disk, mistuning can be imposed on FE models. But these models usually have large numbers of degrees-of-freedom requiring enormous amount of computational time for forced response predictions. Thus, some studies focused on reduced order models which would render dynamic analysis of mistuned bladed disk assemblies affordable in computational time.

Óttarsson et al. [9] proposed to express the mode shapes of a mistuned bladed disk assembly as a summation of cantilevered blade mode shapes and tuned assembly mode shapes with zero density on the blades. Using energy equations and Hamilton's principle the problem is reduced into modal coordinates. Then mistuning is imposed on the part of the modal stiffness matrix which belongs to individual blades. Assuming the tuned case, the method gave close results on natural frequencies but the results can be improved by manually tuning the modal stiffness matrix of cantilevered blades in an iterative manner. This method can be used to carry out statistical studies thanks to its speed. But the modeshapes it yields are not as accurate as those obtained with other methods in the literature [10]. Bladh et al. [11] further developed this model to include shrouds into the analysis. Later, Bladh et al. [12, 13] suggested using component mode synthesis methods for the modal analysis of mistuned bladed disk assemblies. They utilized Craig-Bampton method [14] to connect a number of blades on a perfectly tuned disk. The Craig-Bampton method was chosen "due to its robustness and excellent accuracy". In this model mistuning can be imposed on cantilevered natural frequencies of individual blades. Then

using the idea behind the study made by Yang et al. [15] a new reduced order model is introduced which is faster and yet accurate.

In addition to modal domain methods, Yang and Griffin [16] suggested coupling a tuned disk with mistuned blades via FRF coupling. A transformation which expresses the blade-disk interface motion by a number of translational and rotational rigid body modes is applied to reduce the number of connection degrees-of-freedom. Yet, the FRF matrix for each degree-of-freedom on the blade should be calculated for each point in the frequency range. Afterward, Yang and Griffin [17] developed the method called the subset of nominal modes (SNM) method which is also based on the idea behind their past study [15]. The method assumes that the mistuned mode shapes in a mode family (e.g. first bending) can be expressed by the mode shapes which belong to the same family of modes of the tuned assembly. Slight changes in natural frequencies of individual blades will not result in significant changes in the blade shape but localization throughout the assembly; therefore the assumption seems to be true. Mathematically thinking, for a mode at which the majority of the strain energy is localized on a single blade, the mode shape can be expressed by summation of similar nominal modes having all numbers of nodal diameters (i.e. zero to max nodal diameters) similar to logic behind Fourier expansion. This method requires the knowledge of mode shapes of the tuned assembly and mass and stiffness matrices of a single blade. Feiner and Griffin [18] further improved the method to consider an isolated family of modes and called it the fundamental mistuning model (FMM). With the assumption that the natural frequencies in a single family of modes are close, it is no longer needed to have mass and stiffness matrices of a blade.

Later, Feiner et al. [19, 20] further improved the FMM to calculate transient response of mistuned bladed disk assemblies. FMM is then used to identify individual blade mistuning from experimental measurements.

As an addition to FRF based methods, Petrov et al. [21] proposed using Sherman-Morrison-Woodbury formula to write an exact relationship between FRF's of tuned and mistuned assembly. They introduced mass, stiffness and damping type of mistuning elements which are considered as a modification on the tuned system. The degrees-of-freedom are partitioned as active and passive, the former including the points where mistuning is applied and the response is to be calculated. For the method being based on FRF updating, the linear mistuning elements should be applied at every frequency point in the range of interest. Soon after, Petrov and Ewins [22] utilized this method to calculate the worst mistuning patterns in bladed disk assemblies. They formed an optimization problem in which the mistuning pattern, which is the set of mistuning values for each blade in the assembly, and excitation frequency are main variables. The mistuning amount is constrained within a desired range. In this study, they also developed "an effective method for calculation of the sensitivity coefficients for maximum forced response with respect to blade mistuning." Later Petrov and Ewins [23] used this method to calculate nonlinear forced response of a bladed disk assembly with shroud contacts in the presence of natural frequency mistuning (although it is achieved by point mistuning) and "scatter of contact interface characteristics". The nonlinear aspect of this study will be discussed in the upcoming sections. Recently, Nikolic et al. [24] used the aforementioned method to develop "robust maximum forced response reduction strategies".

1.2.2 Nonlinear Dynamic Response of Bladed Disk Assemblies

The early work on nonlinear dynamic response of bladed disk assemblies used simple models and simple nonlinear oscillators, therefore they will not be discussed here. Only recent and commonly used methods will be briefly described.

In 1990, Wagner and Griffin [25] studied tip shrouded bladed disk assemblies for which the steady-state harmonic response amplitudes vary from blade to blade due to differences in inter-blade gap values for "large enough excitation". They stated that single degree-of-freedom models cannot represent the blade stresses adequately, therefore beam type models should be used. They utilized harmonic balance method (HBM) to approximate the behavior of gap nonlinearity in the system. Later, Yang and Menq [26] formulated a friction element under variable normal load to calculate the steady-state vibrations of tip shrouded blade disk assemblies. They also used HBM to "impose the effective stiffness and damping of the friction joint on the linear structure." They also utilized Newton-Raphson method to trace the multiple solutions over the frequency domain. Their analysis on a two degree-of-freedom oscillator model demonstrated slip, stuck and separation conditions of the contact interface clearly. In the same year Yang and Menq published their work, Şanlıtürk et al. [27] proposed using a microslip model, which is based on the Dahl's friction model, and approximated "an equivalent amplitude-dependent complex stiffness via first order HBM." Also a validation of the calculations with experimental measurements was given besides "a sine-sweep excitation in time marching analysis." Later, Yang et al. [28] formulated a friction contact element under

variable normal load using first order HBM. Case studies presented in this paper showed that the friction element gave accurate results when compared with time integration solutions. In 2001 Chen and Menq [29] introduced a three-dimensional contact element. They determined the stick, slip and separation analytically assuming that the contact interface undergoes a three-dimensional periodic motion. They also combined the friction element with numerical continuation solution procedures to predict the response via multi-harmonic balance method (MHBM) and validated their results with time integration solutions. Again in the same year, Şanlıtürk et al. [30] used experimental recordings of hysteresis loops of basic contact behavior for a given material and used it to calculate the response of a bladed disk assembly with wedge type friction dampers. With a given normal load on the damper-blade contact interface, assuming three-dimensional motion of the damper the responses are compared with experimental measurements. They came up with a conclusion that including only translational degrees-of-freedom on the damper (i.e. only translational motion on three axes) can answer the slight differences between theoretical calculations and experiment measurements.

Ciğeroğlu and Özgüven [31] published a work on a two-slope linear approximation of Dahl's friction model. Later, Ciğeroğlu et al. [32] developed a one-dimensional dynamic micro-slip element in which the inertial effects of the damper is included. The steady-state solution of the shear layer is determined by solving the nonlinear partial differential equations analytically. Then the stick-slip regions are determined at different normal load distributions and the hysteresis curves are calculated. Ciğeroğlu et al. [33] further developed their model to include motion in two

dimensions with variable normal load. They proposed to use a new model with HBM "to determine the forced response of frictionally constrained structures." As an application the response of a single blade which is constrained by a contact interface at the ground is calculated. As an implementation to real problems, Ciğeroğlu et al. [34] utilized their new dynamic micro-slip friction model with a new wedge damper model to be used in forced response analysis of bladed disk assemblies with wedge type friction dampers. In contrast to the previous work of Şanlıtürk et al. [30], in this model the wedge damper can "undergo three-dimensional translation and three-dimensional rotation in addition to the elastic deformation." The damper is constrained only by its contacting faces with the neighboring blade roots.

In parallel to the aforementioned studies, Petrov et al. [35] formulated a multi-harmonic friction element under variable normal load conditions. The MHBM is utilized for linearization of the nonlinearity to calculate the equivalent forcing vector as well as the tangent stiffness matrix. Although the stick-slip and separation instants are determined numerically due to including multiple harmonic terms, the forcing vector and tangent stiffness matrix are calculated analytically. This friction model is implemented in a Newton-Raphson type solution procedure to trace for multiple solutions in frequency domain. A case study on a realistic turbine model is presented in the paper. Later, Petrov and Ewins [36] developed new generic models which can describe the behavior of frictionally constrained contact interfaces for the time domain analysis of bladed disk assemblies. These models can include the effect of normal load variations with or without separation. Friction contact parameters such as friction coefficient and

contact stiffness coefficients can also be time-varying. A numerical analysis is presented for time domain analysis of a shrouded bladed disk assembly. Petrov and Ewins [23] continued their studies with a new method for nonlinear multiharmonic vibration analysis of mistuned bladed disk assemblies. In this study, their previous work on imposing mistuning via exact relationships between tuned and mistuned receptance [21] is combined with analytical formulations of friction contact elements [35] to generate a complete method. The mistuning is imposed not only on natural frequencies of individual blades via point mistuning elements but on contact interface parameters such as gap or interference values, or friction stiffness values. A numerical study on a high-pressure bladed turbine disk is presented to demonstrate changes in FRF's with changing contact parameters. Afterward, they published another work on bladed disk assemblies with dry friction but with both wedge and split type underplatform dampers [37]. In this study, multiharmonic response is calculated for the new damper models for which "inertia forces and the effects of normal load variation on stick-slip transitions at the contact interfaces" is considered. In addition to the studies mentioned hitherto, Petrov [38] developed a new method to analyze the changes in response amplitudes with variations in friction contact interface parameters via a direct parametric approach. The problem is formulated as a function of these parameters with the aid of previously developed analytical formulations of friction contact interface element [35]. As an addition to this study, the effect of aforementioned parameters on resonant amplitudes are examined [39]. This is achieved by introducing another equation which guarantees that the excitation frequency is approximately equal to the resonant frequency.

1.3 Objective

In this thesis, it is aimed to form a new method for nonlinear dynamic analysis of mistuned bladed disk assemblies to be used for stress thus fatigue life predictions. In order to do that, the studies on both mistuning and nonlinear dynamic response of bladed disk assemblies have been investigated in detail.

In the formation of the method, the following requirements are sought:

- The method should be computationally fast even with high density meshes and yet it should yield accurate results both in mistuned natural frequencies, modeshapes and FRFs.
- The method should avoid point type mistuning elements which would eventually distort the blade shapes unless the number of mistuning application points is large and the points are homogeneously distributed. Mistuning could be directly applied to cantilevered natural frequencies of individual blades.
- The method should be able to calculate nonlinear response for various types of nonlinearities such as gaps, friction contact with implemented numerical continuation procedures.

1.4 Scope of the Thesis

The outline of the thesis is given below:

In Chapter 2, firstly background knowledge on mistuned bladed disk assemblies is given. Then cyclic symmetry property, which is essential for analysis of bladed disk assemblies, is briefly discussed. Then engine order excitation and aliasing phenomenon are described.

In Chapter 3, the studies related to mistuning will be discussed in detail. All the selected studies include modal domain methods to avoid using point mistuning elements via FRF related techniques. Namely the fixed interface coupling method and subset of nominal modes method will be described.

In Chapter 4, topics on nonlinear dynamic response will be discussed. Firstly, the equation of motion of a nonlinear system will be presented, and then linearization methods will be discussed. Then, two solution procedures, namely fixed point iteration and Newton-Raphson methods, will be described. Next, continuation methods will be introduced, and the solution procedures in modal coordinates will be given. Finally nonlinear element formulations will be given for macroslip friction and gap elements. They will be validated via time integration results.

In Chapter 5, as a case study, a mid-shrouded bladed compressor disk is given. The linear mistuned response will be calculated by both methods mentioned and will be compared with direct FE approach. Then nonlinear response will be calculated for different types and levels of nonlinearity.

In the last chapter, conclusions on this study will be made. Suggestions on future work and further developments will also be given in this chapter.

CHAPTER 2

BACKGROUND INFORMATION

2.1 Cyclic Symmetry

Due to their rotationally periodic nature, bladed disk assemblies, bladed disks (blisk) and bladed rings (bling) can be represented by a single subpart which is repeated at equally spaced angles around the rotation axis. This property is called cyclic symmetry. In modal analysis terminology, the primary subpart is called a sector.

The modal analysis of such structures can be carried out by exploiting the cyclic symmetry. When the elementary matrices (i.e. mass and stiffness matrices) are transformed into cylindrical coordinate system based on the axis of cyclic symmetry, the resulting matrices are of block-circulant symmetric type. Block-circulant symmetric matrices can be block diagonalized into N number of submatrices, N being the number of identical sectors, by using a Fourier transformation matrix whose elements are defined by

$$E_{j,k} = \frac{1}{\sqrt{N}} e^{\frac{2i\pi}{N}(j-1)(k-1)} \tag{2.1}$$

as

$$\left(E^* \otimes I\right) C (E \otimes I) = Bdiag\left[\Lambda_0, \Lambda_1, ..., \Lambda_N\right] \tag{2.2}$$

where C is the block circulant matrix, I is the identity matrix, $E_{j,k}$ is the element in j^{th} row and k^{th} column, N is the number of sectors, i is unit imaginary number, and Λ_r is the submatrix of the r^{th} subproblem. r in this notation is also called the index of "harmonics", * denotes the Hermitian transpose and $\otimes$ denotes the Kronecker product. Here, $Bdiag[\bullet]$ denotes the block diagonal matrix, the argument being the n^{th} (n=1,2,…) diagonal block. In vibration analysis of axisymmetric disks or cyclic symmetric structures r can be referred to the number of "nodal diameters". Here, nodal diameter refers to the lines which lie on the diameter of the disc and have zero displacements. Then the problem is divided into N number of uncoupled problems. Since it is faster and more efficient to solve N number of problems of a size instead of solving a single problem which is N times of the same size, using cyclic symmetry has the advantage on computational time. In modal analysis of bladed disk assemblies, since each nodal diameter is considered once at a time, the eigenvalues are not as close to each other as in the full size problem. As seen in Figure 2.1, as the nodal diameter increases, the natural frequencies of a mode family converge to a finite value. Therefore, the natural frequencies of a bladed disk appear to be in closely packed clusters unless the problem is treated by considering one nodal diameter at a time. Numerically, solving for well distinct eigenvalues instead of solving for clusters of close eigenvalues will yield more accurate results and it will guarantee faster convergence [17].

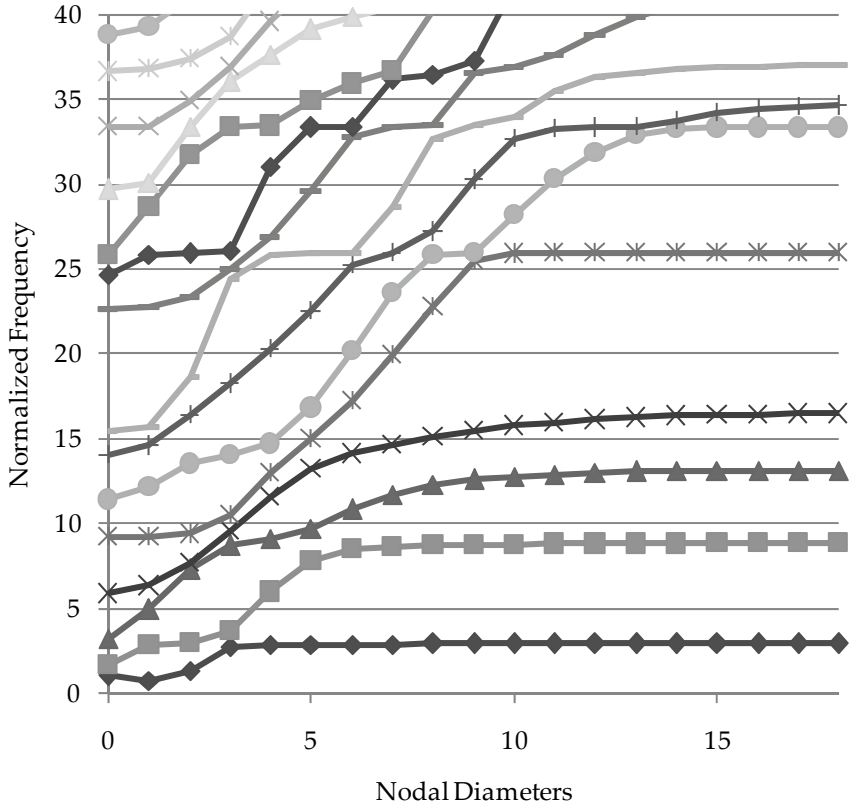

Figure 2.1 – Natural frequency vs. Nodal diameters chart for a bladed disk assembly

In case of block circulant and symmetric matrices, some natural frequencies appear in pairs. If the eigenvalue problem is solved in complex domain, these double modes appear as complex conjugates. The physical interpretation of these complex mode shapes of double modes can be made by counter-rotating traveling wave modes [40].

In practice, sectors are not identical due to manufacturing tolerances, material defects and changes in physical properties during operation. Under such conditions, in some modes the elastic energy is localized in one or more sectors of the whole structure. This phenomenon is called mistuning, disorder or vibration localization. If a structure possesses

mistuning, it is said to be "mistuned". If its sectors are perfectly identical, the structure is said to be "tuned". These terms will be widely used in this work.

Considering mistuning as small perturbations on physical properties of each sector, the sectors will not be identical any more. Therefore the cyclic symmetry is destroyed and the problem can no longer be divided into N number of smaller problems. Hence, double modes are no longer expected.

For further information on circulant matrices, refer to reference [8].

2.2 Expansion of Mode Shapes

After the solutions to smaller eigenvalue problems are determined, the solution for the whole structure is needed. The process of back transformation from subproblems to the original problem is called the "expansion of mode shapes". The formulation of expansion differs depending on whether the Fourier transformation matrix is applied as a complex transformation matrix or its real equivalent [10].

If the transformation is made in complex domain, the following type of formula is used:

$$\left[\phi^*_{j,k}\right] = \frac{1}{\sqrt{N}} e^{\frac{2i\pi}{N}(j-1)/k-1)} \left[\phi^*_k\right] \tag{2.3}$$

where $\left[\phi^*_k\right]$ is the complex eigenvector of the k nodal diameter modes and $\left[\phi^*_{j,k}\right]$ is the complex eigenvector for j^{th} sector for k nodal diameter modes, i

is the unit imaginary number, and N is the number of sectors in the assembly.

In practice, many finite element analysis program vendors usually prefer to carry out cyclic symmetry analysis in real domain. Even if the element matrices are transformed by the complex Fourier transformation matrix the solution of the eigenvalue problem has to be done by using real numbers. Therefore, for simplicity and easy implementation, a duplicate of the original sector is defined and necessary boundary conditions for cyclic symmetry is imposed as follows

$$\begin{aligned}\left\{x_H^{c,m}\right\} &= \left\{x_L^{c,m}\right\}\cos\left(m\alpha\right)+\left\{x_L^{s,m}\right\}\sin\left(m\alpha\right)\\ \left\{x_H^{s,m}\right\} &= -\left\{x_L^{c,m}\right\}\sin\left(m\alpha\right)+\left\{x_L^{s,m}\right\}\cos\left(m\alpha\right)\end{aligned} \tag{2.4}$$

for each m nodal diameters where subscripts H and L denote the high and low edges respectively, and superscripts s and c denote sine and cosine displacements respectively. In analysis in real domain, these sine and cosine displacements are accounted for real and imaginary parts of the mode shapes in analysis in complex domain.

If the transformation is made in real domain then the following formulae are used:

$$\begin{aligned}\left[\phi_j^0\right] &= \frac{1}{\sqrt{N}}\left[\phi^0\right]\\ \left[\phi_j^m\right] &= \sqrt{\frac{2}{N}}\sin\left(\left(j-1\right)m\alpha\right)\left[\phi^{m,s}\right]+\sqrt{\frac{2}{N}}\cos\left(\left(j-1\right)m\alpha\right)\left[\phi^{m,c}\right]\end{aligned} \tag{2.5}$$

where superscript m denotes the number of nodal diameters. If the number of blades is even, the highest nodal diameter modes do not appear in pairs and the transformation becomes

$$\left[\phi_j^{N_{\max}}\right] = (-1)^{j-1}\frac{1}{\sqrt{N}}\left[\phi^{N_{\max}}\right] \tag{2.6}$$

where superscript N_{max} denotes the highest number of nodal diameters.

2.3 Engine Order Excitation and Aliasing

In forced response predictions, the response characteristics are determined by not only the system dynamics but also the external forcing. It is a well known fact that resonant conditions of vibration occur under specific forcing frequencies (i.e. resonant frequencies) and forcing vector. To make a mathematical explanation, the response formula in modal analysis should be checked.

$$\{x(\omega)\} = \sum_{r=1}^{n}\frac{\{\phi_r\}^T\{f\}\{\phi_r\}}{\omega_r^2(1+i\gamma)-\omega^2} \tag{2.7}$$

where $\{x(\omega)\}$ is the vector of complex displacement amplitudes, n is the number of modes retained, $\{\phi_r\}$ and ω_r are the mass normalized eigenvector and natural frequency of the r^{th} mode, $\{f\}$ is the forcing vector and γ is the loss factor. Equation (2.7) shows that resonant conditions can only occur when the denominator is so small unless the numerator nonzero meaning that excitation frequency should be close to one of the natural frequencies and the forcing vector multiplication with the mode shape vector should be nonzero.

In turbomachinery, the external forcing is exerted by the fluid that flows through. The fluctuations in fluid pressure gradients on the blades are the source of the aerodynamic forcing. In modern turbomachinery, the flow of the fluid is altered via stators and vanes to modify the pressure gradient in

favor. Although they provide high speed flow in desired direction, they also create low pressure regions at their rakes. Therefore when a blade passes before a stator, it encounters a high and a low pressure region. Since in one revolution of the engine shaft a single blade passes before all the stators, the excitation frequency on that blade is considered to be the multiplication of the number of stators and the engine rotation frequency. This type of the excitation is called engine order (EO) excitation. As an example, in presence of *n* number of stators, the excitation is said to be an *n-EO* excitation.

In previous discussions, it was stated that the mode shapes of cyclic symmetric structures possess sinusoidal distribution over the circumference ideally. As the way the modeshapes of cyclic symmetric structures are expanded, the forcing vector can also be expanded using a forcing vector definition for a single sector. In ideal case, both mode shapes and forcing vectors resemble sinusoidal functions over the circumference therefore one can conduct that such vectors constructed via sinusoidal functions would be orthogonal which means an *n-EO* excitation will excite *n* nodal diameter modes but not *(n+1)* nodal diameter modes. But since there are a finite number of sectors defined in an assembly, an *n-EO* excitation can excite other nodal diameter modes. This occurs due to aliasing. The nodal diameter modes which can be excited by an *n-EO* excitation can be determined by the following formulae

$$N_{nodal} = kN - n \qquad \text{for } k = 1, 2, \ldots$$

$$N_{nodal} = lN + n \qquad \text{for } l = 0, 1, \ldots \tag{2.8}$$

where N is the number of sectors in the assembly. In practice, since the mode shapes are inevitably mistuned they cannot be classified and expanded as nodal diameter modes. Thus, the forcing and the mode shape vectors are no longer orthogonal. Consequently, the numerator terms in the summation of the equation (2.7) are always nonzero given nonzero forcing.

CHAPTER 3

MISTUNING MODELING

3.1 Modal Coupling Techniques

The dynamic analysis of simple structures (constant cross-section beams, plates, shells) can be made easily thanks to fundamental analytic formulations which were developed decades ago. But as the complexity of the structure increases, for a better understanding on the dynamics, the structure is needed to be divided into smaller structures of which the dynamics is easier to predict. But, whilst dividing system into substructures, the accuracy on dynamic predictions of the whole structure should be kept as much as possible.

In addition, the analysis of complex structures is computationally expensive. Although the capacity of recent processors has increased exponentially, which reduced the time required for computation, the demand for accuracy and detailed models are always increasing. Therefore, fast yet accurate methods are needed.

In modal analysis, the modal characteristics of a structure can be calculated again by substucturing. The dynamics of a structure is expressed by modal characteristics of its substructures. Such techniques that use modal data with or without spatial data are called modal coupling techniques. They

can be classified by how the substructures are analyzed as fixed interface methods and free interface methods [41]. In this work, the implementation of fixed interface method to the mistuned bladed disk assemblies will be used [10].

3.1.1 Fixed Interface Modal Coupling Method

In modal analysis, one of the modal coupling methods is fixed interface modal coupling method which is also known as Craig-Bampton Method [14] or the component mode synthesis methods (CMSM). The method is well known with its robustness and high accuracy. In this method, each substructure is fixed at the interface degrees-of-freedom and a modal analysis is performed. In addition, the substructure is reduced to interface degrees-of-freedom using a static reduction (i.e. Guyan static reduction). Then the dynamics of the system is expressed as a combination of modal coordinates and the physical coordinates of the interface degrees-of-freedom.

The accuracy of the system depends on how much truncation has been made in the modal analysis of substructures. It should be noted that, as the number of modes pertained for each structure is increased to the limit the reduced system becomes the original system.

3.1.1.1 Formulation

Assuming that elementary matrices for all the spatial coordinates are known, a general expression for the equation of motion of an undamped

system is given below. The equation is written in a form such that the physical coordinates are partitioned as primary and secondary coordinates, former being the interface degrees-of-freedom and latter being the interior degrees-of-freedom.

$$\begin{bmatrix} [M_{ss}] & [M_{sp}] \\ [M_{ps}] & [M_{pp}] \end{bmatrix} \begin{Bmatrix} \{\ddot{x}_s\} \\ \{\ddot{x}_p\} \end{Bmatrix} + \begin{bmatrix} [K_{ss}] & [K_{sp}] \\ [K_{ps}] & [K_{pp}] \end{bmatrix} \begin{Bmatrix} \{x_s\} \\ \{x_p\} \end{Bmatrix} = \begin{Bmatrix} \{f_s\} \\ \{f_p\} \end{Bmatrix} \tag{3.1}$$

where $[M]$ and $[K]$ are the mass and stiffness matrices, $\{x\}$ and $\{f\}$ are the physical coordinate and forcing vectors, and subscripts s and p denote the secondary and primary degrees-of-freedom, respectively. Then the interface of the component, which is represented by primary coordinates, is fixed and the equation (3.1) becomes

$$[M_{ss}]\{\ddot{x}_s\} + [K_{ss}]\{x_s\} = \{0\} \tag{3.2}$$

Then a modal analysis is carried out on the following equation assuming a solution in the form

$$\{x\} = \{X\} e^{i\omega t} \tag{3.3}$$

and substituting it in equation (3.2) yields the eigenvalue problem (EVP)

$$\left[-\omega^2 [M_{ss}] + [K_{ss}]\right]\{x_s\} = \{0\} \tag{3.4}$$

Solving equation (3.4) will yield the natural frequencies $\left[\omega_s^2\right]$ and mass normalized eigenvalues matrix $[\phi_S]$. The physical displacements on the secondary partition can be expressed as a summation of fixed interface mode shapes as

$$\{x_s\} = [\phi_s]\{\eta_s\} \tag{3.5}$$

Secondly, a static analysis is made to determine the displacements on secondary coordinates when a single degree-of-freedom on the interface is given unit displacement while other interface degrees-of-freedom are fixed.

This analysis is made for each degree-of-freedom in the interface. These analyses can be written into a single equation in the matrix form as

$$\begin{bmatrix} [K_{ss}] & [K_{sp}] \\ [K_{ps}] & [K_{pp}] \end{bmatrix} \begin{bmatrix} [\psi_s] \\ [I] \end{bmatrix} = \begin{Bmatrix} \{0\} \\ \{f_p\} \end{Bmatrix} \tag{3.6}$$

Solving for $[\psi_s]$ will yield

$$[\psi_s] = -[K_{ss}]^{-1}[K_{sp}] \tag{3.7}$$

Using a truncated set of mode shapes and the resulting shapes of Guyan static reduction, the displacement vector of the component is expressed by a linear combination of both

$$\begin{Bmatrix} \{x_s\} \\ \{x_p\} \end{Bmatrix} = \begin{bmatrix} [\phi_s] & [\psi_s] \\ [0] & [I] \end{bmatrix} \begin{Bmatrix} \{\eta_s\} \\ \{x_p\} \end{Bmatrix} = [T] \begin{Bmatrix} \{\eta_s\} \\ \{x_p\} \end{Bmatrix} \tag{3.8}$$

where $[T]$ is considered as a transformation matrix which transforms reduced coordinates into the physical coordinates of the whole component. Then the equation (3.8) is substituted into the equation of motion (3.1) and pre-multiplied by $[T]^T$. It is assumed that no external force acts on the secondary section.

$$[T]^T \begin{bmatrix} [M_{ss}] & [M_{sp}] \\ [M_{ps}] & [M_{pp}] \end{bmatrix} [T] \begin{Bmatrix} \{\ddot{\eta}_S\} \\ \{\ddot{x}_p\} \end{Bmatrix} + [T]^T \begin{bmatrix} [K_{ss}] & [K_{sp}] \\ [K_{ps}] & [K_{pp}] \end{bmatrix} [T] \begin{Bmatrix} \{\eta_S\} \\ \{x_p\} \end{Bmatrix} = [T]^T \begin{Bmatrix} \{f_s\} \\ \{f_p\} \end{Bmatrix} \tag{3.9}$$

Then the stiffness matrix of the reduced system becomes

$$\begin{aligned} [T]^T [K][T] &= \begin{bmatrix} [\phi_s] & [\psi_s] \\ [0] & [I] \end{bmatrix}^T \begin{bmatrix} [K_{ss}] & [K_{sp}] \\ [K_{ps}] & [K_{pp}] \end{bmatrix} \begin{bmatrix} [\phi_s] & [\psi_s] \\ [0] & [I] \end{bmatrix} \\ &= \begin{bmatrix} [\bar{K}_{\eta\eta}] & [\bar{K}_{\eta p}] \\ [\bar{K}_{p\eta}] & [\bar{K}_{pp}] \end{bmatrix} \end{aligned} \tag{3.10}$$

where

$$
\begin{aligned}
\left[\bar{K}_{\eta\eta}\right] &= \left[\omega_s^2\right] \\
\left[\bar{K}_{\eta p}\right] &= [0] \\
\left[\bar{K}_{p\eta}\right] &= [0] \\
\left[\bar{K}_{pp}\right] &= \left[\left[K_{pp}\right] - \left[K_{ps}\right]\left[K_{ss}\right]^{-1}\left[K_{sp}\right]\right]
\end{aligned}
\tag{3.11}
$$

Then the mass matrix of the reduced system becomes

$$
\begin{aligned}
[T]^T[M][T] &= \begin{bmatrix} [\phi_s] & [\psi_s] \\ [0] & [I] \end{bmatrix}^T \begin{bmatrix} [M_{ss}] & [M_{sp}] \\ [M_{ps}] & [M_{pp}] \end{bmatrix} \begin{bmatrix} [\phi_s] & [\psi_s] \\ [0] & [I] \end{bmatrix} \\
&= \begin{bmatrix} \left[\bar{M}_{\eta\eta}\right] & \left[\bar{M}_{\eta p}\right] \\ \left[\bar{M}_{p\eta}\right] & \left[\bar{M}_{pp}\right] \end{bmatrix}
\end{aligned}
\tag{3.12}
$$

where

$$
\begin{aligned}
\left[\bar{M}_{\eta\eta}\right] &= [I] \\
\left[\bar{M}_{\eta p}\right] &= \left[\left[\phi_s\right]^T\left[M_{ss}\right]\left[\psi_s\right] + \left[\phi_s\right]^T\left[M_{sp}\right]\right] \\
\left[\bar{M}_{p\eta}\right] &= \left[\tilde{M}_{\eta p}\right]^T = \left[\left[\psi_s\right]^T\left[M_{ss}\right]\left[\phi_s\right] + \left[M_{sp}\right]\left[\phi_s\right]\right] \\
\left[\bar{M}_{pp}\right] &= \left[\left[\psi_s\right]^T\left[M_{ss}\right]\left[\psi_s\right] + \left[\psi_s\right]^T\left[M_{sp}\right] + \left[M_{ps}\right]\left[\psi_s\right] + \left[M_{pp}\right]\right]
\end{aligned}
\tag{3.13}
$$

Considering a structure composed of two substructures which are to be coupled, the reduced element matrices are assembled at the interface degrees-of-freedom. The equation of motion of the whole structure becomes

$$
\begin{aligned}
&\begin{bmatrix} [I] & \left[\bar{M}_{\eta p,1}\right] & [0] \\ \left[\bar{M}_{p\eta,1}\right] & \left[\bar{M}_{pp,1}\right] + \left[\bar{M}_{pp,2}\right] & \left[\bar{M}_{p\eta,2}\right] \\ [0] & \left[\bar{M}_{\eta p,2}\right] & [I] \end{bmatrix} \begin{Bmatrix} \{\ddot{\eta}_1\} \\ \{\ddot{x}_p\} \\ \{\ddot{\eta}_2\} \end{Bmatrix} + \\
&+ \begin{bmatrix} \left[\omega_{s,1}^2\right] & [0] & [0] \\ [0] & \left[\bar{K}_{pp,1}\right] + \left[\bar{K}_{pp,2}\right] & [0] \\ [0] & [0] & \left[\omega_{s,1}^2\right] \end{bmatrix} \begin{Bmatrix} \{\eta_1\} \\ \{x_p\} \\ \{\eta_2\} \end{Bmatrix} = \begin{Bmatrix} \{f_{\eta,1}\} \\ \{f_p\} \\ \{f_{\eta,2}\} \end{Bmatrix}
\end{aligned}
\tag{3.14}
$$

where subscripts 1 and 2 denote the first and second components respectively. The transformation of coordinates and force vectors are given below.

$$\begin{Bmatrix} \{x_{s,1}\} \\ \{x_p\} \\ \{x_{s,2}\} \end{Bmatrix} = \begin{bmatrix} [\phi_{s,1}] & [\psi_{s,1}] & [0] \\ [0] & [I] & [0] \\ [0] & [\psi_{s,1}] & [[\phi_{s,1}]] \end{bmatrix} \begin{Bmatrix} \{\eta_1\} \\ \{x_p\} \\ \{\eta_2\} \end{Bmatrix} \tag{3.15}$$

$$\begin{Bmatrix} \{f_{\eta,1}\} \\ \{f_p\} \\ \{f_{\eta,2}\} \end{Bmatrix} = \begin{bmatrix} [\phi_{s,1}] & [\psi_{s,1}] & [0] \\ [0] & [I] & [0] \\ [0] & [\psi_{s,1}] & [[\phi_{s,1}]] \end{bmatrix}^T \begin{Bmatrix} \{f_{s,1}\} \\ \{f_p\} \\ \{f_{s,2}\} \end{Bmatrix} \tag{3.16}$$

3.1.1.2 Formulation for Bladed Disk Assemblies

As an implementation of Craig-Bampton method, Bladh adopted the formulations to bladed disk assemblies [10]. The assembly is divided into a tuned disk and a number of blades. All the substructures are reduced into modal coordinates and physical coordinates at blade disk interfaces. Bladh also studied the secondary modal analysis techniques on the disk and interface and on the interface only. The reduced order model is further reduced via modal reduction. After a suitable reduced system is determined, the mistuning is imposed as perturbations on the modal stiffness matrix of each blade.

In this thesis implementation of the Craig-Bampton method to bladed assemblies will be used without any secondary modal analyses. Here, a complete formulation, which can be found in reference [10], is not given.

The mass and stiffness matrices, $\left[\bar{M}_{dcb}\right]$ and $\left[\bar{K}_{dcb}\right]$, respectively, of the reduced order model are given below:

$$\left[\bar{M}_{dcb}\right]=\begin{bmatrix} [I] & \left[\bar{M}_{dc}\right] & [0] \\ \left[\bar{M}_{dc}\right]^T & \left[\bar{M}_{cc,d}\right]+[I]\otimes\left[\bar{M}_{cc,b}\right] & \left[\hat{F}\right]^T\left[[I]\otimes\left[\bar{M}_{bc}\right]^T\right] \\ [0] & \left[[I]\otimes\left[\bar{M}_{bc}\right]\right]\left[\hat{F}\right] & [I] \end{bmatrix} \tag{3.17}$$

$$\left[\bar{K}_{dcb}\right]=\begin{bmatrix} \left[\left(\omega_r^2\right)_d\right] & [0] & [0] \\ [0] & \left[\bar{K}_{cc,d}\right]+[I]\otimes\left[\bar{K}_{cc,b}\right] & [0] \\ [0] & [0] & [I]\otimes\left[\left(\omega_r^2\right)_b\right] \end{bmatrix} \tag{3.18}$$

Here $[I]$ is the identity matrix, $[0]$ is the zero matrix, $\left[\left(\omega_r^2\right)_d\right]$ is the modal stiffness matrix of the disk, $\left[\left(\omega_r^2\right)_b\right]$ is the modal stiffness matrix of a single cantilevered blade, $\left[\bar{M}_{dcb}\right]$ and $\left[\bar{K}_{dcb}\right]$ are the reduced mass and stiffness matrices, respectively, $\left[\hat{F}\right]$ is the transformation matrix from cyclic coordinates to physical coordinates. Subscripts *b*, *d* and *c* represent the blade, the disk and the connection degrees-of-freedom, respectively.

Note that the lower-right element of the stiffness matrix is a diagonal matrix. It contains the modal stiffness values of each blade in the assembly, which makes modal stiffness mistuning possible. In order to impose mistuning, cantilevered blade modal stiffness values on the diagonal elements of $[I]\otimes\left[\Lambda_b\right]$ are perturbed as:

$$\underset{n=1,\ldots,N}{\text{Bdiag}}\left[\underset{m=1,\ldots,m_b}{\text{diag}}\left(1+\delta_n^k\right)\left[\left(\omega_r^2\right)_b\right]\right] \tag{3.19}$$

Then, the eigenvalue problem

$$\left[\left[\bar{K}\right]-\omega^2\left[\bar{M}\right]\right]\begin{Bmatrix}\{\eta_d\}\\ \{x_i\}\\ \{\eta_b\}\end{Bmatrix}=\{0\} \tag{3.20}$$

is solved for natural frequencies and mode shapes of the mistuned assembly. Here, $\{\eta_d\}$ and $\{\eta_b\}$ are the vectors of modal displacements related to disc and blade modes respectively, and $\{x_i\}$ is the vector of physical displacements on the disk-blade interface.

3.2 Subset of Nominal Modes Method

Another method which exploits modal reduction in calculating modal properties of mistuned bladed disk assemblies is the "subset of nominal modes" method developed by Yang and Griffin [17]. The method is based on their prior work on resolving modal interaction. One of the results of that study is that "closely spaced modes in an altered system can be approximated as a sum of the closely spaced nominal modes." This can be used to approximate the modes of a mistuned bladed assembly since the modes of a typical bladed disk assembly are grouped into clusters of modes which have similar blade motion with different number of nodal diameters disk motion in a narrow frequency range. Therefore the natural frequencies of a mistuned bladed disk assembly in a frequency range can be expressed by the modes of the tuned assembly, which Yang calls the "nominal system", in the same frequency range. The mistuning is imposed on the linear model as modification in mass and stiffness matrices. The structural modification method used in this work was first introduced by Luk and Mitchell [42] in 1982.

Feiner et al. used the subset of nominal modes method to study a single family of modes of mistuned bladed disk assemblies [18]. He further developed the method so that the method does not need the element matrices of the blades any more. The frequency deviations on blade alone cantilevered modes are the only parameters defining mistuning. The other input for the method is the nominal frequencies of the tuned bladed disk assembly.

Feiner et al. implemented this study to identify the mistuning of a bladed disk assembly by experimental data [19]. Given the nominal frequencies of the tuned assembly with a finite number of measurements on mode shapes and natural frequencies of mistuned modes, the method can predict the amount of frequency deviations from nominal frequencies for each sector.

Here, only the formulation for subset of nominal modes method will be given. Here, the effects of aerodynamic and gyroscopic forces will not be included in the analysis.

Assuming a harmonic excitation and steady-state response, the equation of motion of a mistuned bladed disk assembly can be written as

$$\left[[K]+[\Delta K]+i\omega[C]-\omega^2\left([M]+[\Delta M]\right)\right]\{x\}=\{F\} \tag{3.21}$$

Here, $[K]$ and $[M]$ are the stiffness and mass matrices of the tuned system, $[\Delta K]$ and $[\Delta M]$ are the modification matrices on stiffness and mass matrices, $[C]$ is the viscous damping matrix, respectively. $\{x\}$ is the vector of vibration amplitudes, $\{F\}$ is the vector of external forcing, ω is the excitation frequency, and i is the unit imaginary number.

The solution to the eigenvalue problem which is constructed for the undamped nominal system

$$([K]-\omega^2[M])\{x\}=\{0\} \tag{3.22}$$

will yield the eigenvector, $\{\phi_j^0\}$, and the natural frequency square, ω_j^2, for the j^{th} mode. The equation (3.21) is transformed into the modal domain using the following coordinate transformation.

$$\{x\}=[\phi]\{\eta\} \tag{3.23}$$

where $\{\eta\}$ is the modal displacement vector and

$$[\phi]=\left[\{\phi_1\}\{\phi_2\}\cdots\{\phi_N\}\right] \tag{3.24}$$

Then, the equation (3.21) becomes

$$\left[\left(\left[\omega_r^2\right]+[\Delta\bar{K}]\right)+i\omega[\bar{C}]-\omega^2\left([I]+[\Delta\bar{M}]\right)\right]\{\eta\}=[\phi]^T\{F\} \tag{3.25}$$

where

$$\begin{aligned}[\bar{C}]&=[\phi]^T[C][\phi]\\ [\Delta\bar{K}]&=[\phi]^T[\Delta K][\phi]\\ [\Delta\bar{M}]&=[\phi]^T[\Delta M][\phi]\end{aligned} \tag{3.26}$$

Assuming that only the modulus of elasticity of each blade is changed by a portion, the modification matrix for the j^{th} sector can be written as:

$$[\Delta K]=\underset{j=1,\ldots,N}{Bdiag}\left[\left(1+\delta_j\right)[K]\right] \tag{3.27}$$

where

$$[K]=\begin{bmatrix}[K_b] & 0\\ 0 & 0\end{bmatrix} \tag{3.28}$$

Here, $[K_b]$ is the stiffness matrix of a tuned blade. Then, the modification matrix in modal domain can be written as:

$$[\Delta\bar{K}]=\sum_{i=1}^{N}\sum_{j=1}^{N}\left(1+\delta_j\right)\left[E_{i,j}\right]^*\left[\hat{K}_{i-1}\right]\left[E_{i,j}\right] \tag{3.29}$$

where

$$\left[\hat{K}_i\right] = [\phi]_i^* [K][\phi]_i \tag{3.30}$$

which is calculated once. Here, $[\phi]_i$ is the mass normalized complex eigenvector matrix which belongs to *i* nodal diameter modes, and * denotes Hermitian conjugate. For different sets of mistuning, with $\left[\hat{K}_i\right]$'s calculated beforehand, the modification matrix, $[\Delta\bar{K}]$, can be recalculated using equation (3.29). Then, the eigenvalue problem

$$\left[\left(\left[\omega_r^2\right] + [\Delta\bar{K}]\right) - \omega^2 [I]\right]\{\eta\} = \{0\} \tag{3.31}$$

will yield the natural frequencies and mode shapes of the mistuned assembly.

Please see reference [18] for a detailed formulation of fundamental model of mistuning.

CHAPTER 4

NONLINEAR DYNAMIC RESPONSE

4.1 Equation of Motion

The equation of motion of a structure under harmonic external forcing in the presence of non-linearity can be written in the following form.

$$[M]\{\ddot{x}\}+[C]\{\dot{x}\}+[K]\{x\}+i[H]\{x\}+\{f_{NL}\}=\{f\} \tag{4.1}$$

Here, $[M]$, $[K]$, $[C]$ and $[H]$ are the mass, stiffness, viscous damping and structural damping matrices, $\{x\}$, $\{\dot{x}\}$ and $\{\ddot{x}\}$ are the vectors of physical displacements, velocities and accelerations, respectively. $\{f_{NL}\}$ is the vector of non-linear internal forces and $\{f\}$ is the vector of external forces. *i* is the unit imaginary number.

Before looking into the solutions to nonlinear vibratory systems, solutions to linear vibratory response should be examined. For the steady-state linear vibratory response to sinusoidal in the form of

$$\{f(t)\}=\mathrm{Im}\left(\{F\}e^{i\omega t}\right) \tag{4.2}$$

where $\{F\}$ is the complex vector holding the amplitude and phase data, ω is the excitation frequency, the response is assumed to be in the following form:

$$\{x(t)\}=\mathrm{Im}\left(\{X\}e^{i\omega t}\right) \tag{4.3}$$

Then, substituting equations (4.2) and (4.3) into the equation (4.1) one can obtain

$$\left[-\omega^2[M]+i\omega[C]+[K]+i[H]\right]\{X\}=\{F\} \tag{4.4}$$

In nonlinear systems, the response to a simple harmonic excitation at a single frequency will not necessarily be a harmonic response at the same frequency. The response will include other harmonics depending on the nonlinearity in the system. These harmonics will be at frequencies which are the multiples of the excitation frequency.

The general solution approach is based on the assumption that the nonlinear forces can be represented as a sum of sinusoidal functions at harmonics of the excitation frequency. Assuming an external forcing of the form in equation (4.2), the nonlinear internal forces can be expressed as

$$\{f_{NL}(t)\}=\mathrm{Im}\left(\sum_{m=0}^{\infty}\{F_{NL}\}_m e^{im\omega t}\right) \tag{4.5}$$

where m is the harmonics index. Then considering the system as linear with forcing at multiple harmonics, the response is expected to be at the same harmonics and can be expressed as

$$\{x(t)\}=\mathrm{Im}\left(\sum_{m=0}^{\infty}\{X\}_m e^{im\omega t}\right) \tag{4.6}$$

Since there exists nonlinear forcing at multiple harmonics, the external forcing can also be taken in a more general form including components at other harmonics and can be expressed as

$$\{f(t)\}=\mathrm{Im}\left(\sum_{m=0}^{\infty}\{F\}_m e^{im\omega t}\right) \tag{4.7}$$

Substituting equations (4.2), (4.5), (4.6) and (4.7) into equation (4.1) one can write the following equations for each harmonic as

$$\begin{aligned}&[K]\{X\}_0 + \{F_{NL}\}_0 = \{F\}_0 \\ &\left[-(m\omega)^2[M] + i(m\omega)[C] + [K] + i[H]\right]\{X\}_m + \{F_{NL}\}_m = \{F\}_m\end{aligned} \tag{4.8}$$

It should be noted that the amplitudes of the nonlinear forcing depend on the displacements of coordinates at which the nonlinear elements are connected to. Nonlinearity can be expressed as a combination of multiple harmonics using the describing functions method or the harmonic balance method. They will be discussed in the upcoming sections.

4.2 Linearization Methods

In this part, describing functions method (DFM) and harmonic balance method (HBM) will be discussed briefly. They are both based on Fourier expansion formulae. The difference appears in the application of the transformation integrals. In describing functions method, a single integral is calculated in complex domain whereas in harmonic balance method two separate integrals are calculated in real domain. These integrals are equivalent to the real and imaginary parts of the single integral in describing functions method.

4.2.1 Describing Functions Method

Describing functions method has been commonly utilized in control theory. It linearizes the nonlinear elements to make it possible to be used in linear frequency domain analyses. Knowing that the nonlinear elements are functions of frequency and amplitude of the signal (vibration amplitude in

physical systems), the nonlinear element can be assumed to behave linearly at that frequency and amplitude.

The first implementation of describing functions method into vibratory multi-degree-of-freedom physical systems was done by Tanrıkulu et al. [43]. In this study a number of different nonlinearity types have been formulated using the method. Kuran and Özgüven extended this work to include multiple harmonics solution although the main focus was on the response computation using modal superposition [44].

4.2.1.1 Formulation

Considering a multi-degree-of-freedom nonlinear system, the equation of motion will be of the form of equation (4.1). After assuming a solution of the form (4.3), the equation of motion will be

$$\left[-\omega^2[M]+i\omega[C]+[K]+i[H]\right]\{X\}+\{F_{NL}\}=\{F\} \tag{4.9}$$

As Budak and Özgüven [45] suggested, one can write the nonlinear forcing amplitudes vector as

$$\{F_{NL}\}=[\Delta]\{X\} \tag{4.10}$$

where $[\Delta]$ is the response dependent "nonlinearity matrix." Then, the equation of motion can be rewritten as

$$\left[-\omega^2[M]+i\omega[C]+[K]+i[H]+[\Delta]\right]\{X\}=\{F\} \tag{4.11}$$

Considering nonlinearity as discreet elements between specific degrees-of-freedom, each nonlinear element can be treated separately. Assuming that a nonlinear element exists between r^{th} and j^{th} degrees-of-freedom, the elements of the nonlinearity matrix can be written as

$$\Delta_{rr} = v_{rr} + \sum_{\substack{j=1 \\ j\neq r}}^{n} v_{rj}, \qquad r = 1,2,...,n$$
$$\Delta_{rj} = -v_{rj}, \qquad r \neq j, \quad r = 1,2,...,n \tag{4.12}$$

where v_{rj} is the equivalent stiffness of the linearized nonlinear element which can be calculated as

$$v_{rj} = \frac{i}{\pi Y_{rj}} \int_0^{2\pi} n_{rj}(\theta) e^{-i\theta} d\theta \tag{4.13}$$

where Y_{rj} is the complex amplitude of displacements and $n_{rj}(\theta)$ is the nonlinear forcing between r^{th} and j^{th} degrees-of-freedom. It should be noted that, the displacement between two degrees-of-freedom can be written as

$$y_{rj}(\theta) = \mathrm{Im}\left(Y_{rj} e^{i\theta}\right) = \overline{Y}_{rj} \sin\left(\theta + \phi_j\right) \tag{4.14}$$

The formulation is further extended to include multiple harmonics by Kuran and Özgüven [44]. Assuming a solution in the form of equation (4.6), the expression (4.10) can be rewritten as

$$\left\{F_{NL}\right\}_m = [\Delta]_m \{X\}_m \tag{4.15}$$

where $\left\{F_{NL}\right\}_m$ is the amplitude vector, $[\Delta]_m$ is the nonlinearity matrix and $\{X\}_m$ is the displacement vector for the m^{th} harmonic. The nonlinear forcing $n_{rj}(\theta)$ between r^{th} and j^{th} degrees-of-freedom can be expressed by its harmonics as

$$n_{rj}(\theta) = \sum_{m=0}^{N} \left(n_{rj}(\theta)\right)_m \tag{4.16}$$

where N is the highest number of harmonics retained. Then each element of $[\Delta]_m$ is calculated as follows.

$$\left(\Delta_{rr}\right)_m = \left(v_{rr}\right)_m + \sum_{\substack{j=1 \\ j\neq r}}^{n} \left(v_{rj}\right)_m, \qquad r = 1,2,...,n$$
$$\left(\Delta_{rj}\right)_m = -\left(v_{rj}\right)_m, \qquad r \neq j, \quad r = 1,2,...,n \tag{4.17}$$

where

$$\left(v_{rj}\right)_0 = \frac{1}{2\pi\left(Y_{rj}\right)_0}\int_0^{2\pi} n_{rj}(\theta)\,d\theta$$
$$\left(v_{rj}\right)_m = \frac{i}{\pi\left(Y_{rj}\right)_m}\int_0^{2\pi} n_{rj}(\theta)\,e^{-im\theta}d\theta, \quad \text{for } m \geq 1 \tag{4.18}$$

Note that the m^{th} harmonic component of the inter-coordinate displacement is defined as

$$\left(Y_{rj}\right)_m = \left(Y_r\right)_m - \left(Y_r\right)_m,\ r \neq j \tag{4.19}$$

4.2.2 Harmonic Balance Method

Like the describing functions method, the harmonics balance method is based on Fourier transformation integrals. Linear behavior assumption is also made as it is the case in describing functions. In recent studies, multiple harmonics formulation of HBM is commonly used to express strong nonlinearities whereas for barely negligible nonlinearity a single harmonic formulation is sufficient.

Considering the equation of motion of a nonlinear system in the form of equation (4.9), the nonlinear forcing vector can be expressed by the multiplication of a complex stiffness matrix, which is formed by the equivalent stiffness values of linearized nonlinear elements, and displacement vector. Assuming that a nonlinear element exists between r^{th} and j^{th} degrees-of-freedom, the equivalent stiffness is defined as

$$k_{rj} = k_{rj}^R + ik_{rj}^I \tag{4.20}$$

where

$$k_{rj}^{R} = \frac{1}{\pi \bar{Y}_{rj}} \int_0^{2\pi} n_{rj}(\theta)\cos(\theta) d\theta$$
$$k_{rj}^{I} = \frac{-1}{\pi \bar{Y}_{rj}} \int_0^{2\pi} n_{rj}(\theta)\sin(\theta) d\theta \tag{4.21}$$

Here the nonlinear forcing is defined knowing that the inter-coordinate displacement is of the form

$$y_{rj}(t) = \mathrm{Re}\left(Y_{rj} e^{i\omega t}\right) = \bar{Y}_{rj}\cos\left(\omega t + \phi_j\right) \tag{4.22}$$

Then, the equivalent stiffness matrix of the nonlinear elements, $\left[K_{NL}\right]$, can be defined as follows.

$$K_{NL,rr} = k_{rr} + \sum_{\substack{j=1 \\ j\neq r}}^{n} k_{rj}, \quad r = 1,2,...,n$$
$$K_{NL,rj} = -k_{rj}, \quad r \neq j, \quad r = 1,2,...,n \tag{4.23}$$

where

$$k_{rj} = k_{rj}^{R} + i k_{rj}^{I} \tag{4.24}$$

The formulation can be extended for multiple harmonics solutions. It is assumed that the m^{th} harmonic of the nonlinear forcing between r^{th} and j^{th} degrees-of-freedom can be expressed as the multiplication of an equivalent stiffness and the m^{th} harmonic component of the inter-coordinate displacement. The real and imaginary components of the equivalent stiffness for m^{th} harmonic can be written as

$$\left(k_{rj}^{R}\right)_0 = \frac{1}{2\pi\left(\bar{Y}_{rj}\right)_0} \int_0^{2\pi} n_{rj}(\theta)\, d\theta$$
$$\left(k_{rj}^{R}\right)_m = \frac{1}{\pi\left(\bar{Y}_{rj}\right)_m} \int_0^{2\pi} n_{rj}(\theta)\cos(m\theta)\, d\theta, \qquad \text{for } m \geq 1 \tag{4.25}$$
$$\left(k_{rj}^{I}\right)_m = \frac{-1}{\pi\left(\bar{Y}_{rj}\right)_m} \int_0^{2\pi} n_{rj}(\theta)\sin(m\theta)\, d\theta, \qquad \text{for } m \geq 1$$

Then, the equivalent stiffness matrix of nonlinear elements for m^{th} harmonic, $\left[K_{NL}\right]_m$, can be defined as follows.

$$\begin{aligned}\left(K_{NL,rr}\right)_m &= \left(k_{rr}\right)_m + \sum_{\substack{j=1 \\ j\neq r}}^{n}\left(k_{rj}\right)_m,\ r=1,2,...,n \\ \left(K_{NL,rj}\right)_m &= -\left(k_{rj}\right)_m,\quad r\neq j,\quad r=1,2,...,n\end{aligned} \tag{4.26}$$

where

$$\left(k_{rj}\right)_m = \left(k_{rj}^R\right)_m + i\left(k_{rj}^I\right)_m \tag{4.27}$$

Note that the m^{th} harmonic component of the inter-coordinate displacement is defined as it is done in equation (4.19).

4.3 Solution Procedures

In the upcoming sections solution procedures for nonlinear vibratory systems will be discussed. It should be noted that; these procedures are applied with the assumption that all the nonlinearity can be linearized and the solution to the linearized system is stable.

4.3.1 Fixed Point Iteration Method

A function $f(x)$ is said to have a fixed point p if it satisfies the equation

$$p = f(p) \tag{4.28}$$

This point p can be determined by assuming an initial guess p_0 and a sequence is formed by

$$p_{n+1} = f\left(p_n\right) \tag{4.29}$$

If the sequence is convergent, it converges to the fixed point p as

$$p = \lim_{n\to\infty} p_n = \lim_{n\to\infty} f\left(p_n\right) \tag{4.30}$$

The convergence can be defined within a numerical tolerance by defining a relative error being smaller that an error tolerance as

$$\varepsilon_{rel} = \left|\frac{p_{n+1} - p_n}{p_n}\right| \le \varepsilon_{tol} \tag{4.31}$$

Kuran and Özgüven [44] implemented fixed point iteration method in forced response predictions of nonlinear vibratory systems by defining a pseudo-receptance matrix which is a "response dependent" receptance matrix and defined as

$$\left[\Theta(\{X\})\right] = \left(-\omega^2\left[M\right] + i\omega\left[C\right] + \left[K\right] + i\left[H\right] + \left[\Delta(\{X\})\right]\right)^{-1} \tag{4.32}$$

The fixed point for each frequency ω in the range of interest is defined as follows:

$$\{X\} = \left[\Theta(\{X\})\right]\{F\} \tag{4.33}$$

For large systems calculation of the pseudo-receptance matrix is numerically costly, since it consists of a matrix inversion of a large matrix. But if nonlinearity is local then the nonlinearity matrix would be highly sparse. Its elements can be considered as modifications to the receptance matrix of the corresponding linear system at the desired frequency. This kind of modification is generally carried out via Özgüven's method [46] or Sherman-Morrison-Woodbury method [47, 48].

The iteration step is written as

$$\{X\}_{n+1} = \left[\Theta\left(\{X\}_n\right)\right]\{F\} \tag{4.34}$$

and the relative error is defined as follows.

$$\varepsilon_{rel} = \max\left(\left|\frac{X_{n+1}^{j} - X_{n}^{j}}{X_{n}^{j}}\right|\right), \qquad j = 1, 2, ..., N \tag{4.35}$$

where N is the number of degrees-of-freedom.

In case of divergent or numerically unstable solutions relaxation on the fixed point iteration is applied as

$$\{X'\}_{n+1} = (1-\lambda)\{X\}_{n+1} + \lambda\{X\}_{n}, \qquad 0 \le \lambda \le 1 \tag{4.36}$$

4.3.2 Newton-Raphson Method

Newton-Raphson method has proved itself to be one of the fastest methods in optimization. Its quadratic convergence provides the speed to the method given that the necessary initial conditions are set. In nonlinear vibratory systems analysis, Newton-Raphson method has been implemented by several researchers [26, 35, 49]. By introducing numerical continuation techniques, this method can also be used to trace unstable regions of frequency response functions of nonlinear systems in which jump phenomenon is observed. This topic is going to be discussed in the next section.

4.3.2.1 Formulation

The equation of motion of a nonlinear vibratory system in the form of equation (4.9) can be solved by Newton-Raphson method assuming that an estimate point close to the solution curve is known. The equation of motion is rewritten as a residual vector as

$$\left\{R\left(\{X\},\omega\right)\right\} = \left[-\omega^2[M] + i\omega[C] + [K] + i[H]\right]\{X\} + \{F_{NL}\} - \{F\} \tag{4.37}$$

The solution points form a hyper-curve defined by the equation

$$\left\{R\left(\{X\},\omega\right)\right\}=\{0\} \tag{4.38}$$

For an excitation frequency of ω, given an estimate point near the solution curve, the corrector step is applied at the *(i+1)th* iteration as follows.

$$\{X\}_{i+1}=\{X\}_i-\left[\frac{\partial\left\{R\left(\{X\},\omega\right)\right\}}{\partial\{X\}}\right]^{-1}\Bigg|_{\{X\}_i,\omega}\left\{R\left(\{X\}_i,\omega\right)\right\} \tag{4.39}$$

It is evident that the derivative of the residual vector $\left\{R\left(\{X\},\omega\right)\right\}$ with respect to the displacement amplitudes vector $\{X\}$, namely the Jacobian, should be calculated either analytically or numerically. Knowing that the system properties do not change (i.e. time invariant system), the Jacobian can be written as

$$\frac{\partial\left\{R\left(\{X\},\omega\right)\right\}}{\partial\{X\}}=\left[-\omega^2[M]+i\omega[C]+[K]+i[H]\right]+\frac{\partial\{F_{NL}\}}{\partial\{X\}} \tag{4.40}$$

Therefore only the Jacobian of the nonlinear forcing vector with respect to displacement amplitudes is required.

For large systems in which nonlinearity is local, the Jacobian matrix of the nonlinear forcing is highly sparse. Then, the Jacobian of residual vector can be written as

$$\begin{aligned}\left[\frac{\partial\left\{R\left(\{X\},\omega\right)\right\}}{\partial\{X\}}\right]^{-1}&=\left[\left[-\omega^2[M]+i\omega[C]+[K]+i[H]\right]+\frac{\partial\{F_{NL}\}}{\partial\{X\}}\right]^{-1}\\&=\left[[Z(\omega)]+\frac{\partial\{F_{NL}\}}{\partial\{X\}}\right]^{-1}=\left[[\alpha(\omega)]^{-1}+\frac{\partial\{F_{NL}\}}{\partial\{X\}}\right]^{-1}\end{aligned} \tag{4.41}$$

where

$$[Z(\omega)]=[\alpha(\omega)]^{-1}=-\omega^2[M]+i\omega[C]+[K]+i[H] \tag{4.42}$$

Then, the Jacobian can be considered as a modification matrix on the impedance matrix $[Z(\omega)]$ or inverse of the receptance matrix $[\alpha(\omega)]^{-1}$. This kind of modification is generally carried out via Özgüven's method [46] or Sherman-Morrison-Woodbury method [47, 48]. In such an approach, benefits of modal reduction can still be retained.

4.3.2.2 First Order Predictor

The speed and accuracy of Newton-Raphson method can only be of advantage when the estimate is close enough to the solution. Hence, a good estimator should be employed. A first order predictor can be used for such a purpose.

On the solution hyper-curve defined by equation (4.38), one can find a tangent vector by taking a partial derivative of equation (4.38) with respect to the excitation frequency ω:

$$\frac{\partial\{R(\{X\},\omega)\}}{\partial\omega}=\frac{\partial\{R(\{X\},\omega)\}}{\partial\{X\}}\frac{\partial\{X\}}{\partial\omega}+\frac{\partial\{R(\{X\},\omega)\}}{\partial\omega}=\{0\} \tag{4.43}$$

Then, the tangent vector becomes

$$\frac{\partial\{X\}}{\partial\omega}=-\left[\frac{\partial\{R(\{X\},\omega)\}}{\partial\{X\}}\right]^{-1}\frac{\partial\{R(\{X\},\omega)\}}{\partial\omega} \tag{4.44}$$

Substituting the variables in equation (4.44) yields

$$\frac{\partial\{X\}}{\partial\omega}=-\left[[Z(\omega)]+\frac{\partial\{F_{NL}\}}{\partial\{X\}}\right]^{-1}\frac{\partial[Z(\omega)]}{\partial\omega}\{X\} \tag{4.45}$$

At a previous solution point converged by Newton-Raphson corrector given in equation (4.39), the inverse of the matrix is already available. Hence, the initial guess for the next solution can be sought at:

$$\{X\}_k^0 = \{X\}_k + \left(\frac{\partial \{X\}}{\partial \omega}\bigg|_{\{X\}_k} \right) \Delta\omega \tag{4.46}$$

4.3.2.3 Arc Length Method

In the Newton-Raphson procedure discussed above, for each frequency point in the range of interest, the solution is obtained by using the iteration step given in equation (4.39). A solution can be converged given that the initial guess is close enough to the solution and the iteration step is valid. The validity of the iteration step depends on the existence of the inverse of the Jacobian matrix. But in some systems, there exist multiple solutions for some values of the main variable. Therefore, assuming that the solution curve is continuous, the curve should turn and cross these multiple solutions. These points on which the tangent is perfectly vertical are called turning points and at these points the Jacobian in equation (4.39) is singular, indicating that its inverse does not exist.

In vibratory mechanical systems, typical examples for such a phenomenon are systems including cubic stiffness or systems in which motion between contacting surfaces results in partial separation and contact. In Figure 4.1 a typical shift behavior is demonstrated.

To be able to trace over the turning points the curve should be parameterized by another variable. It can be done by selecting the arc length as the additional parameter. Instead of seeking the next solution on the next frequency point, the solution is sought on a hyper-sphere with a

radius of s [50]. This constraint can be imposed by introducing another equation for the k^{th} solution point as follows.

$$\{\Delta q\}_k^T \{\Delta q\}_k = s^2 \tag{4.47}$$

where

$$\{\Delta q\}_k = \left\{\{q\}_k - \{q\}_{k-1}\right\} \tag{4.48}$$

$$\{q\} = \begin{Bmatrix} \{X\} \\ \omega \end{Bmatrix} \tag{4.49}$$

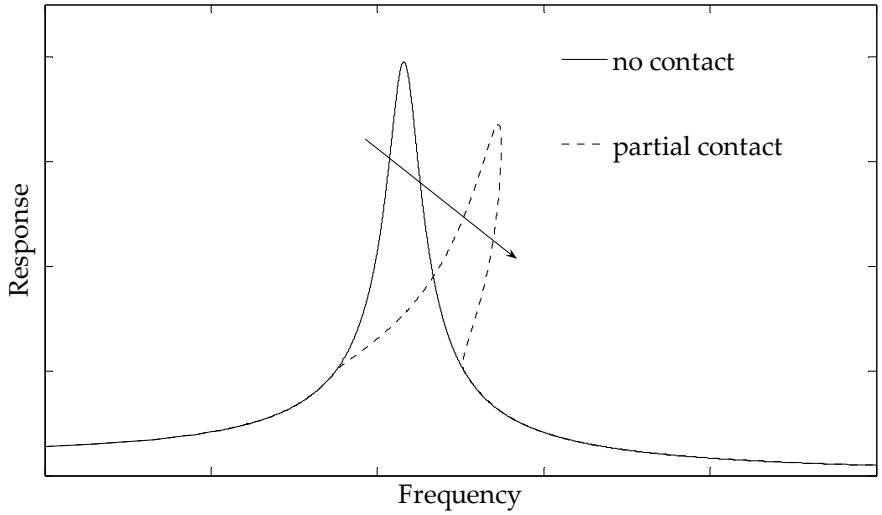

Figure 4.1 – Typical FRF for gap nonlinearity

Arranging terms in equation (4.47), a new equation can be defined as:

$$\left\{g\left(\{X\}_k, \omega_k\right)\right\} = \{\Delta q\}_k^T \{\Delta q\}_k - s^2 = \{0\} \tag{4.50}$$

Then the new corrector step can be rewritten as:

$$\{q\}_k^{i+1} = \{q\}_k^i - \left[\begin{matrix} \dfrac{\partial\left\{R\left(\{X\},\omega\right)\right\}}{\partial\{X\}} & \dfrac{\partial\left\{R\left(\{X\},\omega\right)\right\}}{\partial\omega} \\ \dfrac{\partial g\left(\{X\},\omega\right)}{\partial\{X\}} & \dfrac{\partial g\left(\{X\},\omega\right)}{\partial\omega} \end{matrix}\right]^{-1}\Bigg|_{\{X\}_k^i,\omega_k^i} \begin{Bmatrix} \left\{R\left(\{X\}_k^i, \omega_k^i\right)\right\} \\ g\left(\{X\}_k^i, \omega_k^i\right) \end{Bmatrix} \tag{4.51}$$

where

$$\left[\frac{\partial g\left(\{X\},\omega\right)}{\partial\{X\}} \quad \frac{\partial g\left(\{X\},\omega\right)}{\partial\omega}\right]=\left[2\{\Delta q\}_k^{i\,T}\right] \tag{4.52}$$

and

$$\{\Delta q\}_k^i=\{\Delta q\}_k^i-\{\Delta q\}_k \tag{4.53}$$

By introducing a new equation on the arc length, the corrector is forced to converge to a solution on the hyper-sphere of radius *s*. At the same time, the new Jacobian matrix is not singular at turning points. The first order predictor can still be used with the assumption that, numerically, none of the solution points is perfectly coincident with the turning points.

In the solution process, along the solution curve there may exist sharp turns which may require careful attention. The value of step length at a solution point may not allow following these sharp corners. This situation can be anticipated by continuously checking the number of iterations at each solution point as Crisfield [50] suggested. If the number of iterations at the previous solution point is larger or smaller than a set value, which is not necessarily an integer, the step length can be adjusted accordingly using the following formula [50]:

$$s_k=s_{k-1}\sqrt{\frac{n_{nom}^{iter}}{n_{k-1}^{iter}}} \tag{4.54}$$

Here, s_k is the step length at k^{th} solution point, s_{k-1} and n_{k-1}^{iter} are step length and the number of iterations at $(k\text{-}1)^{th}$ solution point, respectively, and n_{nom}^{iter} is the nominal value of number of iterations. Even though with an adaptive step length, at some points, the method may fail to converge due to the step length being so large. At such a point, the method iterates to converge

relentlessly, and special treatment is needed. To avoid such a case, where convergence cannot be achieved due to large step length, after a limiting number of iterations the step length is reduced and the solution procedure is repeated at the same point.

4.4 Nonlinear Analysis in Modal Domain

Modal reduction is a well known technique which is inevitable and useful at the same time. It is inevitable since each structure in reality has an infinite number of modes all of which cannot be taken into consideration. It is useful, because via modal reduction the number of equations to be solved is reduced to the number of modes retained.

Kuran and Özgüven [44] implemented modal reduction to the solution procedure of nonlinear vibratory systems. They applied the modal reduction to the equation of motion after calculating the nonlinearity matrix. Regardless of the number of nonlinearity in the system, the number of equations is reduced to the number of modes retained. This can be implemented to other solution procedures such as Newton-Raphson method.

Considering a nonlinear system whose equation of motion is of the form (4.9), it can be transformed into the modal domain using the mass normalized modes shapes matrix $[\phi]$ by using the following coordinate transformation.

$$\{X\} = [\phi]\{\eta\} \tag{4.55}$$

where $\{\eta\}$ is the vector of modal displacements. Then the equation of motion becomes

$$\left[-\omega^2[I]+i\omega\left[\bar{C}\right]+\left[\omega_r^2\right]+i\left[\bar{H}\right]\right]\{\eta\}+\left\{\bar{F}_{NL}\right\}=\left\{\bar{F}\right\} \tag{4.56}$$

where $[I]$ is the identity matrix, $\left[\omega_r^2\right]$ is the eigenvalue matrix and

$$\begin{aligned}
\left[\bar{C}\right] &= [\phi]^T[C][\phi] \\
\left[\bar{H}\right] &= [\phi]^T[H][\phi] \\
\left\{\bar{F}_{NL}\right\} &= [\phi]^T\{F_{NL}\} \\
\left\{\bar{F}\right\} &= [\phi]^T\{F\}
\end{aligned} \tag{4.57}$$

The Newton-Raphson solution procedure can be implemented to this modal domain method by transforming the nonlinear forcing vector and its Jacobian matrix into modal coordinates. Assuming that there exists *n* number of nonlinear elements between several degrees-of-freedom of the system, the nonlinear forcing vector can be written as the summation of the forcing vectors of each nonlinear element as

$$\{F_{NL}\}=\sum_{k=1}^{n}\{F_{NL}^k\} \tag{4.58}$$

Therefore, the nonlinear forcing vector transformed into the modal domain will be

$$\left\{\bar{F}_{NL}\right\}=[\phi]^T\{F_{NL}\}=[\phi]^T\sum_{k=1}^{n}\{F_{NL}^k\} \tag{4.59}$$

Knowing that the nonlinear force of each element will act only to the degrees-of-freedom which it is connected to, the forcing vector of each nonlinear element is highly sparse. This vector for the k^{th} element between i^{th} and j^{th} degrees-of-freedom can be represented as

$$\{F_{NL}^k\}=\begin{bmatrix}0\cdots 0 & f_{NL}^k & 0\cdots 0 & -f_{NL}^k & 0\cdots 0\end{bmatrix}^T \tag{4.60}$$

where only the i^{th} and j^{th} columns are nonzero and they have the same force value, f_{NL}^{k}, with opposite signs. Therefore equation (4.59) can be rewritten as

$$\left\{\bar{F}_{NL}\right\} = \sum_{k=1}^{n} \left[\frac{\left\{\phi^{i}\right\}}{\left\{\phi^{j}\right\}}\right]^{T} \begin{Bmatrix} f_{NL}^{k} \\ -f_{NL}^{k} \end{Bmatrix} \tag{4.61}$$

where $\left\{\phi^{i}\right\}$ is the i^{th} row of the mass normalized modal matrix.

Analogously, the derivative of nonlinear forcing vector with respect to the displacements can be written. Knowing that the nonlinear force vector of k^{th} element is a function of the degrees-of-freedom it is connected to, let them be i^{th} and j^{th} degrees-of-freedom, the Jacobian will have nonzero elements only on the intersection of i^{th} and j^{th} rows with i^{th} and j^{th} columns. Therefore the Jacobian can be written in modal domain as

$$\frac{\partial\left\{\bar{F}_{NL}\right\}}{\partial\left\{\eta\right\}} = \sum_{k=1}^{n} \left[\frac{\left\{\phi^{i}\right\}}{\left\{\phi^{j}\right\}}\right]^{T} \begin{bmatrix} \dfrac{\partial f_{NL}^{k}}{\partial x_{i,j}} & -\dfrac{\partial f_{NL}^{k}}{\partial x_{i,j}} \\ -\dfrac{\partial f_{NL}^{k}}{\partial x_{i,j}} & \dfrac{\partial f_{NL}^{k}}{\partial x_{i,j}} \end{bmatrix} \left[\frac{\left\{\phi^{i}\right\}}{\left\{\phi^{j}\right\}}\right] \tag{4.62}$$

where

$$x_{i,j} = x_i - x_j \tag{4.63}$$

4.5 Nonlinear Element Formulations

In this section, a number of basic nonlinear elements will be linearized using either of the methods described in section 4.2. The linearized expressions will be used to determine the equivalent nonlinear force vector and its Jacobian expressions. Verification of the linearization will be carried

out via a comparison of the results with time integration results. *"ode45"* function of MATLAB is utilized for time integration solutions.

4.5.1 Cubic Stiffness Element

Considering a spring element which exerts a force of a magnitude proportional to its extension to the third power, the force expression can be written as:

$$F = k_c x^3 \tag{4.64}$$

where k_c is the coefficient of cubic stiffness. Assuming the displacement of the form:

$$x(\theta) = X\cos(\theta) \tag{4.65}$$

where X is the vibration amplitude. Using HBM the nonlinear forcing for the first harmonics can be linearized as

$$\begin{aligned} k_r &= \frac{1}{\pi X}\int_0^{2\pi} k_c\left(X\cos(\theta)\right)^3\cos(\theta)d\theta = \frac{3}{4}k_c X^2 \\ k_i &= \frac{-1}{\pi X}\int_0^{2\pi} k_c\left(X\cos(\theta)\right)^3\sin(\theta)d\theta = 0 \end{aligned} \tag{4.66}$$

Rewriting the displacement expression with phase difference in terms of sine and cosine functions in matrix form

$$x(\theta) = \{X\}^T \begin{Bmatrix}\cos(\theta)\\ \sin(\theta)\end{Bmatrix} \tag{4.67}$$

where

$$\{X\} = \begin{Bmatrix} X_c \\ X_s \end{Bmatrix} \tag{4.68}$$

The forcing vector can also be written accordingly as follows:

$$F(\theta) = \{F\}^T \begin{Bmatrix}\cos(\theta)\\ \sin(\theta)\end{Bmatrix} = \left[\begin{bmatrix} k_r & 0 \\ 0 & k_r \end{bmatrix}\{X\}\right]^T \begin{Bmatrix}\cos(\theta)\\ \sin(\theta)\end{Bmatrix} \tag{4.69}$$

where

$$\{F\} = \frac{3}{4} k_c \begin{Bmatrix} X_c^3 + X_c X_s^2 \\ X_s X_c^2 + X_s^3 \end{Bmatrix} \tag{4.70}$$

Then the Jacobian of the forcing vector will be

$$\frac{\partial \{F\}}{\partial \{X\}} = \frac{3}{4} k_c \begin{bmatrix} 3X_c^2 + X_s^2 & X_c X_s \\ X_c X_s & 3X_s^2 + X_c^2 \end{bmatrix}$$

4.5.1.1 Verification via Time Domain Integration

For a single degree-of-freedom underdamped system which is grounded by a cubic stiffness spring, the forced response is calculated via Newton-Raphson method using the force vector and Jacobian expressions. The results are compared with time integration results in Figure 4.2. Due to multiple solution points, time integration is applied from low to high frequencies and from high to low frequencies. The results are in good agreement even if a slight difference exists in the resonance amplitude. Time integration method also revealed a negligibly small peak in low frequency region. Those differences can be explained by retaining the fundamental harmonic only.

4.5.2 Macroslip Friction Element under Constant Normal Load

For a macroslip friction element, the force-displacement relationship is shown in Figure 4.3 where k is the friction stiffness, X is the response amplitude and N is the maximum friction force that can occur.

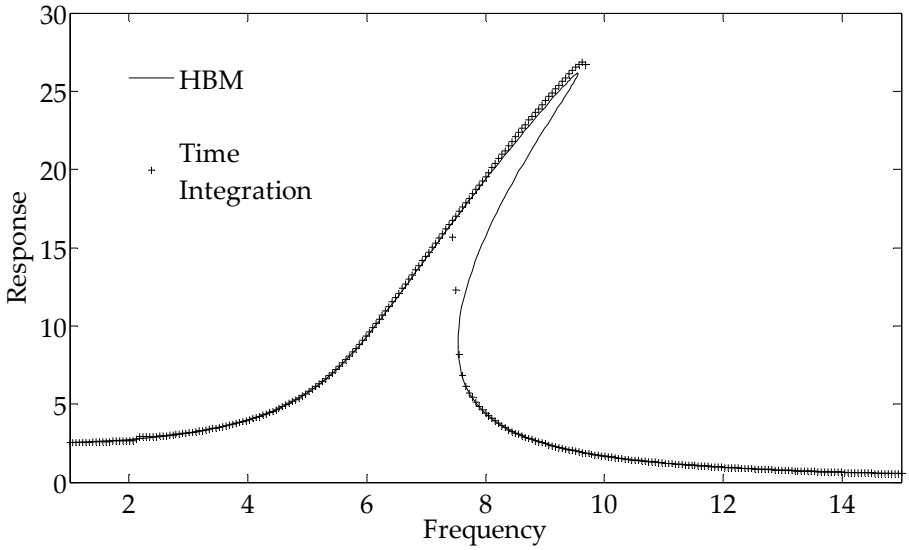

Figure 4.2 – Cubic stiffness: forced response

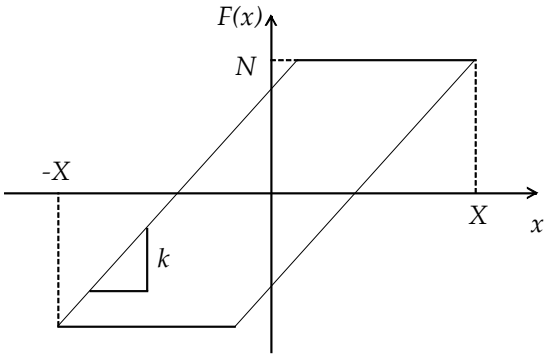

Figure 4.3 – Macroslip friction model

A displacement expression of the following form is considered:

$$x(\theta) = X\cos(\theta) \tag{4.71}$$

The angle which corresponds to the lower right corner of the force-displacement diagram can be determined as

$$\psi = \cos^{-1}\left(\frac{X - 2\delta}{X}\right) \tag{4.72}$$

where

$$\delta = \frac{N}{k} \tag{4.73}$$

Then the force expression, as a function of angle θ, can be written as

$$F(\theta) = \begin{cases} kX\cos(\theta) + N - kX & 0 \le \theta < \psi \\ -N & \psi \le \theta < \pi \\ kX\cos(\theta) - N + kX & \pi \le \theta < \pi + \psi \\ N & \pi + \psi \le \theta < 2\pi \end{cases} \tag{4.74}$$

As it was determined in reference [27], by introducing HBM expressions and using trigonometric relations, the real and imaginary parts of the equivalent stiffness can be determined as

$$\begin{aligned} k_r &= \frac{1}{\pi X}\int_0^{2\pi} F(\theta)\cos(\theta)\,d\theta = \frac{k}{\pi}\left(\psi - \frac{1}{2}\sin(2\psi)\right) \\ k_i &= \frac{-1}{\pi X}\int_0^{2\pi} F(\theta)\sin(\theta)\,d\theta = \frac{4N}{\pi X}\frac{X-\delta}{X} \end{aligned} \tag{4.75}$$

The displacement expression is rewritten with phase difference in complex variables as

$$\begin{aligned} x(t) &= X_c\cos(\theta) + X_s\sin(\theta) \\ &= \mathrm{Re}\left(\left(X_c - iX_s\right)e^{i\omega t}\right) \end{aligned} \tag{4.76}$$

Therefore the vibration amplitude will be

$$X = \sqrt{X_c^2 + X_s^2} \tag{4.77}$$

Then, the forcing induced by the macroslip element can be written as

$$\begin{aligned} F(t) &= F_c\cos(\theta) - F_s\sin(\theta) \\ &= \mathrm{Re}\left(\left(F_c - iF_s\right)e^{i\omega t}\right) \end{aligned} \tag{4.78}$$

where

$$\begin{aligned} F_c &= k_r X_c + k_i X_s \\ F_s &= k_r X_s - k_i X_c \end{aligned} \tag{4.79}$$

Recalling that k_r is a function of ψ and k_i is a function of A, the Jacobian of the nonlinear forcing vector $\begin{bmatrix} F_c & F_s \end{bmatrix}^T$ with respect to the response amplitudes vector $\begin{bmatrix} X_c & X_s \end{bmatrix}^T$ can be calculated as follows.

$$\frac{\partial F_c}{\partial X_c} = \frac{\partial k_r}{\partial \psi}\frac{\partial \psi}{\partial X}\frac{\partial X}{\partial X_c}X_c + k_r + \frac{\partial k_i}{\partial X}\frac{\partial X}{\partial X_c}X_s \tag{4.80}$$

$$\frac{\partial F_c}{\partial X_s} = \frac{\partial k_r}{\partial \psi}\frac{\partial \psi}{\partial X}\frac{\partial X}{\partial X_s}X_c + \frac{\partial k_i}{\partial X}\frac{\partial X}{\partial X_s}X_s + k_i \tag{4.81}$$

$$\frac{\partial F_s}{\partial X_c} = \frac{\partial k_r}{\partial \psi}\frac{\partial \psi}{\partial X}\frac{\partial X}{\partial X_c}X_s - \frac{\partial k_i}{\partial X}\frac{\partial X}{\partial X_c}X_c - k_i \tag{4.82}$$

$$\frac{\partial F_s}{\partial X_s} = \frac{\partial k_r}{\partial \psi}\frac{\partial \psi}{\partial X}\frac{\partial X}{\partial X_s}X_s + k_r - \frac{\partial k_i}{\partial X}\frac{\partial X}{\partial X_s}X_c \tag{4.83}$$

where

$$\frac{\partial k_r}{\partial \psi} = \frac{k}{\pi}\left(1-\cos(2\psi)\right) \tag{4.84}$$

$$\frac{\partial \psi}{\partial X} = -\sqrt{1-\left(1-\frac{2\delta}{X}\right)^2}\,\frac{2\delta}{X^2} \tag{4.85}$$

$$\frac{\partial k_i}{\partial X} = \frac{4N}{\pi X^2}\left(1-\frac{2(X-\delta)}{X}\right) \tag{4.86}$$

$$\frac{\partial X}{\partial X_c} = \frac{X_c}{X} \tag{4.87}$$

$$\frac{\partial X}{\partial X_s} = \frac{X_s}{X} \tag{4.88}$$

4.5.2.1 Verification via Time Domain Integration

For a single degree-of-freedom underdamped system which is grounded through a macroslip friction element, the forced response is calculated via Newton-Raphson method using the force vector and Jacobian expressions. The results are compared with time integration results in Figure 4.4. The

results show a very good match at all frequencies, except at frequencies around subharmonics. The HBM method cannot predict subharmonics since only the fundamental harmonic was used in the analysis.

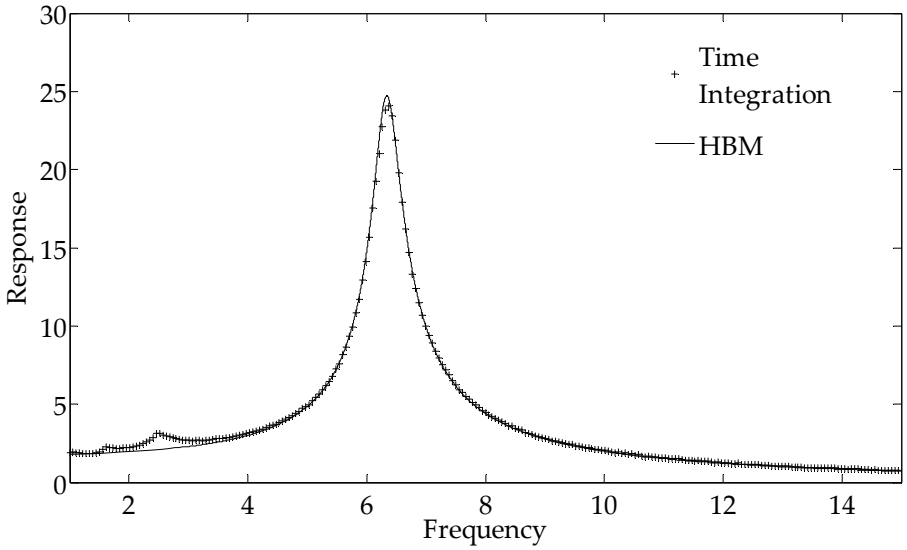

Figure 4.4 – Macroslip friction forced response

4.5.3 Two-slope Macroslip Friction Element

The two-slope macroslip friction element developed by Ciğeroğlu et al. [31], which approximates microslip friction element, can easily be formulated using the force vector and Jacobian expressions for the macroslip friction element. Using graphical construction [31], the two-slope model shown in Figure 4.5 can be expressed as a sum of a macroslip element and a linear spring as shown in Figure 4.6.

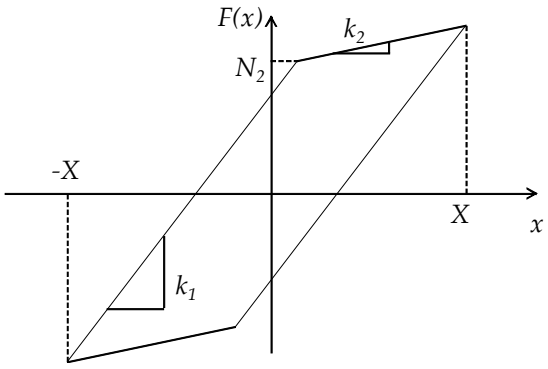

Figure 4.5 – Two-slope microslip friction element

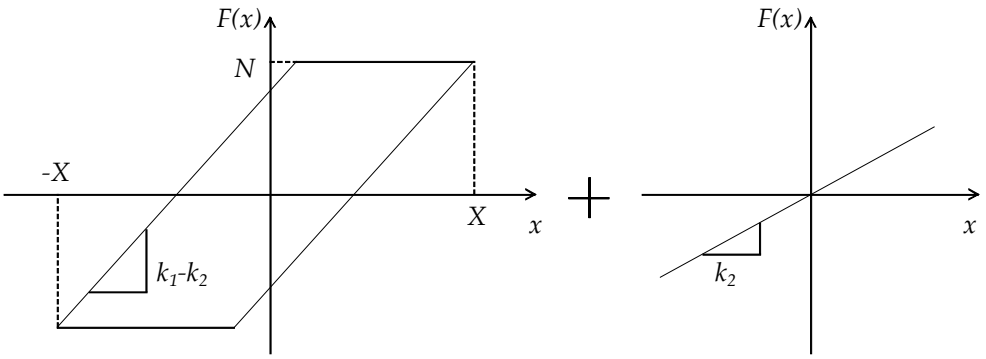

Figure 4.6 – Graphical construction of two-slope microslip friction element

Here, N should be equated to $N_2 - k_2(2\delta - X)$ where δ is defined in equation (4.73). Then the force vector and its Jacobian expressions for the two-slope microslip friction element becomes

$$\{F_{two-slope}\} = \{F_{macro}\} + k_2\{X\} \tag{4.89}$$

$$\frac{\partial\{F_{two-slope}\}}{\partial\{X\}} = \frac{\partial\{F_{macro}\}}{\partial\{X\}} + \begin{bmatrix} k_2 & 0 \\ 0 & k_2 \end{bmatrix} \tag{4.90}$$

where $\{F_{two-slope}\}$ and $\{F_{macro}\}$ are the forcing vectors of two-slope macroslip and macroslip friction elements, $\frac{\partial\{F_{two-slope}\}}{\partial\{X\}}$ and $\frac{\partial\{F_{macro}\}}{\partial\{X\}}$ are their Jacobian matrices, respectively.

Verification to two-slope macroslip model is not given since macroslip element is already justified via time integration results.

4.5.4 Gap/Interference Element

The gaps between mating surfaces can be modeled by using a spring whose one end is attached to one degree-of-freedom and the other end is g amount of far from the ground at equilibrium. In contrast, for interference fits, at equilibrium conditions one end of the spring is in contact with the ground and it is prestretched by an amount of g. It should be noted that the element can loose contact with the ground during motion. A gap element is illustrated in Figure 4.7 where k is the normal stiffness between mating surfaces.

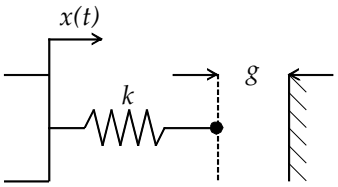

Figure 4.7 – Gap element

The force-displacement relationship for a gap element can be written as follows.

$$F(x) = \begin{cases} k(x-g) & x > g \\ 0 & otherwise \end{cases} \tag{4.91}$$

Here, it should be noted that the interference nonlinearity case can be analyzed by setting negative gap values in a gap element. Therefore the following formulations will be made for a gap element only.

The spring gets in contact with the ground when the displacement is higher than the gap value; otherwise the spring is separated from the ground meaning that no force is exerted by the spring. Once the contact and separation instants are known the linearization can be made by HBM. Here, a multiharmonic solution is given. The fundamental harmonic solution can be determined by setting the number of harmonics to one. It should be noted that the contact periods can be calculated analytically if the fundamental harmonic is retained.

Assuming a multiharmonic response of the form

$$x(\theta) = X_0 + \sum_{m=1}^{n} X_{m,c}\cos(m\theta) + X_{m,s}\sin(m\theta) \tag{4.92}$$

and substituting it into the MHBM integrals by using equation (4.91), the Fourier components of the forcing can be determined as:

$$F_0 = \sum_{k=1}^{n_{contact}} \frac{1}{2\pi} \int_{\theta_c^k}^{\theta_s^k} k\left(x(\theta) - g\right) d\theta \tag{4.93}$$

$$F_{m,c} = \sum_{k=1}^{n_{contact}} \frac{1}{\pi} \int_{\theta_c^k}^{\theta_s^k} k\left(x(\theta) - g\right)\cos(m\theta)\, d\theta \tag{4.94}$$

$$F_{m,s} = \sum_{k=1}^{n_{contact}} \frac{1}{\pi} \int_{\theta_c^k}^{\theta_s^k} k\left(x(\theta) - g\right)\sin(m\theta)\, d\theta \tag{4.95}$$

where $n_{contact}$ is the number of contact periods, θ_c^k and θ_s^k are the contact and separation angles of k_{th} period respectively. Substituting equation (4.92) into the MHBM equations and arranging terms into a matrix form will yield

$$\begin{aligned} \{F\} &= \begin{bmatrix} F_0 & F_{1,c} & F_{1,s} & F_{2,c} & F_{2,s} & \cdots \end{bmatrix}^T \\ &= k\left(\sum_{k=1}^{n_{contact}} \frac{1}{\pi} \int_{\theta_c^k}^{\theta_s^k} \left\{f_t(\theta)\right\}\left\{f_e(\theta)\right\}^T d\theta \right)\{X\} - kg\left(\sum_{k=1}^{n_{contact}} \frac{1}{\pi} \int_{\theta_c^k}^{\theta_s^k} \left\{f_e(\theta)\right\} d\theta \right) \end{aligned} \tag{4.96}$$

where $\{X\}$ is vector of response amplitudes, $\{f_e(\theta)\}$ is the vector of Fourier expansion functions, $\{f_t(\theta)\}$ is the vector of Fourier transformation functions and they are defined as follows.

$$\{X\} = \begin{bmatrix} X_0 & X_{1,c} & X_{1,s} & X_{2,c} & X_{2,s} & \cdots \end{bmatrix}^T \tag{4.97}$$

$$\{f_e(\theta)\} = \begin{bmatrix} 1 & \cos(\theta) & \sin(\theta) & \cos(2\theta) & \sin(2\theta) & \ldots \end{bmatrix}^T \tag{4.98}$$

$$\{f_t(\theta)\} = \begin{bmatrix} 1/2 & \cos(\theta) & \sin(\theta) & \cos(2\theta) & \sin(2\theta) & \ldots \end{bmatrix}^T \tag{4.99}$$

Taking derivative of equation (4.96) with respect to $\{X\}$ will yield the Jacobian matrix as:

$$\frac{\partial\{F\}}{\partial\{X\}} = k\left(\sum_{k=1}^{n_{contact}} \frac{1}{\pi} \int_{\theta_c^k}^{\theta_s^k} \{f_t(\theta)\}\{f_e(\theta)\}^T \, d\theta \right) \tag{4.100}$$

The integral terms can be determined analytically. For

$$[M(\theta)] = \int \{f_t(\theta)\}\{f_e(\theta)\}^T \, d\theta \tag{4.101}$$

the elements of the matrix are determined by the following formulae.

$$M_{1,1} = \theta/2 \tag{4.102}$$

$$\begin{aligned} M_{1,2i} &= \frac{1}{2i}\sin(i\theta) \\ M_{1,2i+1} &= -\frac{1}{2i}\cos(i\theta) \\ M_{2i,1} &= \frac{1}{i}\sin(i\theta) \\ M_{2i+1,1} &= -\frac{1}{i}\cos(i\theta) \end{aligned} \qquad i = 1, 2, \ldots, m \tag{4.103}$$

$$
\begin{aligned}
M_{2i,2i} &= \frac{t}{2} + \frac{1}{4i}\sin(2i\theta) \\
M_{2i,2i+1} &= -\frac{1}{4i}\left(1+\cos(2i\theta)\right) \\
M_{2i+1,2i} &= -\frac{1}{4i}\left(1+\cos(2i\theta)\right) \\
M_{2i+1,2i+1} &= \frac{t}{2} - \frac{1}{4i}\sin(2i\theta)
\end{aligned}
\qquad i = 1,2,\ldots,m \tag{4.104}
$$

$$
\begin{aligned}
M_{2i,2j} &= \frac{1}{2(i-j)}\sin\left((i-j)\theta\right) + \frac{1}{2(i+j)}\sin\left((i+j)\theta\right) \\
M_{2i,2j+1} &= \frac{1}{2(i-j)}\cos\left((i-j)\theta\right) - \frac{1}{2(i+j)}\cos\left((i+j)\theta\right) \\
M_{2i+1,2j} &= -\frac{1}{2(i-j)}\cos\left((i-j)\theta\right) + \frac{1}{2(i+j)}\cos\left((i+j)\theta\right) \\
M_{2i+1,2j+1} &= \frac{1}{2(i-j)}\sin\left((i-j)\theta\right) - \frac{1}{2(i+j)}\sin\left((i+j)\theta\right)
\end{aligned}
\qquad \begin{aligned} &i = 1,2,\ldots,m \\ &j = 1,2,\ldots,m \\ &i \neq j \end{aligned} \tag{4.105}
$$

For

$$
\left\{P(\theta)\right\} = \int \left\{f_t(\theta)\right\} d\theta \tag{4.106}
$$

the elements of the vector are determined by the following formulae.

$$
P_{1,1} = \theta / 2 \tag{4.107}
$$

$$
\begin{aligned}
P_{2i} &= \frac{1}{i}\sin(i\theta) \\
P_{2i+1} &= -\frac{1}{i}\cos(i\theta)
\end{aligned}
\qquad i = 1,2,\ldots,m \tag{4.108}
$$

4.5.4.1 Verification via Time Domain Integration

For a multi-degree-of-freedom underdamped system which is grounded through a gap element, the forced response is calculated via HBM using the force vector and Jacobian expressions. The results are compared with time integration results in Figure 4.8. As expected from gap element,

displacements over the gap value increased the amount of time that the spring is in contact with the ground. This introduces more stiffness to the system causing the response curve shift to higher frequencies. In addition, it is obvious that the fundamental harmonic cannot represent the motion accurately. With higher numbers of harmonics, the HBM solution converges to the actual solution.

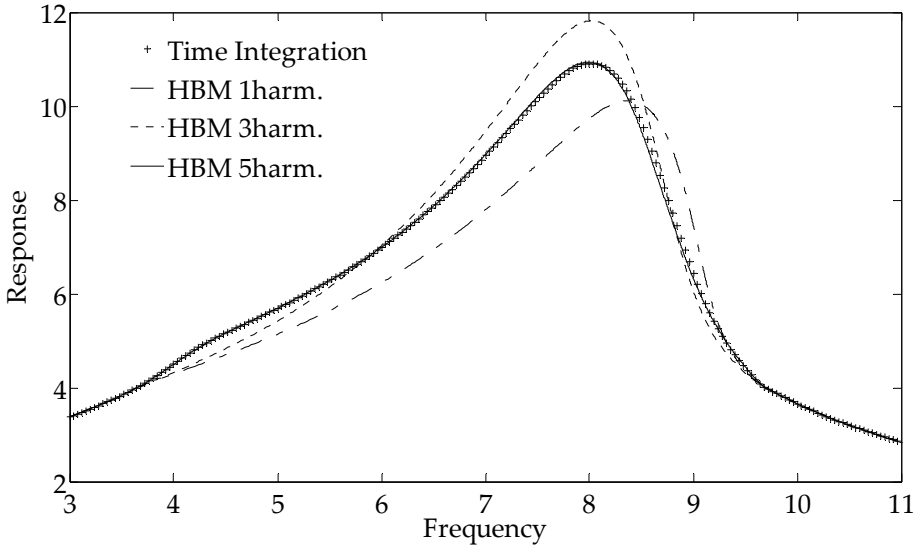

Figure 4.8 – Gap element forced response

CHAPTER 5

CASE STUDIES

In this chapter, the capabilities of the method proposed in this thesis will be demonstrated by several case studies. To begin with, geometry of a sample bladed disk assembly, which is modeled to resemble a realistic rotor of industrial turbomachinery, is introduced. Next, two different reduced order models, namely the component mode synthesis method and subset of nominal modes method, will be utilized to calculate natural frequencies and mode shapes of the bladed disk assembly with different amounts of mistuning. The effect of number of modes retained on the accuracy of the methods will be discussed and the methods will be compared with each other. Subsequently, using the modal data determined by component mode synthesis method, the linear forced response of the bladed disk assembly will be calculated for different mistuned cases as well as the tuned case. Afterwards, again by using the modal data determined by component mode synthesis method, the nonlinear forced response of both tuned and mistuned assemblies will be calculated under different types of nonlinearity, namely the macroslip friction and gap/interference nonlinearity. Finally, the effect of both mistuning and nonlinearity on resonant response amplitudes will be demonstrated by using modal assurance criterion (MAC) calculations for both types of nonlinearity.

5.1 36 Bladed Compressor Model

The implementation of the method discussed in previous chapters will be demonstrated on a compressor rotor. The rotor has 36 blades and a nominal drum diameter of 310mm. The blades are of mid-shroud type and they are modeled with a twist angle to demonstrate a realistic compressor rotor. The geometry of the compressor rotor is given in Figure 5.1 and the material is selected as titanium-nickel alloy and its properties are given in

Table 5.1 – Material properties

Density	8400 kg/m^3
Modulus of Elasticity	270 GPa
Poisson's Ratio	0.3

The modal analysis of the tuned assembly is made by cyclic symmetry analysis using a single sector of the assembly. The finite element model of the sector has 1190 number of 4-noded tetrahedral elements with 415 nodes. In the analysis, the boundary conditions are set such that the sector is clamped at the inner radius and the shroud faces of each blade, which can be seen in Figure 5.2, are free.

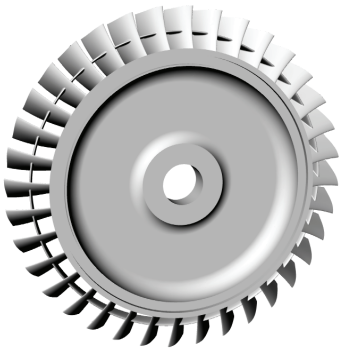

Figure 5.1 – Compressor with mid-shroud blades

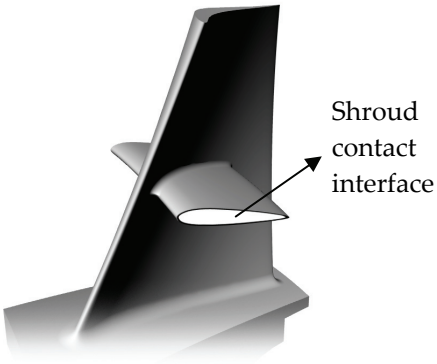

Figure 5.2 – Mid-shrouded blade

In nonlinear forced response analysis, nonlinear elements will be connected between the degrees-of-freedom of neighboring shroud interfaces. The geometry of the sector is shown in Figure 5.3. The natural frequencies of the tuned assembly are plotted with respect to the number of nodal diameters in Figure 5.4.

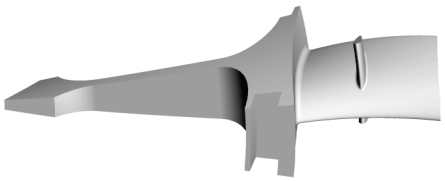

Figure 5.3 – Sector geometry

In Figure 5.4, each data series represents the natural frequencies of a mode family. As the number of nodal diameters increase, the natural frequency of a mode family seems to converge to a value. This results in clusters of close natural frequencies. It should also be noted that, at some regions of the plot, each family of mode seem to veer at some nodal diameters. These regions are called "veering regions". Considering the first family of modes, a

veering region exists for 3 nodal diameters. All the analyses in the upcoming sections will be focused on that veering region. Therefore, a 3EO forcing will be applied at the tip of each blade in order to excite 3 nodal diameter modes, and the tip response will be calculated for each blade in the assembly.

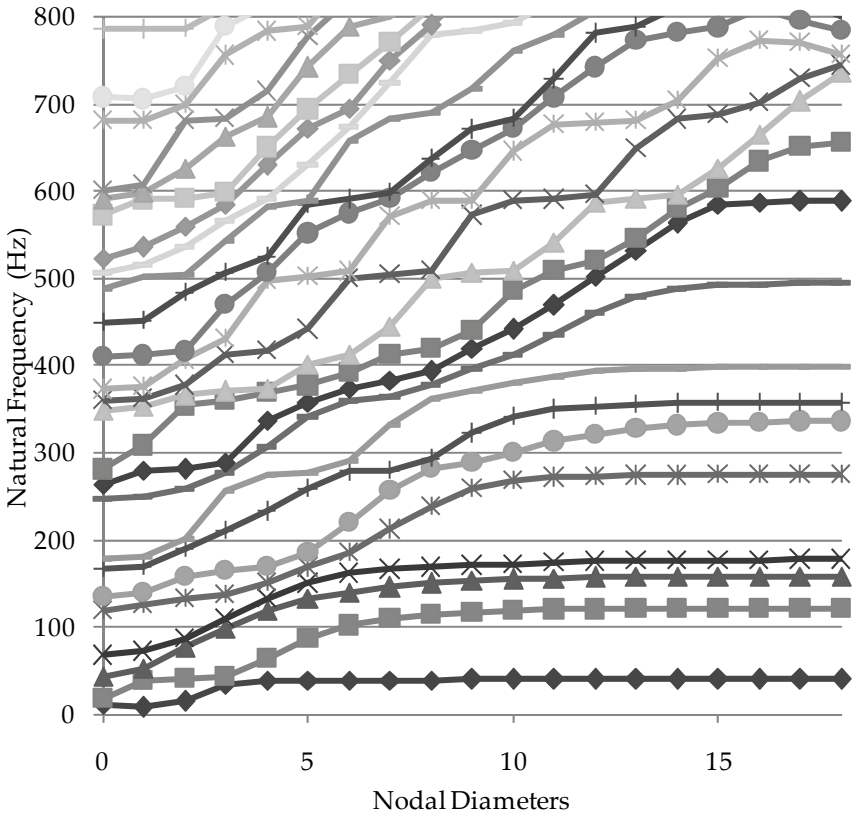

Figure 5.4 – Natural frequencies vs. nodal diameters

For all the response calculations a code, which has been developed in MATLAB®, is used. Finite element work has been carried out in ANSYS®. The MATLAB® source codes and ANSYS® macros are given in the Appendix.

5.2 Modal Analysis of the Mistuned Bladed Disk Assembly

In this section, the modal analysis of the mistuned assembly will be carried out. Two different reduced order models, namely the Component Mode Synthesis Method (CMSM) and the Subset of Nominal Modes Method (SNMM), will be utilized and the results will be discussed in terms of accuracy and computational efficiency. Since in both methods the system matrices are taken from the same FE model, FE results will be used as reference in relative error calculations.

5.2.1 Component Mode Synthesis Method

Using the CMSM formulation for mistuned bladed disk assemblies, the natural frequencies of the tuned assembly will be calculated. To see the effect of number of modes retained per substructures, different number of blade and disk modes will be included in the model. Then, the natural frequencies of the reduced order model will be compared with those obtained from directly from the model itself. Direct FE approach involves cyclic symmetry analysis.

The blade component has 199 nodes and 597 degrees-of-freedom. The blade is connected to the disk through 17 nodes and 51 degrees-of-freedom. The disk component possesses 233 nodes and 699 degrees-of-freedom. 6 nodes which lie on the inner rim of the disk are fixed.

First, to study the effect of number of modes retained for the blades, three different cases, in which 5, 10 and 20 modes are kept for each blade, will be

analyzed. For the disk, 10 modes are kept for each nodal diameter. For the case in which 5 modes are kept for each blade, since in the modal analysis of the disk is made for 19 number of nodal diameters and the assembly has 36 blades, the resulting reduced order model has 2206 degrees-of-freedom whereas the whole FE model has 39852 degrees-of-freedom. The first 200 natural frequencies obtained from the reduced order model are compared with the direct FE analysis results in Figure 5.5. For the cases in which 10 and 20 modes are kept for the blade, the reduced order models have 2386 and 2746 degrees-of-freedom, respectively. For these cases, the same comparison is shown in Figure 5.6 and Figure 5.6, respectively. From the study of these figures, it can be seen that the percentage error is higher at the veering regions. Another thing to be noticed is that, the accuracy of the method does not improve continuously with increasing number of blade modes.

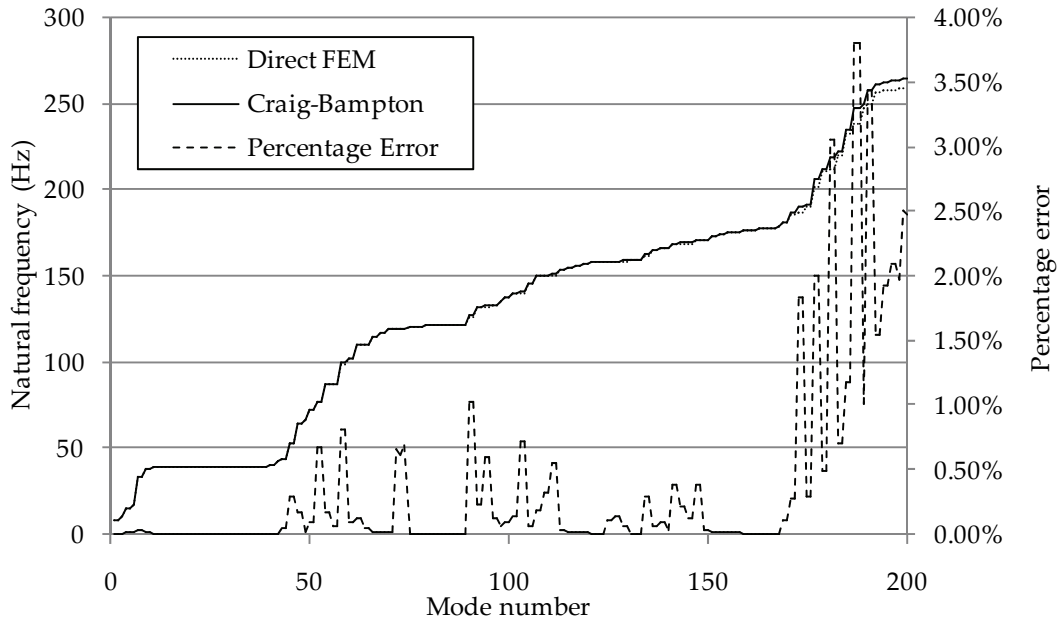

Figure 5.5 - Natural frequency comparison: 5 modes per blade, 10 modes per nodal diameter

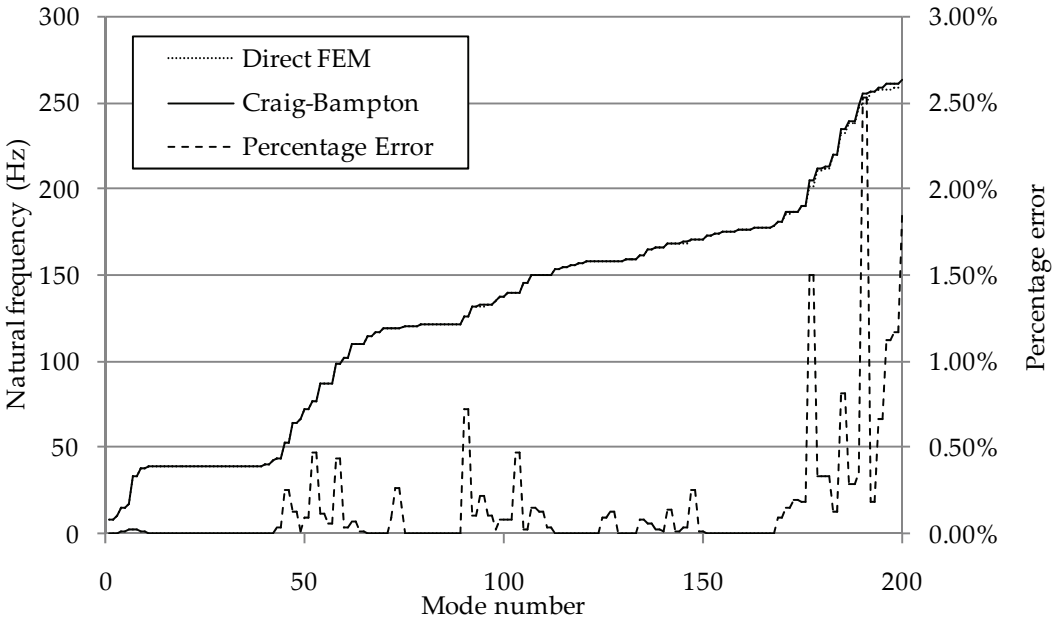

Figure 5.6 – Natural frequency comparison: 10 modes per blade, 10 modes per nodal diameter

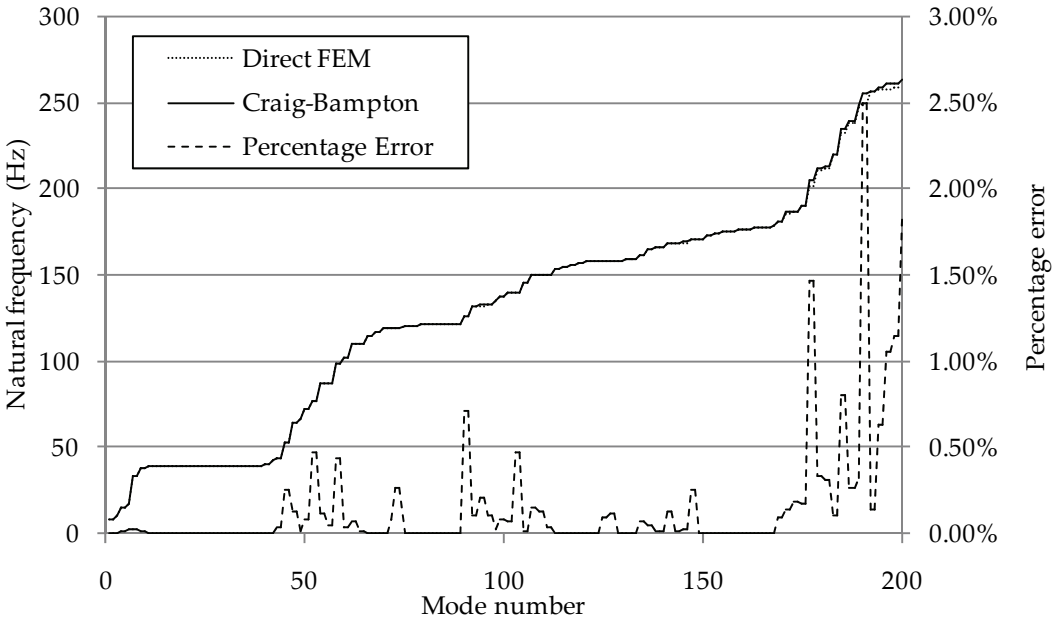

Figure 5.7 – Natural frequency comparison: 20 modes per blade, 10 modes per nodal diameter

Second, to study the effect of number of modes retained for the disk, three different cases, in which 10, 20 and 30 modes are kept for each nodal diameter, will be analyzed. For the blades, 5 modes are kept for each sector. For the case in which 5 modes are kept for each nodal diameter, the first 200 natural frequencies obtained from the reduced order model are already given in Figure 5.5. For the cases in which 20 and 30 modes are kept for each nodal diameter, the reduced order models have 2576 and 2766 degrees-of-freedom, respectively. For these cases, the same comparison is shown in Figure 5.8 and Figure 5.9, respectively. From the study of these figures, it can be seen that, the accuracy of the method does not improve continuously with increasing number of modes retained for the disk.

Lastly, 10 modes for each blade and 20 modes for each nodal diameter of the disk are kept. The resulting reduced order model has 2576 degrees-of-freedom. The first 200 natural frequencies obtained from the reduced order model are again compared with the direct FE analysis results in Figure 5.10. It can be seen that increasing both blade modes and disk modes improved the accuracy of the reduced order model.

From the case studies presented in this section, it can be concluded that the accuracy of CMSM depends on the number of modes retained for blades and for the disk, since the entire interface degrees-of-freedom are inevitably kept in the model and the number of them cannot be reduced. It is seen that CMSM lacks accuracy at veering regions. For better accuracy, it is suggested that the number of modes for both blades and the disk should be increased.

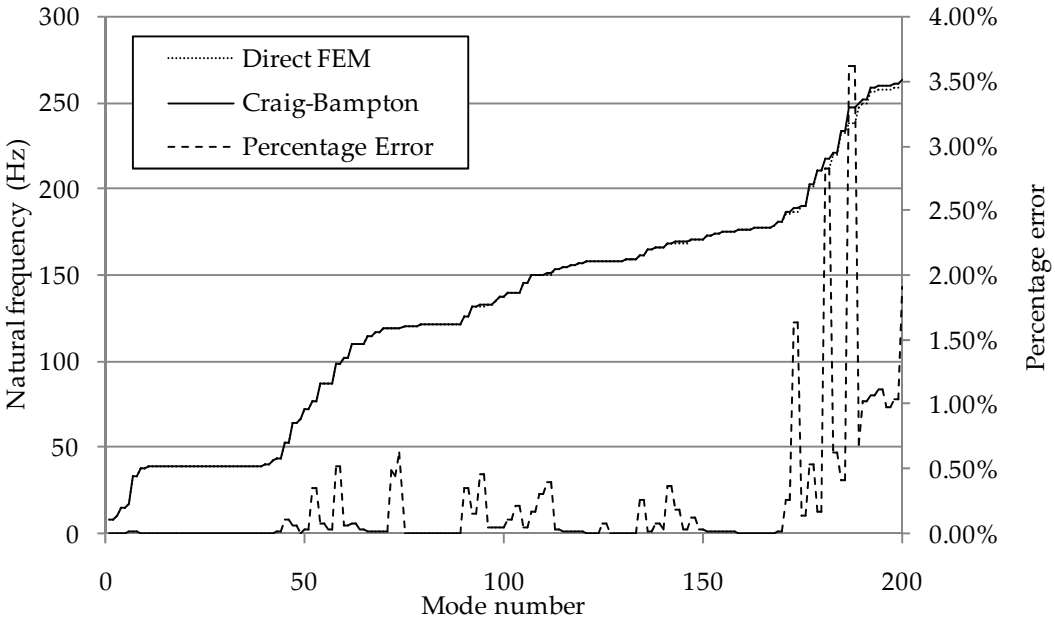

Figure 5.8 - Natural frequency comparison: 5 modes per blade, 20 modes per nodal diameter

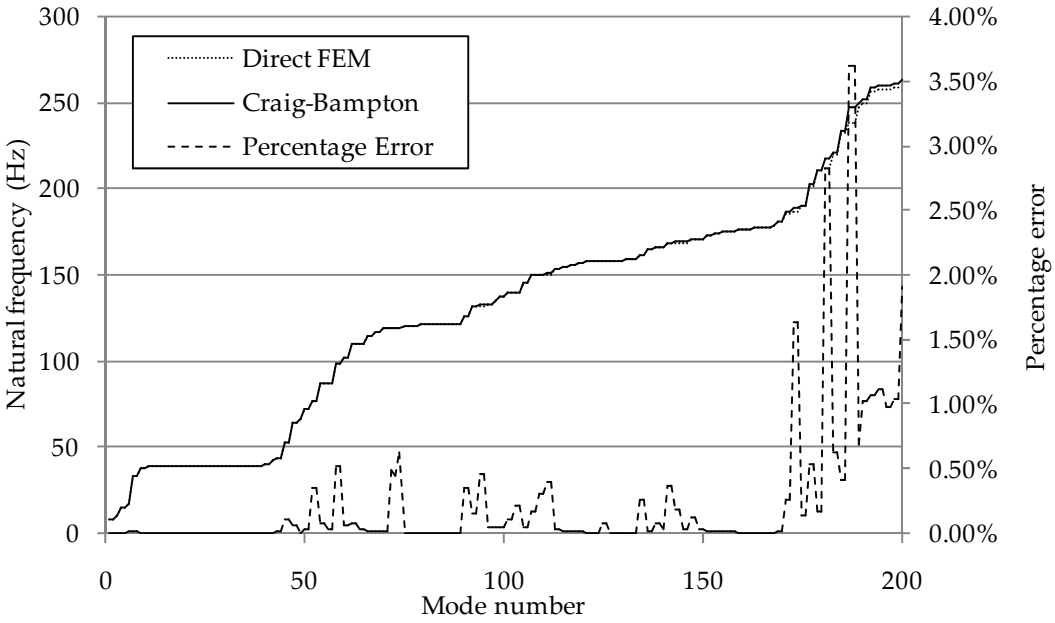

Figure 5.9 - Natural frequency comparison: 5 modes per blade, 30 modes per nodal diameter

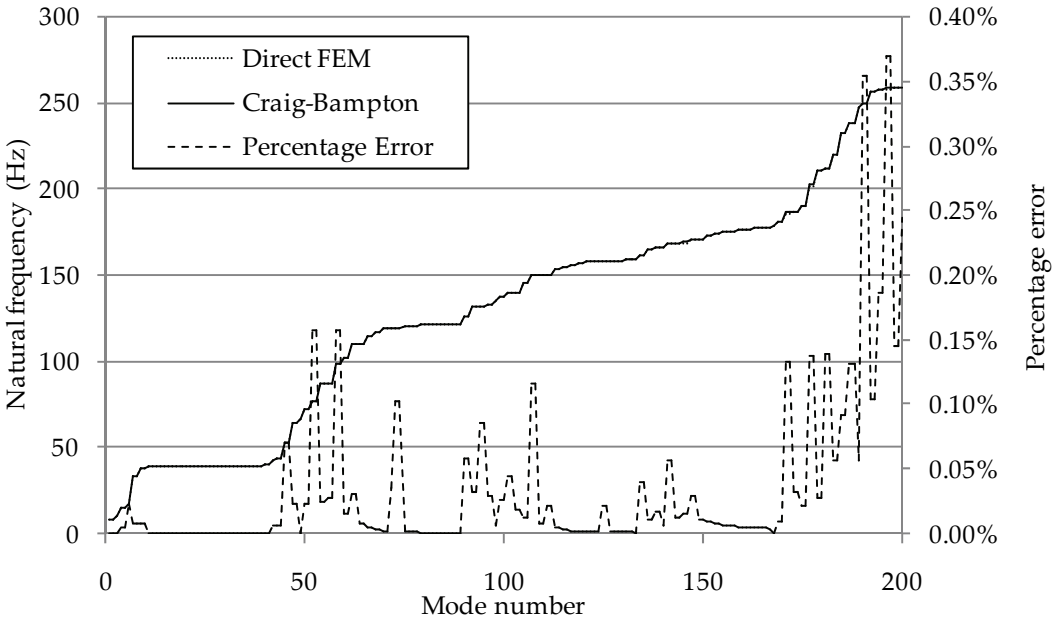

Figure 5.10 – Natural frequency comparison: 10 modes per blade, 20 modes per nodal diameter

5.2.2 Subset of Nominal Modes Method

In this section, the efficiency and accuracy of SNMM will be studied. Natural frequencies of a mistuned bladed disk assembly will be calculated via SNMM and the results will be compared with CMSM and direct FE method results. For different amounts of mistuning the modal analysis will be made using three methods.

In Figure 5.11 and Figure 5.12, natural frequency results of three methods are given with the relative percentage error calculated with respect the direct FE method results considering ±1% and ±5% mistuning, respectively. CMSM and SNMM reduced order models have 2576 and 950 degrees-of-freedom respectively whereas the FE model of the whole assembly has

39852 degrees-of-freedom. For direct FE solution, the modulus of elasticity of each blade in the assembly is mistuned.

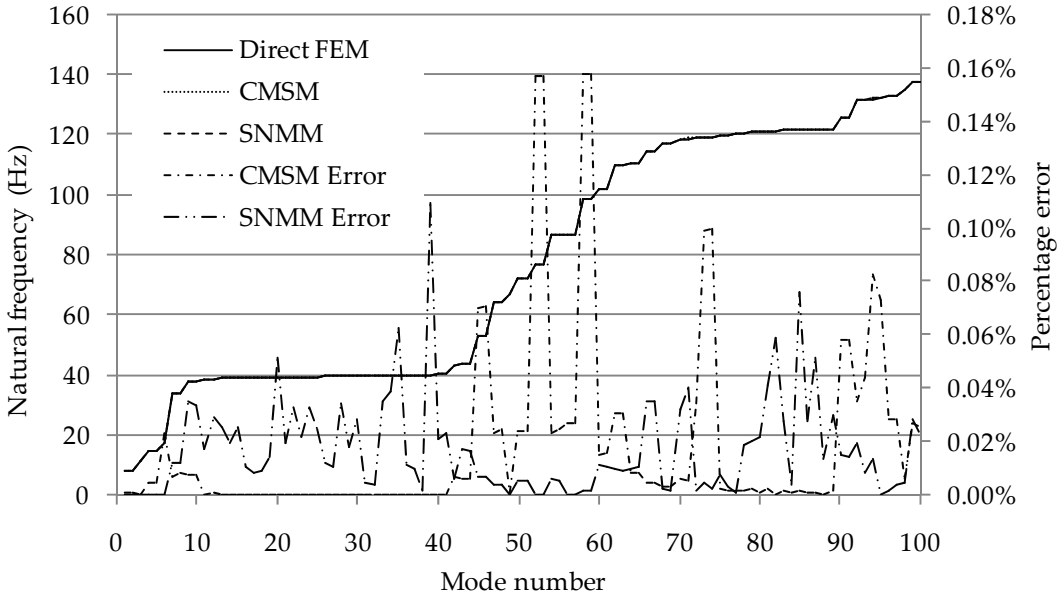

Figure 5.11 – Method comparison for ±1% mistuning

It should be noted that, both two reduced order models yield results with comparable accuracy. The relative error for both methods is within a range of ±0.2% therefore the results for both three methods are coincident in the figure. To study the effect of modes retained in SNMM model, the number of modes kept per nodal diameter is reduced to 6 and 10, and the results are given in Figure 5.13 and Figure 5.14, respectively. The SNMM results are also compared with CMSM and direct FE method results.

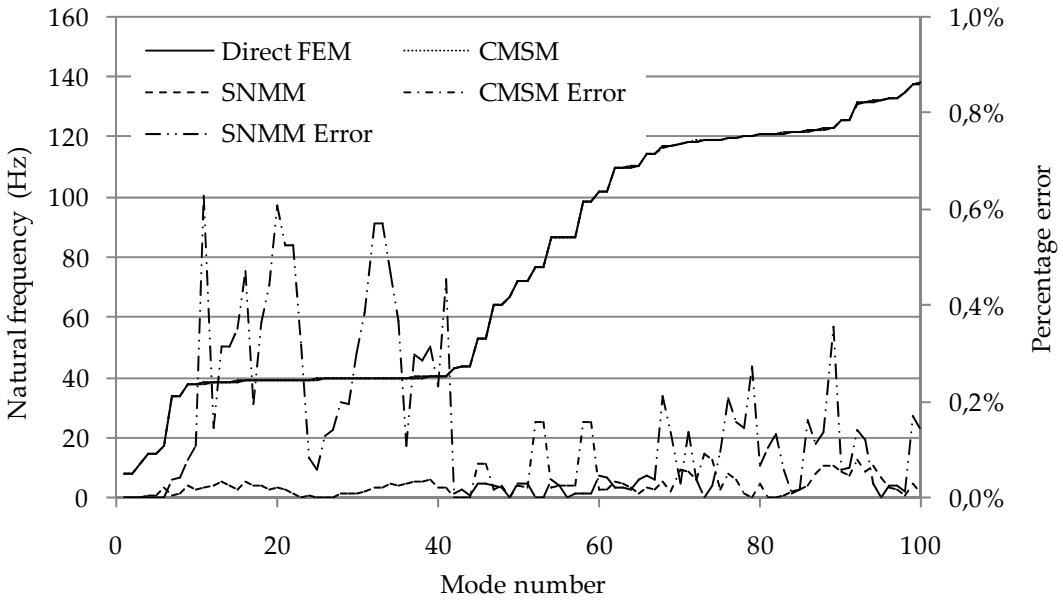

Figure 5.12 – Method comparison for ±5% mistuning

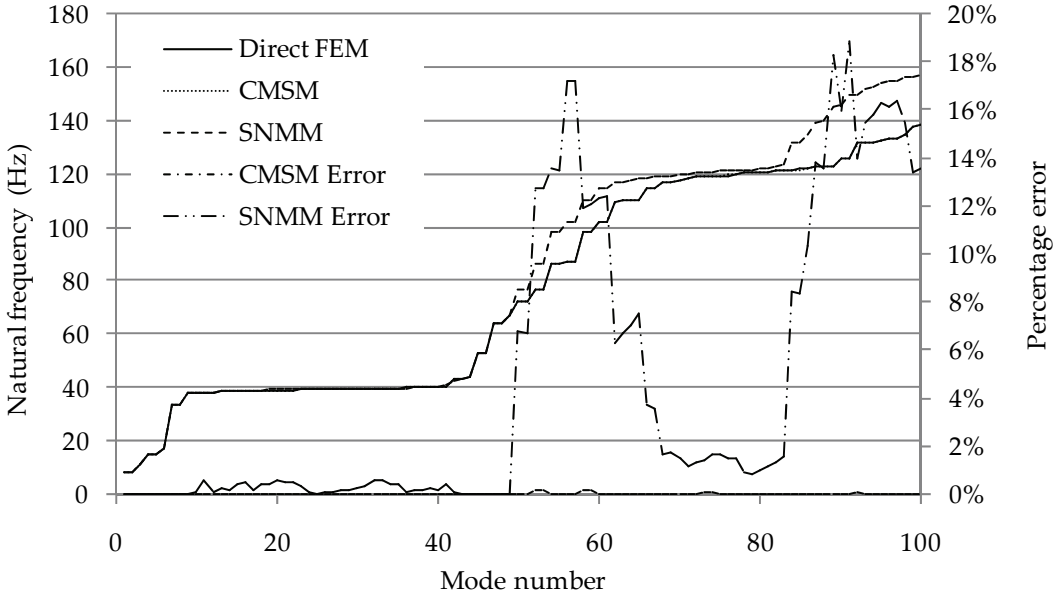

Figure 5.13 – Method comparison for ±5% mistuning – SNMM with 6 modes per ND

From the results of this section it can be concluded that, for low amounts of mistuning, the SNMM method yields more accurate results with less

degrees-of-freedom, but for higher amount of mistuning, the error for SNMM increases. It is also shown that increasing the number of modes retained per nodal diameter in SNMM improves accuracy of the results up to a certain limit. The relative error at this limiting case is higher than the relative error that will be obtained via CMSM. In a numerical point of view, this may be the consequence of analyzing the whole mistuned bladed disk assembly with direct FE method without exploiting cyclic symmetric properties, whereas in SNMM the modes used are determined by cyclic symmetric modal analysis.

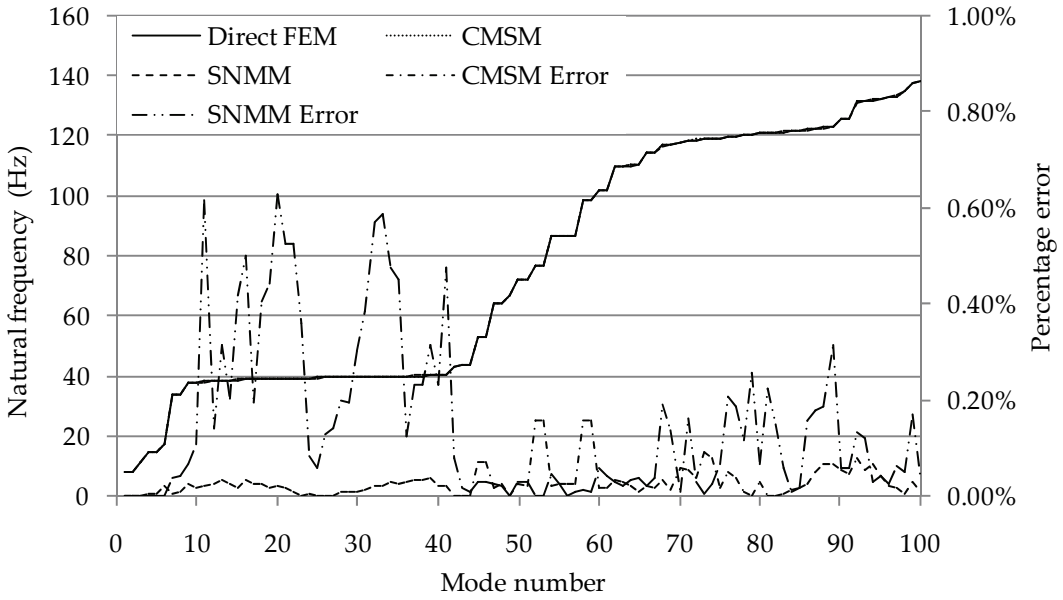

Figure 5.14 – Method comparison for ±5% mistuning – SNMM with 10 modes per ND

5.3 Linear Response

The linear mistuned response of the sample bladed disk assembly will be calculated with different amount of mistuning, which is applied at each

blade with a random value in a range. The results will be compared with the tuned responses and comments will be made on amplification factors.

The assembly is excited at the top side of each blade with an equivalent force of 1 N in axial direction. Excitation in axial direction is chosen since in the following section macroslip elements will be placed at shroud contact interfaces whose motion is desired to be kept in axial direction. In Figure 5.15, the axial component of the response amplitudes of tips for all blades are given as a function of frequency for the tuned assembly. As expected, for the tuned assembly, the blades share the same response amplitudes for all frequencies. Furthermore, by checking the resonant frequencies it is concluded that only the 3 nodal diameter modes are excited.

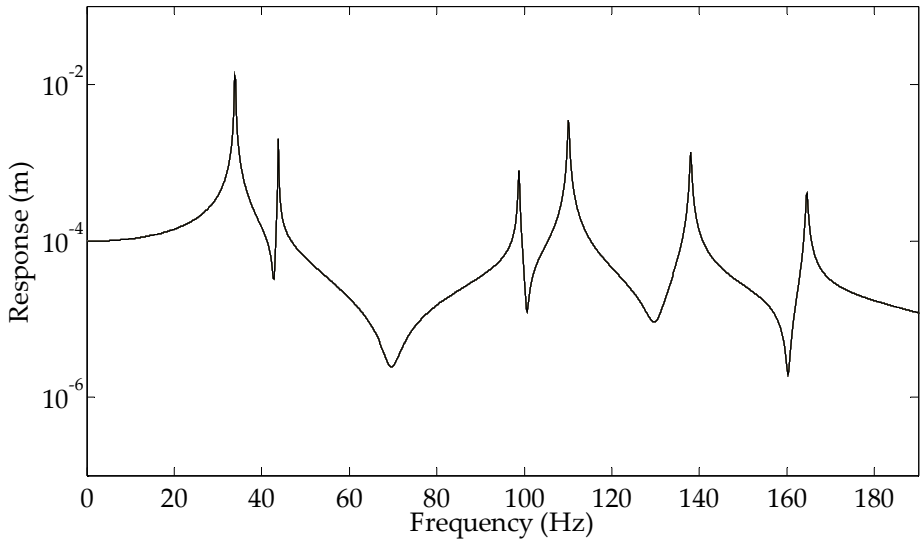

Figure 5.15 – Tuned linear response of blade tips for all sectors

Then the eigenvalues of the blade modes are mistuned within a range of ±1%, and a similar analysis is carried out. In Figure 5.16, the response of the tip in axial direction is given as a function of frequency. In contrast to the

response of the tuned assembly, new resonances appeared. It can be concluded that the 3EO excitation can now excite all the modes instead of exciting 3 nodal diameter modes only. This is consistent with the logic discussed in section 2.3.

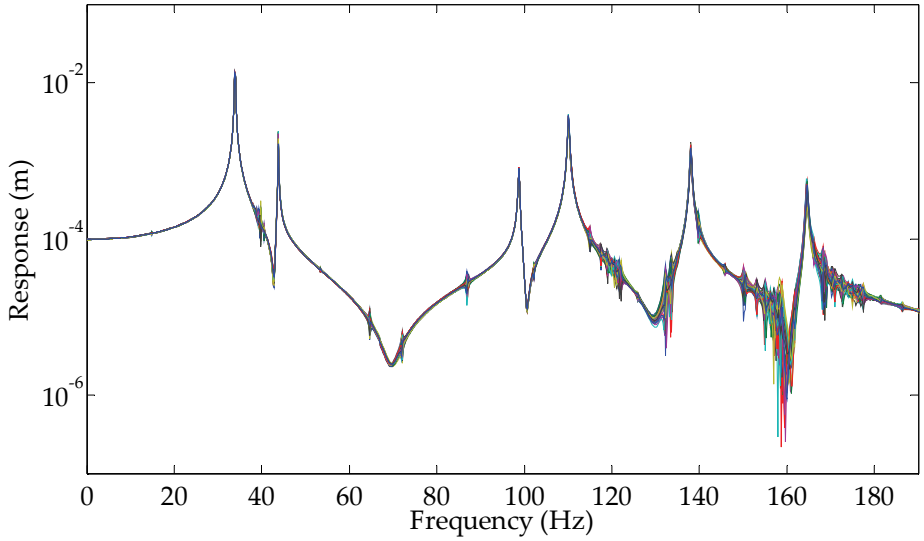

Figure 5.16 – ±1% mistuned, linear response of blade tips for all sectors

When the eigenvalues of the blade modes are given mistuning within a range of ±2% and ±5%, the response of the tip in axial direction is obtained as shown in Figure 5.17 and Figure 5.18, respectively. The natural frequencies of the double modes are split more and the amplitudes of the new resonances are increased. When the response amplitudes are studied, it is noticed that the blades in the mistuned assembly do not reach the resonant amplitudes at the same frequency. This is illustrated by zooming at the first peak in Figure 5.18 and the zoomed view is given in Figure 5.19. Knowing that, the amplitude of the most responding blade at its resonant frequency is used to calculate the maximum amplification factor. Table 5.2 compares the tuned and mistuned responses.

Table 5.2 – Maximum amplification factors at the resonant frequency

Mistuning (%)	Maximum tip amplitude (m)	Maximum amplification factor
0	0.03049	1.000
±1	0.03381	1.109
±2	0.03636	1.192
±5	0.03861	1.266

Although it seems that amount of mistuning is correlated to the maximum amplification factor, some studies in the literature have shown that the maximum amplification factor has the largest value for a specific set of mistuning, not for the largest mistuning.

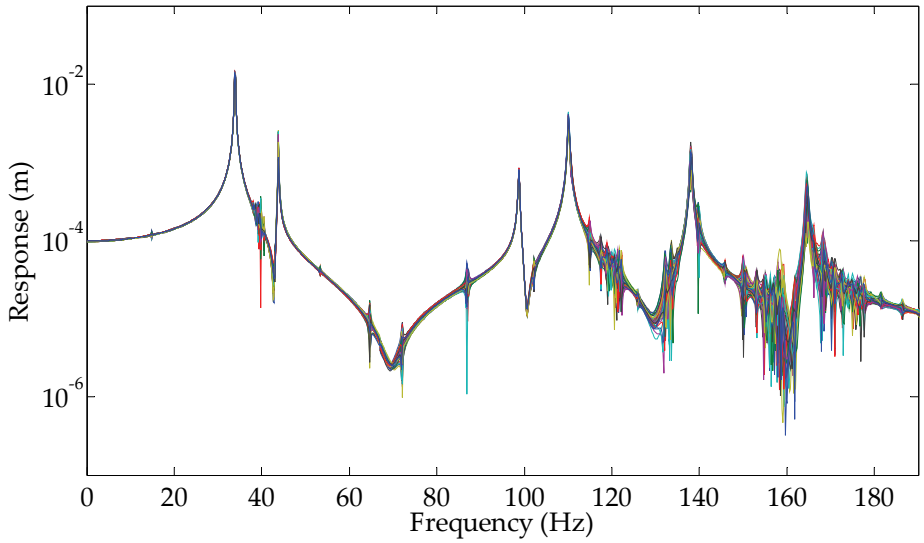

Figure 5.17 – ±2% mistuned, linear response of blade tips for all sectors

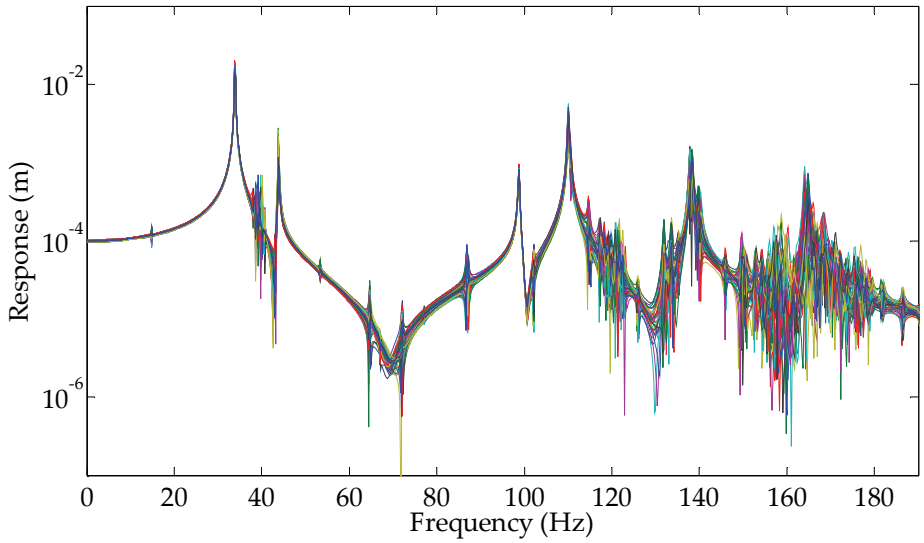

Figure 5.18 – ±5% mistuned, linear response of blade tips for all sectors

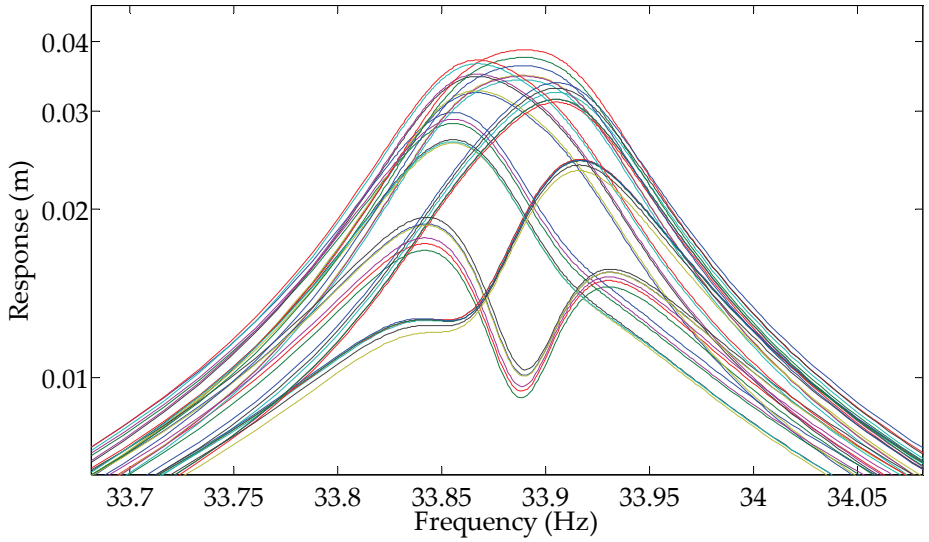

Figure 5.19 – ±5% mistuned, linear response of blade tips for all sectors (close-up)

5.4 Nonlinear Response

In this section, the assembly with macroslip friction or gap elements located between shroud contact interfaces will be analyzed using the modal domain method presented in this study. The contact interfaces consist of 6 nodes. In the analysis, first 30 modes are included. The number of modes is decided by trial error. It is selected as the smallest number of modes after which the response will not be affected significantly. The main interest is focused on the first resonant frequency encountered in tuned assembly. In the analysis, only the fundamental harmonic is considered. Instead of solving for 108 physical degrees-of-freedom, the solution for 30 modal coordinates will be calculated.

5.4.1 Macroslip Friction Nonlinearity

The macroslip elements are placed between shroud contact interfaces. The elements are assumed to be under constant normal load. Therefore any relative motion between the contact interfaces in normal direction is neglected. The relative motion between contact interfaces is assumed to be in only x-direction. Therefore, the macroslip elements are connected to the degrees-of-freedom along axial direction only.

The macroslip elements have a constant normal load of 10 N. The kinetic friction coefficient is selected to be 0.3 and the nominal macroslip friction stiffness values of the elements are taken as 10 kN/m.

In Figure 5.20, tip response of each blade in the assembly is plotted against frequency for the tuned nonlinear case. As expected, in a perfectly tuned nonlinear system, the analysis will yield the same amplitude at all the blades. Furthermore, the resonance amplitudes of the blades are reduced compared with the tuned linear response, due to friction dampers.

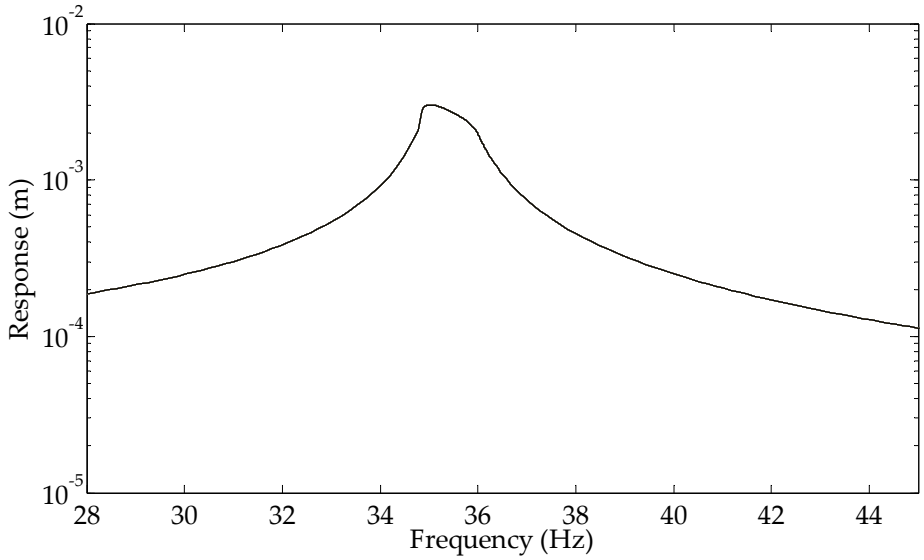

Figure 5.20 – Tuned, nonlinear response of blade tips for all sectors

In Figure 5.21, tip response of each blade in the assembly is plotted against excitation frequency for the mistuned nonlinear case. The mistuning is applied within a range of ±5%. As expected, new resonances have observed in the mistuned response. Mistuning also altered the resonance amplitudes but they are still lower than those of the linear response.

Variations in contact parameters from sector to sector may also introduce a kind of mistuning effect. In Figure 5.22 and Figure 5.23, the effect of contact parameter variations are demonstrated. In the analysis, the blades are perfectly tuned whereas the contact parameters, normal load and friction

stiffness for a macroslip friction element, are varied within a range of 50%. These figures show the tip response of all blades, with normal load deviations and friction stiffness deviations, respectively.

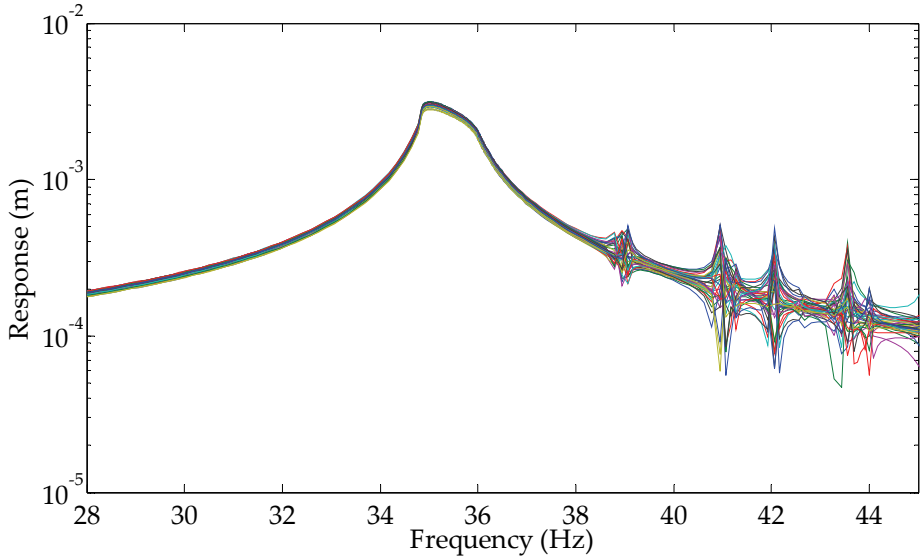

Figure 5.21 – Mistuned nonlinear response of blade tips for all sectors

As can be seen from Figure 5.22 , the effect of normal load variation observed at higher amplitudes only. For constant friction stiffness, only the normal load determines the stick-slip transition displacement; therefore the effect of normal load variation cannot be seen for low vibration amplitudes. In contrast, Figure 5.23 demonstrates that the effect of variations in friction stiffness values can be seen at every frequency in the range. The similarity between Figure 5.21 and Figure 5.23 suggests that both mistuning in structural properties of blades and variations in contact parameters can cause higher vibration amplitudes.

From the results of this section, it is concluded that macroslip nonlinearity can cause changes in resonant frequencies and amplitudes. In addition,

variation in macroslip friction element contact parameters has an effect similar to mistuning is achieved. Therefore, in maximum amplification factor predictions the effect of macroslip friction nonlinearity should be considered.

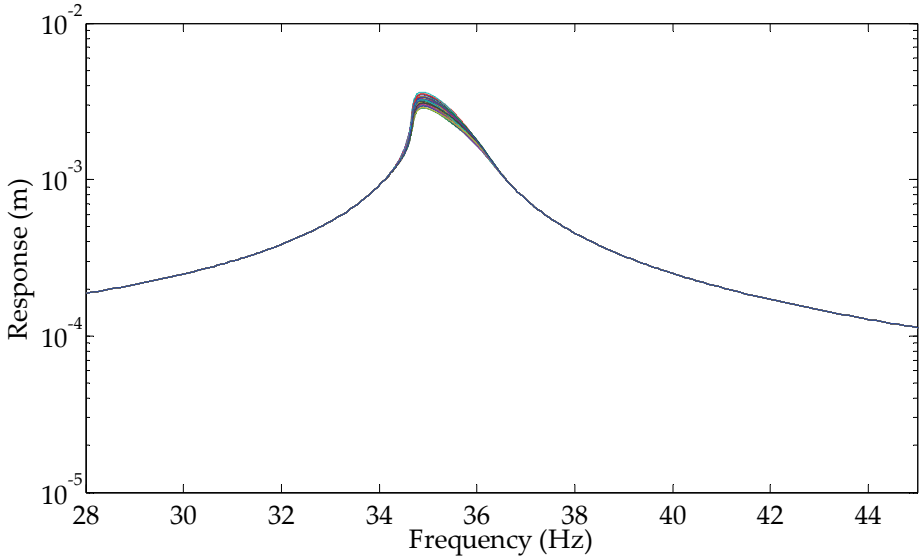

Figure 5.22 – Tuned, nonlinear response of blade tips for all sectors with macroslip normal load variations

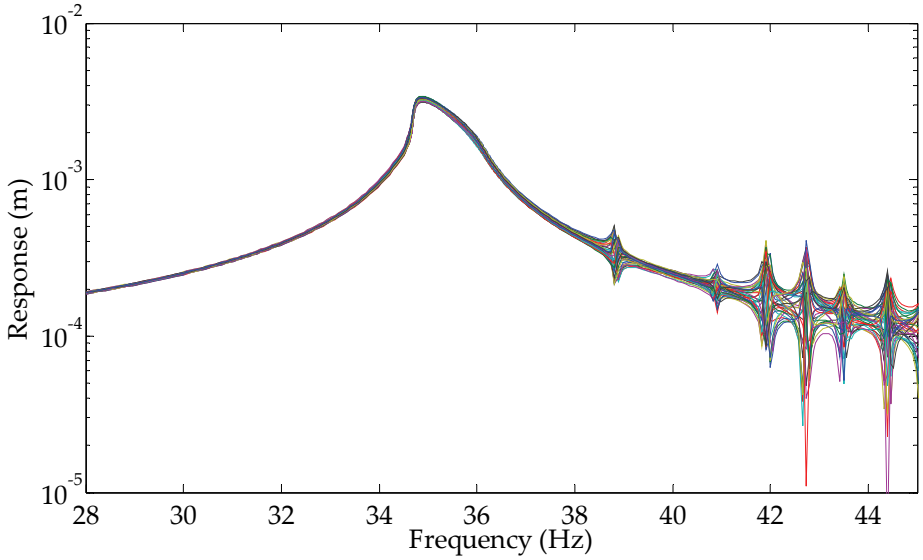

Figure 5.23 – Tuned, nonlinear response of blade tips for all sectors with macroslip friction stiffness variations

5.4.2 Gap/Interference Nonlinearity

In this section, the effect of gap/interference nonlinearity on the forced response will be demonstrated. Gap/interference elements are placed between shroud contact interfaces and only the relative motion in normal direction is considered. Nonlinear responses for both tuned and mistuned assemblies with different amounts of gap/interference nonlinearity are calculated and represented in Figure 5.24 and Figure 5.25. With the same boundary conditions as in the macroslip friction nonlinearity case, the blades are excited at the top edge but the direction of the force is selected to be tangent to the disk circumference so that the relative normal motion between shroud contact interfaces is obtained. The external forcing at each blade tip has an equivalent value of 1 N. The normal stiffness of gap elements is selected to be 10 kN/m. For gap and interference cases different contact states, namely no separation, partial contact and no contact can be encountered.

To demonstrate the effect of interference nonlinearity on forced response when the assembly is mistuned, ±5% mistuning is applied. The forced response of tips of all blades is given in Figure 5.25.

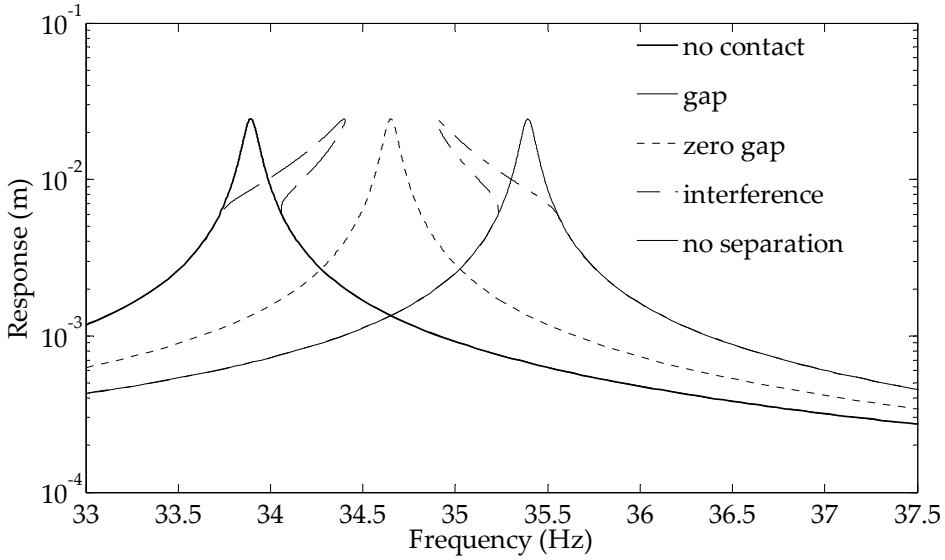

Figure 5.24 – Tuned response of blade tips for all sectors with different amounts of gap/interference nonlinearity

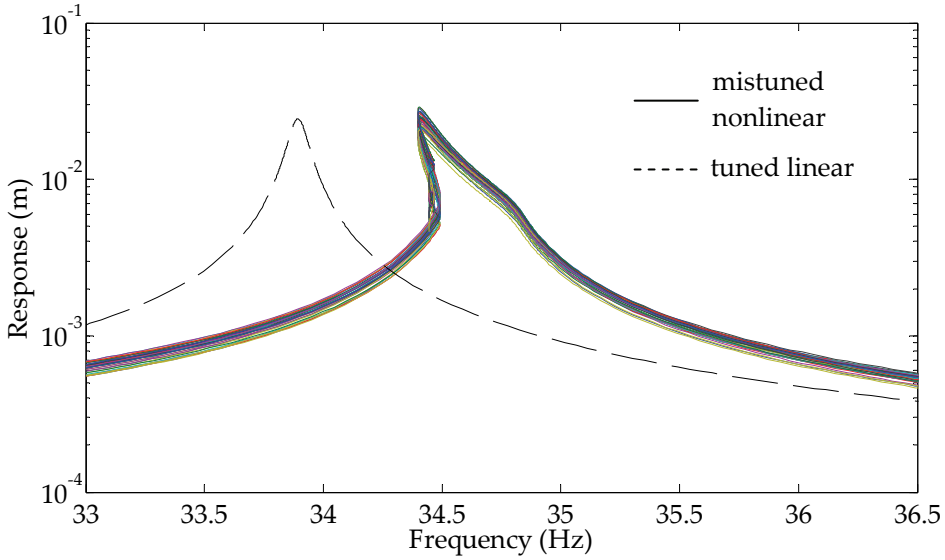

Figure 5.25 – Mistuned response of blade tips for all sectors with interference nonlinearity (±5% mistuning)

In this section, the nonlinear forced response calculation capability of the proposed method is illustrated by several case studies on tuned and

mistuned bladed disk assemblies with gap/interface nonlinearity. It is shown that gap/interface nonlinearity can result in both resonant frequency and amplitudes changes.

5.5 Effect of Mistuning and Nonlinearity on Forced Response

In this section, it is aimed to study the effect of mistuning and nonlinearity on the forced response characteristics of bladed disk assemblies. Several cases with or without mistuning and nonlinearity will be analyzed and the displacements on the most responding blade at the resonance will be compared via modal assurance criterion (MAC).

First, the linear response of the sample bladed disk assembly is calculated for both tuned and mistuned cases. Secondly, the nonlinear response is calculated with or without macroslip friction elements attached between shroud contact interfaces. For all the cases, 200 modes are kept in the analysis. The response vectors for all cases are compared via MAC and they are given in Table 5.3.

Table 5.3 – MAC comparison

	Linear tuned	Linear mistuned	Nonlinear tuned	Nonlinear mistuned
Linear tuned	1	0.9982	0.9992	0.9970
Linear mistuned		1	0.9965	0.9970
Nonlinear tuned			1	0.9983
Nonlinear mistuned				1

All the MAC values are higher than 0.99 which depicts that blade motion for all the cases show high resemblance even though the resonance frequencies and amplitudes are different as demonstrated in section 5.4.

CHAPTER 6

DISCUSSIONS AND CONCLUSIONS

In this thesis, a new method is suggested to analyze the nonlinear forced response of mistuned bladed disk assemblies in order to determine the blade vibrations under resonance conditions. The response, which is calculated in modal domain, is used to find the displacements in physical domain which can be used to determine stress distributions. Under such conditions, the stress distributions, which have major importance on the fatigue life of blades in the assembly, can be used in the design process.

6.1 The Mathematical Model

The component mode synthesis method (CMSM) formulation for mistuned bladed disk assemblies is utilized to determine the natural frequencies and mode shapes of the linear assembly. The method is preferred since distributed parameter mistuning (e.g., variations in modulus of elasticity due to material imperfections) can be imposed on blade substructures. Such an approach avoids using point mistuning elements which is the state-of-the-art for nonlinear mistuned cases and can distort the mode shapes of blades unless their numbers are high and they are well distributed along the blade. The displacements on the blades are of top importance since they lead to stress distribution information which is the main design parameter for blades. The method is also preferred due to its accuracy and robustness.

In nonlinear forced response analysis, Newton-Raphson method is used for the solution of nonlinear equations. Thanks to the arc length parameterization, the method is capable of tracing turning points. Moreover, the robustness of the method is improved by introducing an adaptive step length strategy. In addition, the Jacobian matrices required for Newton-Raphson iteration step are determined analytically for different types of nonlinearity such as gap/interference and macroslip elements. The response is calculated in modal domain for multiple harmonics by a transformation from physical coordinates into modal coordinates. Then, the Newton-Raphson method is applied to the equation in modal domain.

The advantage of the method is that, transforming the problem into modal coordinates, the size of the problem is reduced and the new size does not depend on of the number of nonlinear elements. Therefore, the computational speed can be considerably improved by modal truncation. Another advantage of the method is that, it yields the nonlinear forced response solution in modal domain. Consequently, the response can be back transformed into physical coordinates making it possible to calculate displacements along the blades under resonant conditions. The analysis can be extended to make stress analysis by using the physical displacements.

6.2 Accuracy and Efficiency of the Method

Case studies presented in this thesis have clearly shown that the number of modes retained in reduced order models is crucial. In CMSM, the accuracy of the reduced order model depends on both number of modes retained per

blade and number of modes retained per disk. If the model is not accurate enough and the lack of accuracy is due to inadequate number of blade modes, increasing the number of disk modes will not have significant effect and vice versa. Meaning that, the number of modes should be adjusted for both substructures at the same time. When compared with the subset of nominal modes method (SNMM), CMSM proved to yield more accurate results for higher amounts of mistuning. Although the relative error can be improved by introducing more degrees-of-freedom in CMSM, it is not possible to improve the accuracy beyond a limit in SNMM by introducing more modes per nodal diameter.

In forced response analysis, the number of modes retained in the model is important. It should be adequate to represent the motion correctly, especially where nonlinear elements are attached. Therefore, it should be selected so that increasing the number further for a frequency range of interest will have negligible effect on the response. This number can be decided by trial and error. Moreover, the number of harmonics is important for the accuracy of forced response. In systems with strong nonlinearity, subharmonic components become larger and their effect on resonance amplitudes becomes significant. For this reason, the number of harmonics included in the analysis should be selected so that further increase has no significant effect on the forced response.

6.3 The Effects of Mistuning and Nonlinearity on the Forced Response

In this thesis, using the proposed method, the effects of mistuning and nonlinearity on forced response characteristics of mistuned bladed disk

assemblies have been investigated. A number of cases were analyzed and response at each blade in the assembly was calculated. Besides, the response patterns were compared for different cases including linear and nonlinear response of tuned and mistuned assemblies.

Both mistuning and nonlinearity caused significant changes in resonance conditions in terms of frequency and amplitude. For instance, due to mistuning the double modes split and the resonance amplitudes are increased. In another case, both macroslip friction and gap/interference nonlinearity caused shifts in resonance frequency and changes in resonance amplitudes. In contrast, the modal assurance criterion calculations have shown that although mistuning and nonlinearity can alter the resonance conditions, the blade shapes may not change significantly.

6.4 Suggestions for Future Work

In this thesis, some assumptions have been made on the application of nonlinearity on the sample model in forced response analysis. Despite these simplifying assumptions, the results have shown the importance of both mistuning and nonlinearity on forced response. For instance, considering gap/interference nonlinearity, in all calculations it was assumed that the relative motion between mating surfaces is only in normal direction and its tangential component is neglected. Whereas, for macroslip friction nonlinearity, the relative motion is assumed to be only in tangential direction and the normal load, which may vary with displacements in normal direction, is assumed to be constant. Hence, a better nonlinear

element, in which friction contact under variable normal load is considered, will improve the accuracy of the results.

In general, the design of a structure is a process that depends on the stress levels that can be encountered during operation. Therefore, stress distributions is a better measure of structural integrity than the displacements although they are strongly linked. In this thesis, the effects of mistuning and nonlinearity on blade motion have been illustrated by MAC comparison between the ideally tuned linear response, and the mistuned and nonlinear cases. It has been observed that the blade motions were similar. However, since slight localized variations in displacements can result in severe changes in stress distributions, the stress levels should be studied. In addition, a software can be developed that can calculate stress distributions from displacements, including multiharmonic response, and can depict the results in a graphical environment. Then, instead of comparing the displacement patterns, stress levels can be used to study the effect of mistuning and nonlinearity in forced response.

REFERENCES

[1] T. Nicholas, *High Cycle Fatigue: A Mechanics of Materials Perspective*. Oxford: Elsevier Ltd., 2006.

[2] D. S. Whitehead, "Effect of Mistuning on the Vibration of Turbomachine Blades Induced by Wakes," *Journal of Mechanical Engineering Science,* vol. 8, pp. 15-21, 1966.

[3] D. J. Ewins, "The Effects of Detuning upon the Vibration of Bladed Discs." vol. Doctor of Philosophy Cambridge: University of Cambridge, 1966.

[4] D. S. Whitehead, "Research Note: Effect of Mistuning on Forced Vibration of Blades with Mechanical Coupling," *Journal of Mechanical Engineering Science,* vol. 18, pp. 306-307, 1976.

[5] D. S. Whitehead, "The Maximum Factor by Which Forced Vibration of Blades Can Increase Due to Mistuning," *ASME Journal of Engineering for Gas Turbines and Power,* vol. 120, pp. 115-119, 1998.

[6] S.-H. Lim, M. P. Castanier, and C. Pierre, "Predicting Mistuned Blade Amplitude Bounds and Stress Increases from Energy Formulations," in *Proceedings of 9th National Turbine Engine High Cycle Fatigue Conference*, Pinehurst, NC, 2004.

[7] J. A. Kenyon, J. H. Griffin, and D. M. Feiner, "Maximum Bladed Disk Forced Response From Distortion of a Structural Mode," *ASME Journal of Turbomachinery,* vol. 125, 2003.

[8] P. J. Davis, *Circulant Matrices*, second ed. New York, New York: Chelsea Publishing, 1994.

[9] M. P. Castanier, G. Óttarsson, and C. Pierre, "A Reduced Order Modeling Technique for Mistuned Bladed Disks," *ASME Journal of Vibration and Acoustics,* vol. 119, pp. 439-447, 1997.

[10] J. R. Bladh, "Efficient Predictions of the Vibratory Response of Mistuned Bladed Disks by Reduced Order Modeling," in *Mechanical Engineering*. vol. Doctor of Philosophy Michigan: University of Michigan, 2001.

[11] R. Bladh, M. P. Castanier, and C. Pierre, "Reduced Order Modeling and Vibration Analysis of Mistuned Bladed Disk Assemblies with Shrouds," *ASME Journal of Engineering for Gas Turbines and Power,* vol. 121, pp. 515-522, 1999.

[12] R. Bladh, M. P. Castanier, and C. Pierre, "Component-Mode-Based Reduced Order Modeling Techniques for Mistuned Bladed Disks - Part I: Theoretical Models," *ASME Journal of Engineering for Gas Turbines and Power,* vol. 123, pp. 89-99, 2001.

[13] R. Bladh, M. P. Castanier, and C. Pierre, "Component-Mode-Based Reduced Order Modeling Techniques for Mistuned Bladed Disks - Part II: Application," *ASME Journal of Engineering for Gas Turbines and Power,* vol. 123, pp. 100-108, 2001.

[14] R. R. Craig and M. C. C. Bampton, "Coupling of Substructures for Dynamics Analysis," *AIAA Journal,* vol. 6(7), pp. 1313-1319, 1968.

[15] M.-T. Yang and J. H. Griffin, "A Normalized Modal Eigenvalue Approach for Resolving Modal Interaction," *ASME Journal of Engineering for Gas Turbines and Power,* vol. 119, pp. 647-650, 1997.

[16] M.-T. Yang and J. H. Griffin, "A Reduced Order Approach for the Vibration of Mistuned Bladed Disk Assemblies," *ASME Journal of Engineering for Gas Turbines and Power,* vol. 119, pp. 161-167, 1997.

[17] M.-T. Yang and J. H. Griffin, "A Reduced-Order Model of Mistuning Using a Subset of Nominal System Modes," *ASME Journal of Engineering for Gas Turbines and Power,* vol. 123, pp. 893-900, 2001.

[18] D. M. Feiner and J. H. Griffin, "A Fundamental Model of Mistuning for a Single Family of Modes," *ASME Journal of Turbomachinery,* vol. 124, pp. 597-605, 2002.

[19] D. M. Feiner and J. H. Griffin, "Mistuning Identification of Bladed Disks Using a Fundamental Mistuning Model - Part I: Theory," *ASME Journal of Turbomachinery,* vol. 126, pp. 150-158, 2004.

[20] D. M. Feiner and J. H. Griffin, "Mistuning Identification of Bladed Disks Using a Fundamental Mistuning Model - Part II: Application," *ASME Journal of Turbomachinery,* vol. 126, pp. 159-165, 2004.

[21] E. P. Petrov and K. Y. Şanlıtürk, "A New Method for Dynamic Analysis of Mistuned Bladed Disks Based on the Exact Relationship Between Tuned and Mistuned Systems," *ASME Journal of Engineering for Gas Turbines and Power,* vol. 124, pp. 586-597, 2002.

[22] E. P. Petrov and D. J. Ewins, "Analysis of the Worst Mistuning Patterns in Bladed Disk Assemblies," *ASME Journal of Turbomachinery,* vol. 125, pp. 623-631, 2003.

[23] E. P. Petrov and D. J. Ewins, "Method for Analysis of Nonlinear Multiharmonic Vibrations of Mistuned Bladed Disks With Scatter of Contact Interface Characteristics," *ASME Journal of Turbomachinery,* vol. 127, pp. 128-136, 2006.

[24] M. Nikolic, E. P. Petrov, and D. J. Ewins, "Robust Strategies for Forced Response Reduction of Bladed Disks Based on Large Mistuning Concept," *ASME Journal of Engineering for Gas Turbines and Power,* vol. 130, pp. 022501-1-11, 2008.

[25] J. H. Griffin and L. F. Wagner, "Blade Vibration With Nonlinear Tip Constraint: Model Development," *ASME Journal of Turbomachinery,* vol. 112, pp. 778-785, 1990.

[26] B.-D. Yang and C.-H. Menq, "Modeling of Friction Contact and Its Application to the Design of Shroud Contact," *ASME Journal of Engineering for Gas Turbines and Power,* vol. 119, pp. 958-963, 1997.

[27] K. Y. Şanlıtürk, M. İmregün, and D. J. Ewins, "Harmonic Balance Vibration Analysis of Turbine Blades With Friction Dampers," *ASME Journal of Vibration and Acoustics,* vol. 119, pp. 96-103, 1997.

[28] B. D. Yang, M. K. Chu, and C. H. Menq, "Stick-Slip-Separation Analysis and Non-linear Stiffness and Damping Characterization of Friction Contacts Having Variable Normal Load," *Journal of Sound and Vibration,* vol. 210, pp. 461-481, 1998.

[29] C.-H. Menq and J. J. Chen, "Periodic Response of Blades Having Three-Dimensional Nonlinear Shroud Constraints," *ASME Journal of Engineering for Gas Turbines and Power,* vol. 123, pp. 901-909, 2001.

[30] K. Y. Şanlıtürk, D. J. Ewins, and A. B. Stanbridge, "Underplatform Dampers for Turbine Blades: Theoretical Modeling, Analysis, and Comparison With Experimental Data," *ASME Journal of Engineering for Gas Turbines and Power,* vol. 123, pp. 919-929, 2001.

[31] E. Ciğeroğlu and H. N. Özgüven, "Non-linear Vibration Analysis of Bladed Disks With Dry Friction Dampers," *Journal of Sound and Vibration,* vol. 292, pp. 1028-1043, 2006.

[32] E. Ciğeroğlu, W. Lu, and C.-H. Menq, "One-dimensional Dynamic Microslip Friction Model," *Journal of Sound and Vibration,* vol. 292, pp. 881-898, 2006.

[33] E. Ciğeroğlu, N. An, and C.-H. Menq, "A microslip friction model with normal load variation induced by normal motion," *Nonlinear Dynamics,* vol. 50, pp. 609-626, 2007.

[34] E. Ciğeroğlu, N. An, and C.-H. Menq, "Wedge Damper Modeling and Forced Response Prediction of Frictionally Constrained Blades," in *ASME Turbo Expo 2007*, Montréal, Canada, 2007, pp. 519-528.

[35] E. P. Petrov and D. J. Ewins, "Analytical Formulation of Friction Interface Elements for Analysis of Nonlinear Multi-Harmonics Vibrations of Bladed Disks," *ASME Journal of Turbomachinery,* vol. 125, pp. 364-371, 2003.

[36] E. P. Petrov and D. J. Ewins, "Generic Friction Models for Time-Domain Vibration Analysis of Bladed Disks," *ASME Journal of Turbomachinery,* vol. 126, pp. 184-192, 2004.

[37] E. P. Petrov and D. J. Ewins, "Advanced Modeling of Underplatform Friction Dampers for Analysis of Bladed Disk Vibration," *ASME Journal of Turbomachinery,* vol. 129, pp. 143-150, 2007.

[38] E. P. Petrov, "Method for Direct Parametric Analysis of Nonlinear Forced Response of Bladed Disks With Friction Contact Interfaces," *ASME Journal of Turbomachinery,* vol. 126, 2004.

[39] E. P. Petrov, "Direct Parametric Analysis of Resonance Regimes for Nonlinear Vibrations of Bladed Disks," *ASME Journal of Turbomachinery,* vol. 129, pp. 495-502, 2007.

[40] G. S. Óttarsson, "Dynamic Modeling and Vibration Analysis of Mistuned Bladed Disks," in *Mechanical Engineering*. vol. Doctor of Philosophy Michigan: University of Michigan, 1994.

[41] N. M. M. Maia, J. M. M. Silva, J. He, N. A. J. Lieven, R. M. Lin, G. W. Skingle, W.-M. To, and A. P. V. Urgueira, *Theoretical and Experimental Modal Analysis*. Hertfordshire: Research Studies Press Ltd., 1997.

[42] Y. W. Luk and L. D. Mitchell, "System Modeling and Modification via Modal Analysis," *1st International Modal Analysis Conference,* vol. 1, pp. 423-429, 1982.

[43] Ö. Tanrıkulu, B. Kuran, H. N. Özgüven, and M. İmregün, "Forced Harmonic Response Analysis of Non-linear Structures Using Describing Functions," *American Institute of Aeronautics and Astronautics Journal,* vol. 31, pp. 1313-1320, 1993.

[44] B. Kuran and H. N. Özgüven, "A Modal Superposition Method for Non-linear Structures," *Journal of Sound and Vibration,* vol. 189, pp. 315-339, 1996.

[45] E. Budak and H. N. Özgüven, "A Method for Harmonic Response of Structures with Symmetric Non-linearities," in *Proceedings of the 15th International Seminar on Modal Analysis*, Leuven, 1990, pp. 901-915.

[46] H. N. Özgüven, "A New Method for Harmonic Response of Non-proportionally Damped Structures Using Undamped Modal Data," *Journal of Sound and Vibration,* vol. 117, pp. 313-328, 1987.

[47] J. Sherman and W. J. Morrison, "Adjustment of an Inverse Matrix Corresponding to Changes in the Elements of a Given Column or a Given Row of the Original Matrix," *Ann. Math. Stat.,* vol. 20, p. 621, 1949.

[48] M. Woodbury, "Inverting Modified Matrices," Princeton University, Princeton, NJ 1950.

[49] M. Berthillier, C. Dupont, R. Mondal, and J. J. Barrau, "Blades Forced Response Analysis with Friction Dampers," *ASME Journal of Vibration and Acoustics,* vol. 120, pp. 468-474, 1998.

[50] M. A. Crisfield, "A Fast Incremental/Iterative Solution Procedure that Handles "Snap-through"," *Computers and Structures,* vol. 13, pp. 55-62, 1981.

APPENDIX A. CODE FOR NONLINEAR RESPONSE CALCULATION

```
function [ w , u , state] = UniSolveM( m , c , k , loss , f , OPTIONS )
%
%
% [ w , u ] = UniSolve( m , c , k , loss , f , OPTIONS )
% Universal non-linear solver
%
% OPTIONS Structure
%
% SolutionSpace:
%     1 : Solution procedure in Spatial Domain
%     m, c, k, f stays as they are.
%     2 : Solution procedure in Modal Domain
%     m, c, k, f become phi, cbar, wr, fbar.
%     ( 1 by default )
%
% SolutionProcedure:
%     1 : Solution procedure using Path Following
%     2 : Solution procedure using Fixed Point Iteration
%     ( 1 by default )
%
% ResponseType:
%     Valid for solution procedure in Modal Domain
%     1 : In Spatial Coords
%     2 : In Modal Coords
%     ( 1 by default )
%
% Harmonics:
%     Number of harmonics to be included in the analysis
%     ( 1 by default )
%
% FreqRange:
%     [ w_min w_max ];
%
% StepSize:
%     Valid for Path Following
%     ( 1E-2 by default )
%
% FreqStep:
%     Valid for Fixed Point Iteration
%     ( 1E3 by default )
%
% SweepDir:
%     1 : Low to High frequencies
%     2 : High to Low Frequencies
%     ( 1 by default )
%
% ErrorTolerance:
%     Global relative error tolerance
%     ( 1E-8 by default )
%
% IterNorm:
%     Valid for Path Following
%     Number of iterations at normal circumstances
%     ( 1.2 by default )
%
% IterMax:
%     Maximum number of iterations allowed
%     ( 1E2 by default )
%
% Relaxation:
%     Valid for Fixed Point Iteration
%     Relaxation parameter
%     ( 0.5 by default )
%
% NormalFlow:
%     0 : Normal flow algorithm NOT used
%     1 : Normal flow algorithm IS used
%     ( 1 by default )
%
% Nonlinear:
```

```
%     List of non-linearity with type and parameters
%
% ResponseDofs:
%     List of dofs at which the response is desired

d_SolutionSpace = 1;
d_SolutionProcedure = 1;
d_ResponseType = 1;
d_Harmonics = 1;
d_StepSize = 1E-2;
d_FreqStep = 1E3;
d_SweepDir = 1;
d_ErrorTolerance = 1E-8;
d_IterNorm = 1.2;
d_IterMax = 1E2;
d_Relaxation = 0.5;
d_NormalFlow = 1;

f_halt = 0;

w = -1;
u = -1;

if nargin < 5
    disp('Solver Stopped: Not enough arguments!');
    f_halt = 1;
end

% Preferences with predefined default values

if ( isfield( OPTIONS , 'SolutionSpace' ) )
    SolutionSpace = OPTIONS.SolutionSpace;
    if ( SolutionSpace ~= 1 && SolutionSpace ~= 2 )
        disp('Solver Altered Preference: Invalid SolutionSpace, value changed to default!');
        SolutionSpace = d_SolutionSpace;
    end
else
    SolutionSpace = d_SolutionSpace;
    disp('Solver Altered Preference: Default value used for SolutionSpace!');
end

if ( isfield( OPTIONS , 'SolutionProcedure' ) )
    SolutionProcedure = OPTIONS.SolutionProcedure;
    if ( SolutionProcedure ~= 1 && SolutionProcedure ~= 2 )
        disp('Solver Altered Preference: Invalid SolutionProcedure, value changed to
default!');
        SolutionProcedure = d_SolutionProcedure;
    end
else
    SolutionProcedure = d_SolutionProcedure;
    disp('Solver Altered Preference: Default value used for SolutionProcedure!');
end

if ( isfield( OPTIONS , 'ResponseType' ) )
    ResponseType = OPTIONS.ResponseType;
    if ( ResponseType ~= 1 && ResponseType ~= 2 )
        disp('Solver Altered Preference: Invalid ResponseType, value changed to default!');
        ResponseType = d_ResponseType;
    end
else
    ResponseType = d_ResponseType;
    disp('Solver Altered Preference: Default value used for ResponseType!');
end

if ( isfield( OPTIONS , 'Harmonics' ) )
    Harmonics = OPTIONS.Harmonics;
    if ( Harmonics <= 0 )
        disp('Solver Altered Preference: Invalid Harmonics, value changed to default!');
        Harmonics = d_Harmonics;
    end
else
    Harmonics = d_Harmonics;
    disp('Solver Altered Preference: Default value used for ResponseType!');
end

if ( isfield( OPTIONS , 'StepSize' ) )
    StepSize = OPTIONS.StepSize;
    if ( StepSize <= 0 )
        disp('Solver Altered Preference: Invalid StepSize, value changed to default!');
        StepSize = d_StepSize;
```

```
    end
else
    StepSize = d_StepSize;
    disp('Solver Altered Preference: Default value used for StepSize!');
end

if ( isfield( OPTIONS , 'FreqStep' ) )
    n_FreqStep = OPTIONS.FreqStep;
    if ( n_FreqStep < 1 )
        disp('Solver Altered Preference: Invalid FreqStep, value changed to default!');
        n_FreqStep = d_FreqStep;
    end
else
    n_FreqStep = d_FreqStep;
    disp('Solver Altered Preference: Default value used for FreqStep!');
end

if ( isfield( OPTIONS , 'SweepDir' ) )
    SweepDir = OPTIONS.SweepDir;
    if ( SweepDir ~= 1 && SweepDir ~= 2 )
        disp('Solver Altered Preference: Invalid SweepDir, value changed to default!');
        SweepDir = d_SweepDir;
    end
else
    SweepDir = d_SweepDir;
    disp('Solver Altered Preference: Default value used for SweepDir!');
end

if ( isfield( OPTIONS , 'ErrorTolerance' ) )
    ErrorTolerance = OPTIONS.ErrorTolerance;
    if ( ErrorTolerance <= 0 )
        disp('Solver Altered Preference: Invalid ErrorTolerance, value changed to default!');
        ErrorTolerance = d_ErrorTolerance;
    end
else
    ErrorTolerance = d_ErrorTolerance;
    disp('Solver Altered Preference: Default value used for ErrorTolerance!');
end

if ( isfield( OPTIONS , 'IterNorm' ) )
    IterNorm = OPTIONS.IterNorm;
    if ( IterNorm <= 0 )
        disp('Solver Altered Preference: Invalid IterNorm, value changed to default!');
        IterNorm = d_IterNorm;
    end
else
    IterNorm = d_IterNorm;
    disp('Solver Altered Preference: Default value used for IterNorm!');
end

if ( isfield( OPTIONS , 'IterMax' ) )
    IterMax = OPTIONS.IterMax;
    if ( IterMax <= 0 )
        disp('Solver Altered Preference: Invalid IterMax, value changed to default!');
        IterMax = d_IterMax;
    end
else
    IterMax = d_IterMax;
    disp('Solver Altered Preference: Default value used for IterMax!');
end

if ( isfield( OPTIONS , 'Relaxation' ) )
    Relaxation = OPTIONS.Relaxation;
    if ( Relaxation <= 0 )
        disp('Solver Altered Preference: Invalid Relaxation, value changed to default!');
        Relaxation = d_Relaxation;
    end
else
    Relaxation = d_Relaxation;
    disp('Solver Altered Preference: Default value used for Relaxation!');
end

if ( isfield( OPTIONS , 'NormalFlow' ) )
    f_NormalFlow = OPTIONS.NormalFlow;
    if ( f_NormalFlow <= 0 )
        disp('Solver Altered Preference: Invalid NormalFlow, value changed to default!');
        f_NormalFlow = d_NormalFlow;
    end
else
    f_NormalFlow = d_NormalFlow;
```

```
        disp('Solver Altered Preference: Default value used for NormalFlow!');
    end

    if ( isfield( OPTIONS , 'ResponseDofs' ) )
        f_ResponseDofs = 1;
        ResponseDofs = OPTIONS.ResponseDofs;
    else
        f_ResponseDofs = 0;
    end

    f_square = 1;

    if ( SolutionSpace == 1 )
        % Element matrices should be square with same size
        if ( size(m,1) ~= size(m,2) )
            disp('Solver Stopped: m matrix is not square!');
            f_halt = 1;
            f_square = 0;
        end
        if ( size(k,1) ~= size(k,2) )
            disp('Solver Stopped: k matrix is not square!');
            f_halt = 1;
            f_square = 0;
        end
        if ( size(c,1) ~= size(c,2) )
            disp('Solver Stopped: c matrix is not square!');
            f_halt = 1;
            f_square = 0;
        end
        if ( (f_square == 1) && (size(m,1) ~= size(k,1) || size(c,1) ~= size(k,1)) )
            disp('Solver Stopped: Matrix sizes mismatch!');
        end
    elseif ( SolutionSpace == 2 )
        if ( size(k,1) ~= size(k,2) )
            disp('Solver Stopped: wr matrix is not square!');
            f_halt = 1;
        elseif ( size(m,2) ~= size(k,1) )
            disp('Solver Stopped: Number of modes in phi and wr mismatch! Considering less
modes.');
            if ( size(m,2) > size(k,1) )
                m = m( : , 1:size(k,1) );
            else
                k = k( 1:size(m,2) , 1:size(m,2) );
            end
        end
    end

    if ( isfield( OPTIONS , 'FreqRange' ) )
        FreqRange = OPTIONS.FreqRange;
        if ( max(size(FreqRange)) == 2 && max(size(FreqRange)) == 1 )
            disp('Solver Stopped: Frequency range is not valid!');
            f_halt = 1;
        end
    else
        disp('Solver Stopped: Frequency range is not defined!');
        f_halt = 1;
    end

    if ( isfield( OPTIONS , 'Nonlinear' ) )
        if ( size( OPTIONS.Nonlinear , 2 ) >= 6 )
            f_Nonlinear = 1;
            Nonlinear_data = OPTIONS.Nonlinear;
        else
            disp('Solver Altered Preference: Invalid Nonlinear data, nonlinearity omitted!');
            f_Nonlinear = 0;
        end
    else
        f_Nonlinear = 0;
    end

    if ( f_halt == 1 )
        return;
    end

    % SETTING SOLVER PARAMETERS

    w_min = min ( FreqRange );
    w_max = max ( FreqRange );
    w_step = (w_max - w_min) / n_FreqStep;
```

```
s = StepSize;

n_dof = size(m,1);
n_eig = size(m,2);

n_harm = Harmonics;
n_terms = 2*n_harm + 1;

if ( f_Nonlinear )
    n_Nonlinear = size(Nonlinear_data,1);
end

% SETTING UP ELEMENTARY MATRICES

if ( SolutionSpace == 2 )
    phi = m;
    m = eye(n_eig);
end

k_multp = eye( n_terms );
ch_multp = zeros( n_terms );
m_multp = zeros( n_terms );

for ( n = 1 : Harmonics )
    p = 2*n+1;
    m_multp(p-1:p,p-1:p) = n^n * eye(2);
    ch_multp(p-1,p) = -n;
    ch_multp(p,p-1) = n;
end

K = kron(k_multp,k);

M = kron(m_multp,m);

C = kron(ch_multp,c);

H = kron(ch_multp,loss*k);

F = zeros(n_eig*n_terms,1);

fc =  real(f);
fs = -imag(f);

F(n_eig+1:2*n_eig) = fc;
F(2*n_eig+1:3*n_eig) = fs;

% PATH FOLLOWING PROCEDURE

if ( SolutionProcedure == 1 )

    r = 1;
    if ( SweepDir == 1 )
        w_act = w_min;
    else
        w_act = w_max;
    end

    r = 1;
    w = w_act;

    Z = K + H - w^2 * M + w * C;
    Y = inv(Z)*F; % Linear solution as initial guess

    error = 1;
    iter(r) = 0;
    while ( error > ErrorTolerance )

        F_Elem = zeros(n_terms*n_eig,1);
        Kf_Elem = zeros(n_terms*n_eig);

        if ( f_Nonlinear )
            if ( SolutionSpace == 1 )
                process_nonlinear_spatial;
            else
                process_nonlinear_modal;
            end
        end

        R0 = Z * Y + F_Elem - F;
        dRdY_inv = inv(Z+Kf_Elem);
```

```
    Ytemp = Y - dRdY_inv * R0;
    Ytemp_size = Ytemp' * Ytemp;
    error = sqrt( R0'*R0 );

    Y = Ytemp;

    iter(r) = iter(r) + 1;

end
disp(sprintf('Omega = %8.4f and sqrt|R0".R0| = %e with iter = %d',w,error,iter(r)))
dYdw(:,r) = dRdY_inv * ( 2*w*M - C ) * Y ;
q(:,r) = [ Y ; w ];

r = r+1;
if ( SweepDir == 1 )
    w = w_min + (r-1)*w_step;
else
    w = w_max - (r-1)*w_step;
end

Z = K + H - w^2 * M + w * C;
Y = inv(Z)*F; % Linear solution as initial guess

error = 1;
iter(r) = 0;
while ( error > ErrorTolerance )

    F_Elem = zeros(n_terms*n_eig,1);
    Kf_Elem = zeros(n_terms*n_eig);

    if ( f_Nonlinear )
        if ( SolutionSpace == 1 )
            process_nonlinear_spatial;
        else
            process_nonlinear_modal;
        end
    end

    R0 = Z * Y + F_Elem - F;
    dRdY_inv = inv(Z+Kf_Elem);
    Ytemp = Y - dRdY_inv * R0;
    Ytemp_size = Ytemp' * Ytemp;
    error = sqrt( R0'*R0 );

    Y = Ytemp;

    iter(r) = iter(r) + 1;

end
disp(sprintf('Omega = %8.4f and sqrt|R0".R0| = %e with iter = %d',w,error,iter(r)))
dYdw(:,r) = dRdY_inv * ( 2*w*M - C ) * Y ;
q(:,r) = [ Y ; w ];

while (w < w_max && w > w_min)

    s_new = s * sqrt ( IterNorm / iter(r) );
    if( s_new < StepSize )
        s = s_new;
    else
        s = StepSize;
    end

    dYdw(:,r) = dRdY_inv * ( 2*w*M - C ) * Y ;

    deltaq = q(:,r) - q(:,r-1);

    dq = [ dYdw(:,r) ; 1 ];
    dq = (s / sqrt(dq'*dq))*dq;

    corr = deltaq'*dq;
    if (corr < 0)
        dq = -dq;
    end

    q(:,r+1) = q(:,r) + dq;

    Y = q(1:n_eig*n_terms,r+1);
    w = q(n_eig*n_terms+1,r+1);

    Z = K + H - w^2 * M + w * C;
```

```
          F_Elem = zeros(n_terms*n_eig,1);
          Kf_Elem = zeros(n_terms*n_eig);

          if ( f_Nonlinear )
              if ( SolutionSpace == 1 )
                  process_nonlinear_spatial;
              else
                  process_nonlinear_modal;
              end
          end

          deltaq = dq;

          R0 = ( Z ) * Y + F_Elem - F;
          g0 = deltaq'*deltaq - s^2;

          error = sqrt( R0'*R0 );
          iter(r+1) = 0;
          while (error > ErrorTolerance)

              dq = -inv( [ Z+Kf_Elem (-2*w*M + C)*Y ; 2*deltaq' ] )*[R0 ; g0];

              q(:,r+1) = q(:,r+1) + dq;

              deltaq = q(:,r+1) - q(:,r);

              Y = q(1:n_eig*n_terms,r+1);
              w = q(n_eig*n_terms+1,r+1);

              Z = K + H - w^2 * M + w * C;

              F_Elem = zeros(n_terms*n_eig,1);
              Kf_Elem = zeros(n_terms*n_eig);

              if ( f_Nonlinear )
                  if ( SolutionSpace == 1 )
                      process_nonlinear_spatial;
                  else
                      process_nonlinear_modal;
                  end
              end

              R0 = ( Z ) * Y + F_Elem - F;
              g0 = deltaq'*deltaq - s^2;

              error = sqrt( R0'*R0 );
              iter(r+1) = iter(r+1) + 1;

          end

          dRdY_inv = inv(Z+Kf_Elem);

          r = r + 1;

          disp(sprintf('Omega = %8.4f and sqrt|R0".R0| = %e and |g0| = %e with iter =
%d',w,error,abs(g0),iter(r)))

      end

   % FIXED POINT ITERATION PROCEDURE

   else

      r = 1;
      if ( SweepDir == 1 )
          w = w_min;
      else
          w = w_max;
      end

      while ( w >= w_min && w <= w_max )

          Z = K + H - w^2 * M + w * C;
          invZ = inv(Z);

          if ( f_Nonlinear ) % if there exist nonlinearity

              state_Nonlinear(:,r) = zeros( n_Nonlinear , 1 );
              error = 1;
```

```
            if ( r == 1 )
                Y = invZ * F;
            elseif ( r == 2 );
                Y = q(1:n_terms*n_eig,r-1);
            elseif ( r > 2 )
                Y = 2*q(1:n_terms*n_eig,r-1) - q(1:n_terms*n_eig,r-2);
            end

            iter = 0;

            while ( error > ErrorTolerance )

                F_Elem = zeros(n_terms*n_eig,1);
                Kf_Elem = zeros(n_terms*n_eig);

                if ( SolutionSpace == 1 )
                    process_nonlinear_spatial;
                else
                    process_nonlinear_modal;
                end

                Ytemp = invZ * ( F - F_Elem );
                error_temp = 1;

                for s=1:n_terms*n_eig
                    if ( Ytemp(s) ~= 0 )
                        error_temp = abs( (Ytemp(s)-Y(s))/Ytemp(s) );
                        if ( error_temp < error )
                            error = error_temp;
                        end
                    end
                end

                Y = Ytemp * (1-Relaxation) + Y * Relaxation;

                iter = iter + 1;

            end

            q(:,r) = [ Y ; w ];

            disp(sprintf('Omega = %f and iter = %d',w,iter))

            % Next step
            r = r + 1;
            if ( SweepDir == 1 )
                w = w_min + (r-1)*w_step;
            else
                w = w_max - (r-1)*w_step;
            end

        else

            % Solution
            Y = invZ * F;

            q(:,r) = [ Y ; w ];

            % Next step
            r = r + 1;
            if ( SweepDir == 1 )
                w = w_min + (r-1)*w_step;
            else
                w = w_max - (r-1)*w_step;
            end

            disp(sprintf('Omega = %f',w))
        end



    end

end

if( f_Nonlinear )
    state = state_Nonlinear;
else
    state = -1;
```

```
end

w = q(n_terms*n_eig+1 , :);
if ( SolutionSpace == 1 )
    u = q(1:n_terms*n_eig , :);
else
    u = kron(eye(n_terms),phi) * q(1:n_terms*n_eig , :);
end
```

```
% Process Nonlinearity in Spatial Domain MULTIHARMONICS
for k=1:n_Nonlinear

    dof_1 = Nonlinear_data(k,1);
    dof_2 = Nonlinear_data(k,2);

    type = Nonlinear_data(k,3);

    param1 = Nonlinear_data(k,4);
    param2 = Nonlinear_data(k,5);
    param3 = Nonlinear_data(k,6);

    if ( dof_1 == 0 || dof_2 == 0 )

        if ( dof_1 == 0 )
            dof_1 = dof_2;
        end

        for n=1:n_terms
            DY(n,1) = Y((n-1)*n_eig+dof_1);
        end

        switch type
            case 1 % Gap element
                if ( n_harm == 1 )
                    [ F_Elem_k , Kf_Elem_k , state ] = gap_elem(DY,param1,param2);
                else
                    [ F_Elem_k , Kf_Elem_k , state ] =
gap_elem_multiharmonic(DY,param1,param2);
                end
                state_Nonlinear(k,r) = state;
            case 2 % Macroslip friction element
                [ F_Elem_k , Kf_Elem_k , state ] = friction_elem(DY,param1,param2,param3);
                state_Nonlinear(k,r) = state;
            case 3 % Macroslip Analytical - Non-Petrov
                [ F_Elem_k , Kf_Elem_k , state ] =
friction_elem_macroslip(DY,param1,param2,param3);
                state_Nonlinear(k,r) = state;
            otherwise
                F_Elem_k = zeros(n_terms,1);
                state_Nonlinear(k,r) = -666;
        end

        for n=1:n_terms
            F_Elem( dof_1 + (n-1)*n_eig , 1) = F_Elem( dof_1 + (n-1)*n_eig ) + F_Elem_k(n);
        end

        for p=1:n_terms
            for t=1:n_terms
                Kf_Elem( (p-1)*n_eig + dof_1 , (t-1)*n_eig + dof_1 ) = Kf_Elem( (p-1)*n_eig +
dof_1 , (t-1)*n_eig + dof_1 ) + Kf_Elem_k(p,t);
            end
        end

    else

        for n=1:n_terms
            DY(n,1) = Y((n-1)*n_eig+dof_1) - Y((n-1)*n_eig+dof_2);
        end

        switch type
            case 1 % Gap element
                if ( n_harm == 1 )
                    [ F_Elem_k , Kf_Elem_k , state ] = gap_elem(DY,param1,param2);
                else
```

```
                    [ F_Elem_k , Kf_Elem_k , state ] =
gap_elem_multiharmonic(DY,param1,param2);
                end
                state_Nonlinear(k,r) = state;
            case 2 % Macroslip friction element
                [ F_Elem_k , Kf_Elem_k , state ] = friction_elem(DY,param1,param2,param3);
                state_Nonlinear(k,r) = state;
            otherwise
                F_Elem_k = zeros(n_terms,1);
                state_Nonlinear(k,r) = -666;
        end

        for n=1:n_terms
            F_Elem( dof_1 + (n-1)*n_eig , 1) = F_Elem( dof_1 + (n-1)*n_eig ) + F_Elem_k(n);
            F_Elem( dof_2 + (n-1)*n_eig , 1) = F_Elem( dof_2 + (n-1)*n_eig ) - F_Elem_k(n);
        end

        for p=1:n_terms
            for t=1:n_terms
                Kf_Elem( (p-1)*n_eig + dof_1 , (t-1)*n_eig + dof_1 ) = Kf_Elem( (p-1)*n_eig +
dof_1 , (t-1)*n_eig + dof_1 ) + Kf_Elem_k(p,t);
                Kf_Elem( (p-1)*n_eig + dof_2 , (t-1)*n_eig + dof_2 ) = Kf_Elem( (p-1)*n_eig +
dof_2 , (t-1)*n_eig + dof_2 ) + Kf_Elem_k(p,t);
                Kf_Elem( (p-1)*n_eig + dof_1 , (t-1)*n_eig + dof_2 ) = Kf_Elem( (p-1)*n_eig +
dof_1 , (t-1)*n_eig + dof_2 ) - Kf_Elem_k(p,t);
                Kf_Elem( (p-1)*n_eig + dof_2 , (t-1)*n_eig + dof_1 ) = Kf_Elem( (p-1)*n_eig +
dof_2 , (t-1)*n_eig + dof_1 ) - Kf_Elem_k(p,t);
            end
        end

    end

end
```

```
% Process Nonlinearity in Modal Domain MULTIHARMONICS
for k=1:n_Nonlinear

    dof_1 = Nonlinear_data(k,1);
    dof_2 = Nonlinear_data(k,2);

    type = Nonlinear_data(k,3);

    param1 = Nonlinear_data(k,4);
    param2 = Nonlinear_data(k,5);
    param3 = Nonlinear_data(k,6);

    if ( dof_1 == 0 || dof_2 == 0 )

        if ( dof_1 == 0 )
            dof_1 = dof_2;
        end

        phi_1 = phi( dof_1 , : );

        for n=1:n_terms
            DY(n,1) = phi_1 * Y( (n-1)*n_eig+1 : n*n_eig );
        end

        phi_Elem = kron( eye(n_terms) , phi_1 );

        switch type
            case 1 % Gap element
                if ( n_harm == 1 )
                    [ F_Elem_k , Kf_Elem_k , state ] = gap_elem(DY,param1,param2);
                else
                    [ F_Elem_k , Kf_Elem_k , state ] =
gap_elem_multiharmonic(DY,param1,param2);
                end
                state_Nonlinear(k,r) = state;
            case 2 % Macroslip friction element
                [ F_Elem_k , Kf_Elem_k , state ] = friction_elem(DY,param1,param2,param3);
                state_Nonlinear(k,r) = state;
            otherwise
                F_Elem_k = zeros(n_terms,1);
```

```
                state_Nonlinear(k,r) = -666;
            end

            F_Elem = F_Elem + phi_Elem' * F_Elem_k;

            Kf_Elem = Kf_Elem + phi_Elem' * Kf_Elem_k * phi_Elem;

        else

            phi_1 = phi( dof_1 , : );
            phi_2 = phi( dof_2 , : );

            for n=1:n_terms
                DY(n,1) = phi_1 * Y( (n-1)*n_eig+1 : n*n_eig ) - phi_2 * Y( (n-1)*n_eig+1 :
n*n_eig );
            end

            phi_Elem = [ kron(eye(n_terms),phi_1) ; kron(eye(n_terms),phi_2) ];

            switch type
                case 1 % Gap element
                    if ( n_harm == 1 )
                        [ F_Elem_k , Kf_Elem_k , state ] = gap_elem(DY,param1,param2);
                    else
                        [ F_Elem_k , Kf_Elem_k , state ] =
gap_elem_multiharmonic(DY,param1,param2);
                    end
                    state_Nonlinear(k,r) = state;
                case 2 % Macroslip friction element
                    [ F_Elem_k , Kf_Elem_k , state ] = friction_elem(DY,param1,param2,param3);
                    state_Nonlinear(k,r) = state;
                otherwise
                    F_Elem_k = zeros(n_terms,1);
                    state_Nonlinear(k,r) = -666;
            end

            F_Elem = F_Elem + phi_Elem' * [ F_Elem_k ; -F_Elem_k ];
            Kf_Elem = Kf_Elem + phi_Elem' * [ Kf_Elem_k -Kf_Elem_k ; -Kf_Elem_k Kf_Elem_k ] *
phi_Elem;

        end

    end
```

APPENDIX B. CODE FOR COMPONENT MODE SYNTHESIS METHOD

```
clear;
clc;

max_mode_blade = 5;
max_modeperND_disk = 30;

file_disk_mass = 'DISK_MASS.MATRIX';
file_disk_stiffness = 'DISK_STIFFNESS.MATRIX';
file_blade_mass = 'BLADE_MASS.MATRIX';
file_blade_stiffness = 'BLADE_STIFFNESS.MATRIX';

file_disk_nodeno = 'DISK_NODENO.TXT';
file_disk_nodecoord = 'DISK_NODECOORD.TXT';
file_disk_fixedno = 'DISK_FIXEDNODENO.TXT';
file_disk_freq = 'DISK_FREQ.TXT';
file_disk_modal = 'DISK_MODAL.TXT';

file_interfacenodeno = 'INTERFACENODENO.TXT';

file_blade_nodeno = 'BLADE_NODENO.TXT';
file_blade_freq = 'BLADE_FREQ.TXT';
file_blade_modal = 'BLADE_MODAL.TXT';

[ Kd , Md ] = ansys_mat_import ( file_disk_mass , file_disk_stiffness );
[ Kb , Mb ] = ansys_mat_import ( file_blade_mass , file_blade_stiffness );

node_list_disk = uint32 ( importdata( file_disk_nodeno ) );
node_coord_disk = importdata( file_disk_nodecoord );
node_list_disk_fixed = uint32 ( importdata( file_disk_fixedno ) );
FREQ_DISK = importdata ( file_disk_freq );
MODAL_DISK = importdata ( file_disk_modal );

node_list_interface = uint32 ( importdata( file_interfacenodeno ) );

node_list_blade = uint32 ( importdata( file_blade_nodeno ) );
FREQ_BLADE = importdata ( file_blade_freq );
MODAL_BLADE = importdata ( file_blade_modal );

n_node_disk = size( node_list_disk , 1 );
n_node_blade = size ( node_list_blade , 1 );
n_node_disk_fixed = size ( node_list_disk_fixed , 1 );
n_node_interface = size ( node_list_interface , 1 );
n_node_blade = size ( node_list_blade , 1 );

n_mode_blade = size ( FREQ_BLADE , 1 );
n_mode_disk = size ( FREQ_DISK , 1 );
n_ND_disk = max ( FREQ_DISK(:,1) );
n_modeperND_disk = max ( FREQ_DISK(:,2) );

% CORRECT ANSYS OUTPUT FORMAT

FREQ_BLADE( : , 3 ) = FREQ_BLADE( : , 3 ) * 2*pi;
FREQ_DISK( : , 3 ) = FREQ_DISK( : , 3 ) * 2*pi;

if (n_mode_blade > max_mode_blade)
    FREQ_BLADE = FREQ_BLADE( 1:max_mode_blade , : );
    MODAL_BLADE = MODAL_BLADE( : , 1:max_mode_blade );
    n_mode_blade = max_mode_blade;
end

if (n_modeperND_disk > max_modeperND_disk)

    FREQ_TEMP = zeros( n_ND_disk * max_modeperND_disk , 3 );
    MODAL_TEMP = zeros( size(MODAL_DISK,1) , n_ND_disk * max_modeperND_disk );

    for n=1:n_ND_disk
        FREQ_TEMP( (n-1)*max_modeperND_disk+1 : n*max_modeperND_disk , : ) = FREQ_DISK( (n-
1)*n_modeperND_disk+1 : (n-1)*n_modeperND_disk + max_modeperND_disk , : );
        MODAL_TEMP( : , (n-1)*max_modeperND_disk+1 : n*max_modeperND_disk ) = MODAL_DISK( : ,
(n-1)*n_modeperND_disk+1 : (n-1)*n_modeperND_disk + max_modeperND_disk );
```

```
       end
       n_modeperND_disk = max_modeperND_disk;
       FREQ_DISK = FREQ_TEMP;
       MODAL_DISK = MODAL_TEMP;
       n_mode_disk = size( FREQ_DISK , 1 );
       clear *_TEMP;
   end

   symm_axis = 1; % Cyclic symmetry axis: x-axis
   e_tol = 1E-4; % Matching tolerance

   qc = node_coord_disk;
   qp = zeros(n_node_disk*3,1);

   node_list_disk_free = uint32( pop(node_list_disk,node_list_disk_fixed) ); % All nodes on the
disk other than fixed nodes
   node_list_disk_free_fixedinterface = uint32( pop(node_list_disk_free,node_list_interface) );
% All nodes on the disk other than fixed nodes and interface nodes

   node_list_blade_fixedinterface = uint32( pop(node_list_blade , node_list_interface) );

   n_node_fixed = size(node_list_disk_fixed,1);
   n_node_interface = size(node_list_interface,1);
   n_node_disk_free = size(node_list_disk_free,1);
   n_node_disk_free_fixedinterface = size(node_list_disk_free_fixedinterface,1);
   n_node_blade_fixedinterface = size(node_list_blade_fixedinterface,1);

   MODAL_DISK_LOW = MODAL_DISK( 1:n_node_disk*3 , : );
   MODAL_DISK_HIGH = MODAL_DISK( n_node_disk*3+1:n_node_disk*3*2 , : );

   % ************************************************************************
   %                                    DISK
   % ************************************************************************

   lamda_d = diag ( FREQ_DISK(:,3).^2 );

   % Transform the coordinate frame from cartesian to cylindrical

   qc_free = zeros( n_node_disk_free*3 , 1 );
   for n=1:n_node_disk_free
       m = pick(node_list_disk,node_list_disk_free(n));
       qc_free( (n-1)*3+1 : n*3 , 1 ) = qc( (m-1)*3+1 : m*3 , 1 );
   end

   for n=1:n_node_disk_free

       x(n) = qc_free ( (n-1)*3 + 1 );
       y(n) = qc_free ( (n-1)*3 + 2 );
       z(n) = qc_free ( n*3 );

       r(n) = sqrt( y(n)^2 + z(n)^2 );
       teta(n) = atan2( z(n) , y(n) );
       h(n) = x(n);

   end

   % ************************************************************************

   rotation = @(rot_angle) [ 1 0 0 ; 0 cos(rot_angle) -sin(rot_angle) ; 0 sin(rot_angle)
cos(rot_angle) ];

   % Matching Low and High edges by duplicate sector

   n_matching = 0;

   N = round( 2*pi/(max(teta)-min(teta)) ) - 1;

   while ( n_matching == 0 )

       N = N + 1;

       alfa = 2*pi / N;

       T_rot = rotation( alfa );

       T_rot_assm = kron( eye(n_node_disk_free) , T_rot );

       qc_free_rot = T_rot_assm * qc_free;

       node_list_high = uint32(0);
```

```
      node_list_low = uint32(0);

      for n=1:n_node_disk_free

          x_r1 = qc_free( (n-1)*3 + 1 );
          y_r1 = qc_free( (n-1)*3 + 2 );
          z_r1 = qc_free( n*3 );

          for m=1:n_node_disk_free

              x_r2 = qc_free_rot( (m-1)*3 + 1 );
              y_r2 = qc_free_rot( (m-1)*3 + 2 );
              z_r2 = qc_free_rot( m*3 );

              delta = sqrt( (x_r2-x_r1)^2 + (y_r2-y_r1)^2 + (z_r2-z_r1)^2 );
              if delta < e_tol
                  n_matching = n_matching + 1;
                  node_list_high(n_matching,1) = node_list_disk_free(n);
                  node_list_low(n_matching,1) = node_list_disk_free(m);
              end
          end

      end

   end

   P = round ( N/2 );

   node_list_disk_interior = uint32( pop( node_list_disk_free_fixedinterface , [ node_list_low ;
node_list_high ]) );
   n_node_disk_interior = size(node_list_disk_interior,1);

   % ************************************************************************

   % Partition the element matrices

   node_list_disk_ordered = [ node_list_disk_interior ; node_list_interface ; node_list_low ;
node_list_high ];

   n_node_disk_ordered = size(node_list_disk_ordered,1);

   K_free = zeros(n_node_disk*3);
   M_free = zeros(n_node_disk*3);
   phi_d = zeros(n_node_disk_ordered*3 , n_mode_disk);

   for n=1:n_node_disk_ordered
       picked(n,1) = pick( node_list_disk , node_list_disk_ordered(n) );
   end

   for n=1:n_node_disk_ordered
       node_x = picked(n);
       phi_d_LOW( (n-1)*3+1 : n*3 , : ) = MODAL_DISK_LOW( (node_x-1)*3+1 : node_x*3 , : );
       phi_d_HIGH( (n-1)*3+1 : n*3 , : ) = MODAL_DISK_HIGH( (node_x-1)*3+1 : node_x*3 , : );
       for m=1:n_node_disk_ordered
           node_y = picked(m);

           K_free( (n-1)*3+1 : n*3 , (m-1)*3+1 : m*3 ) = Kd( (node_x-1)*3+1 : node_x*3 ,
(node_y-1)*3+1 : node_y*3 );
           M_free( (n-1)*3+1 : n*3 , (m-1)*3+1 : m*3 ) = Md( (node_x-1)*3+1 : node_x*3 ,
(node_y-1)*3+1 : node_y*3 );

       end
   end

   phi_d_LOW_D = phi_d_LOW ( 1:n_node_disk_interior*3 , : );
   phi_d_LOW_R = phi_d_LOW ( n_node_disk_interior*3+1 :
(n_node_disk_interior+n_node_interface)*3 , : );
   phi_d_LOW_a = phi_d_LOW ( (n_node_disk_interior+n_node_interface)*3+1 :
(n_node_disk_interior+n_node_interface+n_matching)*3 , : );

   phi_d_HIGH_D = phi_d_HIGH ( 1:n_node_disk_interior*3 , : );
   phi_d_HIGH_R = phi_d_HIGH ( n_node_disk_interior*3+1 :
(n_node_disk_interior+n_node_interface)*3 , : );
   phi_d_HIGH_a = phi_d_HIGH ( (n_node_disk_interior+n_node_interface)*3+1 :
(n_node_disk_interior+n_node_interface+n_matching)*3 , : );

   phi_d = [ phi_d_HIGH_a ; phi_d_HIGH_D ; phi_d_LOW_a ; phi_d_LOW_D ];

   clear phi_d_*;
   clear MODAL_DISK_*;
```

```
   K_DD = K_free( 1:n_node_disk_interior*3 , 1:n_node_disk_interior*3 );
   K_DR = K_free( 1:n_node_disk_interior*3 , n_node_disk_interior*3+1 :
(n_node_disk_interior+n_node_interface)*3 );
   K_Da = K_free( 1:n_node_disk_interior*3 , (n_node_disk_interior+n_node_interface)*3+1 :
(n_node_disk_interior+n_node_interface+n_matching)*3 );
   K_Db = K_free( 1:n_node_disk_interior*3 ,
(n_node_disk_interior+n_node_interface+n_matching)*3+1 :
(n_node_disk_interior+n_node_interface+n_matching*2)*3 );

   K_RR = K_free( n_node_disk_interior*3+1 : (n_node_disk_interior+n_node_interface)*3 ,
n_node_disk_interior*3+1 : (n_node_disk_interior+n_node_interface)*3 );
   K_Ra = K_free( n_node_disk_interior*3+1 : (n_node_disk_interior+n_node_interface)*3 ,
(n_node_disk_interior+n_node_interface)*3+1 :
(n_node_disk_interior+n_node_interface+n_matching)*3 );
   K_Rb = K_free( n_node_disk_interior*3+1 : (n_node_disk_interior+n_node_interface)*3 ,
(n_node_disk_interior+n_node_interface+n_matching)*3+1 :
(n_node_disk_interior+n_node_interface+n_matching*2)*3 );

   K_aa = K_free( (n_node_disk_interior+n_node_interface)*3+1 :
(n_node_disk_interior+n_node_interface+n_matching)*3 ,
(n_node_disk_interior+n_node_interface)*3+1 :
(n_node_disk_interior+n_node_interface+n_matching)*3 );
   K_ab = K_free( (n_node_disk_interior+n_node_interface)*3+1 :
(n_node_disk_interior+n_node_interface+n_matching)*3 ,
(n_node_disk_interior+n_node_interface+n_matching)*3+1 :
(n_node_disk_interior+n_node_interface+n_matching*2)*3 );

   K_bb = K_free( (n_node_disk_interior+n_node_interface+n_matching)*3+1 :
(n_node_disk_interior+n_node_interface+n_matching*2)*3 ,
(n_node_disk_interior+n_node_interface+n_matching)*3+1 :
(n_node_disk_interior+n_node_interface+n_matching*2)*3 );

   M_DD = M_free( 1:n_node_disk_interior*3 , 1:n_node_disk_interior*3 );
   M_DR = M_free( 1:n_node_disk_interior*3 , n_node_disk_interior*3+1 :
(n_node_disk_interior+n_node_interface)*3 );
   M_Da = M_free( 1:n_node_disk_interior*3 , (n_node_disk_interior+n_node_interface)*3+1 :
(n_node_disk_interior+n_node_interface+n_matching)*3 );
   M_Db = M_free( 1:n_node_disk_interior*3 ,
(n_node_disk_interior+n_node_interface+n_matching)*3+1 :
(n_node_disk_interior+n_node_interface+n_matching*2)*3 );

   M_RR = M_free( n_node_disk_interior*3+1 : (n_node_disk_interior+n_node_interface)*3 ,
n_node_disk_interior*3+1 : (n_node_disk_interior+n_node_interface)*3 );
   M_Ra = M_free( n_node_disk_interior*3+1 : (n_node_disk_interior+n_node_interface)*3 ,
(n_node_disk_interior+n_node_interface)*3+1 :
(n_node_disk_interior+n_node_interface+n_matching)*3 );
   M_Rb = M_free( n_node_disk_interior*3+1 : (n_node_disk_interior+n_node_interface)*3 ,
(n_node_disk_interior+n_node_interface+n_matching)*3+1 :
(n_node_disk_interior+n_node_interface+n_matching*2)*3 );

   M_aa = M_free( (n_node_disk_interior+n_node_interface)*3+1 :
(n_node_disk_interior+n_node_interface+n_matching)*3 ,
(n_node_disk_interior+n_node_interface)*3+1 :
(n_node_disk_interior+n_node_interface+n_matching)*3 );
   M_ab = M_free( (n_node_disk_interior+n_node_interface)*3+1 :
(n_node_disk_interior+n_node_interface+n_matching)*3 ,
(n_node_disk_interior+n_node_interface+n_matching)*3+1 :
(n_node_disk_interior+n_node_interface+n_matching*2)*3 );

   M_bb = M_free( (n_node_disk_interior+n_node_interface+n_matching)*3+1 :
(n_node_disk_interior+n_node_interface+n_matching*2)*3 ,
(n_node_disk_interior+n_node_interface+n_matching)*3+1 :
(n_node_disk_interior+n_node_interface+n_matching*2)*3 );

   T = kron( eye(n_matching) , T_rot );

   K_Db = K_Db * T;
   K_Rb = K_Rb * T;
   K_ab = K_ab * T;
   K_bb = T' * K_bb * T;

   % ************************************************************************

   MU_dc_d = zeros( n_mode_disk , N*n_node_interface*3 );
   MU_cc_d = zeros( N*n_node_interface*3 );
   K_cc_d = zeros( N*n_node_interface*3 );

   for ND = 1 : n_ND_disk
```

```
       h = ND-1; % number of nodal diameters (harmonics)
       sine_h = sin(h*alfa);
       cosine_h = cos(h*alfa);

       if ( h == 0 )

           phi_dh = phi_d( (n_node_disk_interior+n_matching)*3+1 :
(n_node_disk_interior+n_matching)*3*2 , 1 : n_modeperND_disk );

           temp = (K_Da+K_Db*cosine_h);

           K_d_SS = [ (K_aa + (K_ab+K_ab')*cosine_h + K_bb)    temp' ;
                                  temp                        K_DD ];

           K_d_SR = [ (K_Ra'+K_Rb'*cosine_h) ;
               K_DR ];

           K_d_RR = K_RR;

           temp = (M_Da+M_Db*cosine_h);

           M_d_SS = [ (M_aa + (M_ab+M_ab')*cosine_h + M_bb)    temp' ;
                                  temp                        M_DD ];

           M_d_SR = [ (M_Ra'+M_Rb'*cosine_h) ;
               M_DR ];

           M_d_RR = M_RR;

           psi_dh = -inv(K_d_SS)*K_d_SR;

           MU_dc_d( 1 : n_modeperND_disk , 1 : n_node_interface*3 ) = phi_dh'*( M_d_SS*psi_dh +
M_d_SR);
           MU_cc_d( 1 : n_node_interface*3 , 1 : n_node_interface*3 ) = psi_dh'*( M_d_SS*psi_dh
+ M_d_SR) + M_d_SR'*psi_dh + M_d_RR ;
           K_cc_d( 1 : n_node_interface*3 , 1 : n_node_interface*3 ) = K_d_RR + K_d_SR'*psi_dh;

       elseif ( h == P )

           phi_dh = phi_d( (n_node_disk_interior+n_matching)*3+1 :
(n_node_disk_interior+n_matching)*3*2 , h*n_modeperND_disk+1 : (h+1)*n_modeperND_disk );

           temp = (K_Da+K_Db*cosine_h);

           K_d_SS = [ (K_aa + (K_ab+K_ab')*cosine_h + K_bb)    temp' ;
                                  temp                        K_DD ];

           K_d_SR = [ (K_Ra'+K_Rb'*cosine_h) ;
               K_DR ];

           K_d_RR = K_RR;


           temp = (M_Da+M_Db*cosine_h);

           M_d_SS = [ (M_aa + (M_ab+M_ab')*cosine_h + M_bb)    temp' ;
                                  temp                        M_DD ];

           M_d_SR = [ (M_Ra'+M_Rb'*cosine_h) ;
               M_DR ];

           M_d_RR = M_RR;

           Mtemp = [ M_d_SS M_d_SR ; M_d_SR' M_d_RR ];
           Ktemp = [ K_d_SS K_d_SR ; K_d_SR' K_d_RR ];

           psi_dh = -inv(K_d_SS)*K_d_SR;

           MU_dc_d( h*n_modeperND_disk+1 : (h+1)*n_modeperND_disk , (N-1)*n_node_interface*3+1 :
N*n_node_interface*3 ) = phi_dh'*( M_d_SS*psi_dh + M_d_SR);
           MU_cc_d( (N-1)*n_node_interface*3+1 : N*n_node_interface*3 , (N-
1)*n_node_interface*3+1 : N*n_node_interface*3 ) = psi_dh'*( M_d_SS*psi_dh + M_d_SR) +
M_d_SR'*psi_dh + M_d_RR ;
           K_cc_d( (N-1)*n_node_interface*3+1 : N*n_node_interface*3 , (N-
1)*n_node_interface*3+1 : N*n_node_interface*3 ) = K_d_RR + K_d_SR'*psi_dh;

       else

           phi_dh = phi_d( : , h*n_modeperND_disk+1 : (h+1)*n_modeperND_disk );
```

```
          temp = (K_Da+K_Db*cosine_h);

          K_d_SS0 = [ (K_aa + (K_ab+K_ab')*cosine_h + K_bb)    temp' ;
                                 temp                         K_DD ];

          temp = K_Db*sine_h;

          K_d_SS1 = [ (K_ab-K_ab')*sine_h            -temp' ;
                               temp    zeros(n_node_disk_interior*3) ];

          temp = K_Rb'*sine_h;
          temp2 = (K_Ra' + K_Rb'*cosine_h);

          K_d_SR = [ temp2 -temp;
              K_DR                    zeros(n_node_disk_interior*3,n_node_interface*3);
              temp            temp2;
              zeros(n_node_disk_interior*3,n_node_interface*3)    K_DR ];

          K_d_RR = [ K_RR zeros(n_node_interface*3);
              zeros(n_node_interface*3) K_RR ];

          K_d_SS = [ K_d_SS0  K_d_SS1 ;
              K_d_SS1' K_d_SS0 ];

          temp = (M_Da+M_Db*cosine_h);

          M_d_SS0 = [ (M_aa + (M_ab+M_ab')*cosine_h + M_bb)    temp' ;
                                 temp                         M_DD ];

          temp = M_Db*sine_h;

          M_d_SS1 = [ (M_ab-M_ab')*sine_h            -temp' ;
                               temp    zeros(n_node_disk_interior*3) ];

          temp = M_Rb'*sine_h;
          temp2 = (M_Ra' + M_Rb'*cosine_h);

          M_d_SR = [ temp2 -temp;
              M_DR                    zeros(n_node_disk_interior*3,n_node_interface*3);
              temp            temp2;
              zeros(n_node_disk_interior*3,n_node_interface*3)    M_DR ];

          M_d_RR = [ M_RR zeros(n_node_interface*3);
              zeros(n_node_interface*3) M_RR ];

          M_d_SS = [ M_d_SS0  M_d_SS1 ;
              M_d_SS1' M_d_SS0 ];

          psi_dh = -inv(K_d_SS)*K_d_SR;

          MU_dc_d( h*n_modeperND_disk+1 : (h+1)*n_modeperND_disk , n_node_interface*3+(h-
1)*n_node_interface*3*2+1 : n_node_interface*3+h*n_node_interface*3*2 ) = phi_dh'*(
M_d_SS*psi_dh + M_d_SR);
          MU_cc_d( n_node_interface*3+(h-1)*n_node_interface*3*2+1 :
n_node_interface*3+h*n_node_interface*3*2 , n_node_interface*3+(h-1)*n_node_interface*3*2+1 :
n_node_interface*3+h*n_node_interface*3*2 ) = psi_dh'*( M_d_SS*psi_dh + M_d_SR) + M_d_SR'*psi_dh
+ M_d_RR ;
          K_cc_d( n_node_interface*3+(h-1)*n_node_interface*3*2+1 :
n_node_interface*3+h*n_node_interface*3*2 , n_node_interface*3+(h-1)*n_node_interface*3*2+1 :
n_node_interface*3+h*n_node_interface*3*2 ) = K_d_RR + K_d_SR'*psi_dh;

       end

   end

   clear temp*;

   disp(sprintf('Disk components are calculated!'))

   % ************************************************************************
   %                                BLADE
   % ************************************************************************

   lamda_b = diag( FREQ_BLADE(:,3).^2 );

   node_list_blade_ordered = [ node_list_blade_fixedinterface ; node_list_interface ] ;

   n_node_blade_ordered = size(node_list_blade_ordered,1);

   Kb_free = zeros(n_node_blade_ordered*3);
```

```
   Mb_free = zeros(n_node_blade_ordered*3);
   phi_b = zeros(n_node_blade_ordered*3,n_mode_blade);

   for n=1:n_node_blade_ordered
       picked(n,1) = pick( node_list_blade , node_list_blade_ordered(n) );
   end

   for n=1:n_node_blade_ordered
       node_x = picked(n);
       phi_b( (n-1)*3+1 : n*3 , : ) = MODAL_BLADE( (node_x-1)*3+1 : node_x*3 , : );
       for m=1:n_node_blade_ordered
           node_y = picked(m);

           Kb_free( (n-1)*3+1 : n*3 , (m-1)*3+1 : m*3 ) = Kb( (node_x-1)*3+1 : node_x*3 ,
(node_y-1)*3+1 : node_y*3 );
           Mb_free( (n-1)*3+1 : n*3 , (m-1)*3+1 : m*3 ) = Mb( (node_x-1)*3+1 : node_x*3 ,
(node_y-1)*3+1 : node_y*3 );

       end
   end

   phi_b = phi_b ( 1:n_node_blade_fixedinterface*3 , :);

   K_BB = Kb_free( 1:n_node_blade_fixedinterface*3 , 1:n_node_blade_fixedinterface*3 );
   K_BR = Kb_free( 1:n_node_blade_fixedinterface*3 , n_node_blade_fixedinterface*3+1 :
(n_node_blade_fixedinterface+n_node_interface)*3 );

   K_RR = Kb_free( n_node_blade_fixedinterface*3+1 :
(n_node_blade_fixedinterface+n_node_interface)*3 , n_node_blade_fixedinterface*3+1 :
(n_node_blade_fixedinterface+n_node_interface)*3 );

   M_BB = Mb_free( 1:n_node_blade_fixedinterface*3 , 1:n_node_blade_fixedinterface*3 );
   M_BR = Mb_free( 1:n_node_blade_fixedinterface*3 , n_node_blade_fixedinterface*3+1 :
(n_node_blade_fixedinterface+n_node_interface)*3 );

   M_RR = Mb_free( n_node_blade_fixedinterface*3+1 :
(n_node_blade_fixedinterface+n_node_interface)*3 , n_node_blade_fixedinterface*3+1 :
(n_node_blade_fixedinterface+n_node_interface)*3 );

   psi_b = -inv(K_BB)*K_BR;

   MU_bc_b = phi_b' * ( M_BB*psi_b + M_BR );
   MU_cc_b = psi_b' * ( M_BB*psi_b + M_BR ) + M_BR'*psi_b + M_RR;
   K_cc_b = K_RR + K_BR'*psi_b;

   disp(sprintf('Blade components are calculated!'))

   % ************************************************************************
   %                                   ASSEMBLY
   % ************************************************************************

   % Constructing Fourier expansion matrix F

   F = zeros(N);

   F(:,1) = ones(N,1)/sqrt(N);

   for i = 1:n_ND_disk-2
       for j = 1:N
           F( j , 1+(i-1)*2+1 ) = sqrt(2/N)*cos( alfa*i*(j-1) );
           F( j , 1+(i-1)*2+2 ) = sqrt(2/N)*sin( alfa*i*(j-1) );
       end
   end

   if ( mod(N,2) == 0 )
       for j = 1:N
           F(j,N) = (-1)^(j+1)/sqrt(N);
       end
   end

   Fcap = kron( F , eye(n_node_interface*3) );

   mist_percentage = 0;
   mist_pattern = importdata( 'MistuningData.txt' );
   mist_pattern = mist_pattern * mist_percentage;

   a_M = [ eye(n_mode_disk)              MU_dc_d
zeros(n_mode_disk,n_mode_blade*N) ;
              MU_dc_d'         (MU_cc_d+kron(eye(N),MU_cc_b))         temp' ;
          zeros(n_mode_blade*N,n_mode_disk)    temp  eye(n_mode_blade*N) ];
```

```
   a_K = [ lamda_d       zeros(n_mode_disk,n_node_interface*3*N)
zeros(n_mode_disk,n_mode_blade*N);
         zeros(n_node_interface*3*N,n_mode_disk)       (K_cc_d+kron(eye(N),K_cc_b))
zeros(n_node_interface*3*N,n_mode_blade*N) ;
         zeros(n_mode_blade*N,n_mode_disk)     zeros(n_mode_blade*N,n_node_interface*3*N)
kron(diag(1+mist_pattern),lamda_b) ];

   clear K*;
   clear M*;

   toc;
   disp(sprintf('Assembly successful!'))

   % Correct symmetry
   a_K = (a_K/2 + a_K'/2);
   a_M = (a_M/2 + a_M'/2);

   n_eig = 200;

   % [V,D] = eig( a_K , a_M );
   tic;
   [V,D] = eigs( a_K , a_M , n_eig , 'SM' );
   disp('Eigenvalues and eigenvectors are extracted!')
   toc;

   wr_sq = max ( real (D) );

   [Dsorted,I] = sort(wr_sq);

   for n=1:n_eig
       wr_sq_sorted(n) = wr_sq(I(n));
       V_sorted(:,n) = V(:,I(n));
   end

   wr_sq = wr_sq_sorted;
   V = real( V_sorted );

   clear a_*;
   clear T_rot_assm;
   clear temp;

   save modalexport.mat
```

APPENDIX C. CODE FOR SUBSET OF NOMINAL MODES METHOD

```
clear;
clc;

N = 36;
max_modeperND = 10;
mist_percentage = 5;

file_blade_mass = 'BLADE_MASS.MATRIX';
file_blade_stiffness = 'BLADE_STIFFNESS.MATRIX';
file_mistuning = 'MISTUNING_DATA.TXT';

file_tuned_nodeno = 'TUNED_NODENO.TXT';
file_tuned_freq = 'TUNED_FREQ.TXT';
file_tuned_modal = 'TUNED_MODAL.TXT';

[ K , M ] = ansys_mat_import ( file_blade_mass , file_blade_stiffness );

node_list = uint32 ( importdata( file_tuned_nodeno ) );
FREQ = importdata ( file_tuned_freq );
MODAL = importdata ( file_tuned_modal );
c = importdata ( file_mistuning ) * mist_percentage;

n_mode = size ( FREQ , 1 );
n_ND = max ( FREQ(:,1) );
n_modeperND = max ( FREQ(:,2) );
n_dof = size ( K , 1 );


eb = @(j,k) exp( i*(j-1)*(k-1)*2*pi/N ) / sqrt(N);


clear file_*;

% CORRECT ANSYS OUTPUT FORMAT

FREQ( : , 3 ) = FREQ( : , 3 ) * 2*pi;

% SET MAXIMUM NUMBER OF MODES/ND

if (n_modeperND > max_modeperND)

    FREQ_TEMP = zeros( n_ND * max_modeperND , 3 );
    MODAL_TEMP = zeros( size(MODAL,1) , n_ND * max_modeperND );

    n = 1;
    while n<=n_ND
        FREQ_TEMP( (n-1)*max_modeperND+1 : n*max_modeperND , : ) = FREQ( (n-1)*n_modeperND+1
: (n-1)*n_modeperND + max_modeperND , : );
        if ( (n==n_ND) || (n==1) )
            MODAL_TEMP( : , (n-1)*max_modeperND+1 : n*max_modeperND ) = MODAL( : , (n-
1)*n_modeperND+1 : (n-1)*n_modeperND + max_modeperND ) / sqrt(2);
        else
            MODAL_TEMP( : , (n-1)*max_modeperND+1 : n*max_modeperND ) = MODAL( : , (n-
1)*n_modeperND+1 : (n-1)*n_modeperND + max_modeperND );
        end
        n = n + 1;
    end

    n_modeperND = max_modeperND;
    FREQ = FREQ_TEMP;
    MODAL = MODAL_TEMP;
    n_mode = size( FREQ , 1 );
    clear *_TEMP;

end

% CALCULATING MATRIX MULTIPLICATIONS

clear i;
MODAL_COMPLEX = MODAL(1:n_dof , :) + i*MODAL(n_dof+1:2*n_dof , :);
```

```
   mod = zeros(n_ND);

   j = 1;
   while j <= n_ND
       k = j;
       while k <= n_ND
           n = 1;
           while n<=N
               mod(j,k) = mod(j,k) + eb(j,n)'*c(n)*eb(k,n);
               n = n + 1;
           end
           mod(k,j) = mod(j,k)';
           k = k + 1;
       end
       j = j + 1;
   end

   dK = zeros(n_mode,n_mode);

   j = 1;
   while j <= n_ND
       k = 1;
       while k <= n_ND
           dK( (j-1)*n_modeperND+1 : j*n_modeperND , (k-1)*n_modeperND+1 : k*n_modeperND ) =
MODAL_COMPLEX(:,(j-1)*n_modeperND+1 : j*n_modeperND)' * K * MODAL_COMPLEX(:,(k-1)*n_modeperND+1
: k*n_modeperND) * mod(j,k);
           dK( (k-1)*n_modeperND+1 : k*n_modeperND , (j-1)*n_modeperND+1 : j*n_modeperND ) = dK(
(j-1)*n_modeperND+1 : j*n_modeperND , (k-1)*n_modeperND+1 : k*n_modeperND )';
           if ( j == k )
               dK( (j-1)*n_modeperND+1 : j*n_modeperND , (k-1)*n_modeperND+1 : k*n_modeperND ) =
dK( (j-1)*n_modeperND+1 : j*n_modeperND , (k-1)*n_modeperND+1 : k*n_modeperND )/2 + dK( (j-
1)*n_modeperND+1 : j*n_modeperND , (k-1)*n_modeperND+1 : k*n_modeperND )'/2;
           end
           k = k + 1;
       end
       j = j + 1;
   end

   n_eig = 100;
   lamda = FREQ(:,3).^2;
   [ V , D ] = eigs( diag(lamda)+dK , eye(n_mode) , n_eig , 'SM' );

   wr_sq = max ( real (D) );

   [Dsorted,I] = sort(wr_sq);

   for n=1:n_eig
       wr_sq_sorted(n) = wr_sq(I(n));
       V_sorted(:,n) = V(:,I(n));
   end

   wr_sq = wr_sq_sorted;
   V = real( V_sorted );
```

APPENDIX D. CODE FOR NONLINEAR ELEMENTS

```
function [ F , Kf , state] = friction_elem_macroslip( X , N0 , mu , kx )

N = N0*mu;

Xc = X(2);
Xs = X(3);
Xbar = sqrt(Xc^2+Xs^2);
Xcr = N/kx;

if ( Xbar > Xcr )

    state = 2;

    Xr = Xc;
    Xi = -Xs;

    ho = (Xbar-2*Xcr)/Xbar;
    beta = acos( ho );

    kr = (kx/pi)*(beta - 0.5*sin(2*beta));
    ki = ((4*N)/(pi*Xbar))*(Xbar-Xcr)/Xbar;

    Fr = kr*Xr - ki*Xi;
    Fi = kr*Xi + ki*Xr;

    dkrdbeta = kx*(1-cos(2*beta))/pi;
    dkidX = 4*N/(pi*Xbar^2)-8*N*(Xbar-Xcr)/(pi*Xbar^3);

    dbetadX = (-1/sqrt(1-ho^2)*(1-ho)/Xbar);

    dXdXr = Xr/Xbar;
    dXdXi = Xi/Xbar;

    dkrdXr = dkrdbeta*dbetadX*dXdXr;
    dkidXr = dkidX*dXdXr;
    dkrdXi = dkrdbeta*dbetadX*dXdXi;
    dkidXi = dkidX*dXdXi;

    dFrdXr = kr + Xr*dkrdXr - dkidXr*Xi;
    dFrdXi = Xr*dkrdXi - dkidXi*Xi - ki;
    dFidXr = dkrdXr*Xi + dkidXr*Xr + ki;
    dFidXi = dkrdXi*Xi + kr + dkidXi*Xr;

    F = [ 0 ; Fr ; -Fi ];

    Kf = [ 0 0 0 ; 0 dFrdXr -dFrdXi ; 0 -dFidXr dFidXi ];

else

    F = kx * X;
    Kf = eye(3) * kx;
    Kf(1,1) = 0;
    state = 1;

end
```

```
function [ F , Kf , state] = friction_elem_twoslope_microslip( X , F1 , k1 , k2 )

kb = max([k1,k2]);
ks = min([k1,k2]);

kx = kb - ks;

N = F1;
```

```
Xc = X(2);
Xs = X(3);
Xbar = sqrt(Xc^2+Xs^2);
Xcr = N/kx;

if ( Xbar > Xcr )

    state = 2;

    Xr = Xc;
    Xi = -Xs;

    ho = (Xbar-2*Xcr)/Xbar;
    beta = acos( ho );

    kr = (kx/pi)*(beta - 0.5*sin(2*beta));
    ki = ((4*N)/(pi*Xbar))*(Xbar-Xcr)/Xbar;

    Fr = kr*Xr - ki*Xi;
    Fi = kr*Xi + ki*Xr;

    dkrdbeta = kx*(1-cos(2*beta))/pi;
    dkidX = 4*N/(pi*Xbar^2)-8*N*(Xbar-Xcr)/(pi*Xbar^3);

    dbetadX = -1/sqrt(1-ho^2)*(1-ho)/Xbar;

    dXdXr = Xr/Xbar;
    dXdXi = Xi/Xbar;

    dkrdXr = dkrdbeta*dbetadX*dXdXr;
    dkidXr = dkidX*dXdXr;
    dkrdXi = dkrdbeta*dbetadX*dXdXi;
    dkidXi = dkidX*dXdXi;

    dFrdXr = kr + Xr*dkrdXr - dkidXr*Xi;
    dFrdXi = Xr*dkrdXi - dkidXi*Xi - ki;
    dFidXr = dkrdXr*Xi + dkidXr*Xr + ki;
    dFidXi = dkrdXi*Xi + kr + dkidXi*Xr;

    F = [ 0 ; Fr ; -Fi ] + ks * X;

    Kf = [ 0 0 0 ; 0 dFrdXr -dFrdXi ; 0 -dFidXr dFidXi ] + eye(3) * ks;
    Kf(1,1) = 0;

else

    F = kb * X;
    Kf = eye(3) * kb;
    Kf(1,1) = 0;
    state = 1;

end
```

```
function [ F , Kf , state ] = gap_elem_singleharmonic( Y , ky , g )
% [ F , Kf , state ] = gap_elem( Y , ky , g )
%
% Friction element calculation procedure.
% X: Tangential displacement components
% Y: Normal displacement components
% kx: Tangential stiffness
% ky: Normal stiffness
% N0: Normal loading ( initial gap obtained by negative loading )
% mu: Coefficient of friction

m = 1;
len = 2*m+1;

F = zeros(len,1);
Kf = zeros(len);

if ( ky == 0 )
    state = -1;
    return;
```

```
end

N0 = -g*ky;

Y0 = Y(1);
Yc = Y(2);
Ys = Y(3);

Ybar = sqrt( Ys^2 + Yc^2 );
psi = atan2( Yc , Ys );

ratio_gap2Ybar = (g-Y0)/Ybar;

if ( ratio_gap2Ybar > 1 )

    % Full seperation
    state = 0;

elseif ( ratio_gap2Ybar < -1 )

    % Full contact
    state = 2;

    F = ky * Y;
    F(1,1) = F(1,1) + N0;
    Kf = ky * eye(len);

else

    % Partial contact
    state = 1;

    phi1 = asin( ratio_gap2Ybar );
    phi2 = pi - phi1;

    teta1 = phi1 - psi;
    teta2 = phi2 - psi;

    if ( teta1 < 0 )
        teta1 = teta1 + 2*pi;
    end

    if ( teta2 < 0 )
        teta2 = teta2 + 2*pi;
    end

    teta = sort( [ teta1 ; teta2 ] );

    y_mid = Hminus( (teta(1)+teta(2))/2 , m )' * Y;

    if (y_mid < g)
        teta = [ teta(2) (teta(1)+2*pi) ];
    end

    W = 1/pi * (HmHp_int(teta(2),m) - HmHp_int(teta(1),m));
    w = 1/pi * (Hp_int(teta(2),m) - Hp_int(teta(1),m));

    F = N0 * w + ky * W * Y;

    Kf = ky * W;

end
```

```
function [ F , Kf , state ] = gap_elem( Y , ky , g )
% Friction element calculation procedure.
%
% Y: Normal displacement components
% ky: Normal stiffness
% g: Initial gap

len = length(Y);

F = zeros(len,1);
Kf = zeros(len);
```

```
   if ( ky == 0 )
       state = -1;
       return;
   end

   N0 = -g*ky;

   m = ( len-1 ) / 2; % number of harmonics

   flag_print = 0;

   % Calculating seperation instants
   N = 2*m; % Number of brackets equal to twice the number of harmonics

   % Bracketing
   k = 0;
   for i = 1:N
       t(i) = (i-1)*2*pi/N;
       y(i) = Hminus( t(i) , m )' * Y;
       dy(i) = dHminus( t(i) , m )' * Y;
   end
   t(N+1) = t(1)+2*pi;
   y(N+1) = y(1);
   dy(N+1) = dy(1);

   s = N0 + ky * y;

   n_root = 0;
   for i = 1:N
       if( sign(s(i))*sign(s(i+1)) < 0 )
           n_root = n_root + 1;
           t_sep(n_root) = root_bracket( @(tao) N0 + ky * Hminus( tao , m )' * Y , t(i) , t(i+1)
);
       elseif ( (sign(dy(i))*sign(dy(i+1)) < 0) && (sign(s(i))*sign(dy(i)) < 0) )
           t_ext = root_bracket( @(tao) dHminus( tao , m )' * Y , t(i) , t(i+1) );
           s_ext = N0 + ky * Hminus( t_ext , m )' * Y;
           if ( sign(s(i))*sign(s_ext) < 0 )
               n_root = n_root + 1;
               t_sep(n_root) = root_bracket( @(tao) N0 + ky * Hminus( tao , m )' * Y , t(i) ,
t_ext );
               n_root = n_root + 1;
               t_sep(n_root) = root_bracket( @(tao) N0 + ky * Hminus( tao , m )' * Y , t_ext ,
t(i+1) );
           end
       end
   end

   % Check if full seperated!
   if ( (n_root == 0) && (s(i) < 0) )
       state = 0;
       if ( flag_print)
           disp('Full seperation');
       end
       return;


   % Check for no seperation!
   elseif ( (n_root == 0) && (s(i) > 0) )
       state = 2;
       if ( flag_print )
           disp(sprintf('No seperation '));
       end

       F = ky * Y;
       F(1) = F(1) + N0; % Modification
       Kf = ky * eye(len);

   else
       % Partial contact
       state = 1;
       if ( flag_print )
           disp('Partial contact');
       end

       t_sep = sort(t_sep); % Seperation/Contact instants calculated!
       contact_data = [ 0 0 ];
       c = 0;

       t_sep(n_root+1) = t_sep(1)+2*pi;
```

```
    for i=1:n_root
        t_mid = (t_sep(i)+t_sep(i+1))/2;
        normal = N0 + ky * Hminus( t_mid, m )' * Y;
        if ( normal > 0 )
            c = c + 1;
            contact_data(c,:) = [ t_sep(i) t_sep(i+1) ];
        end
    end

    % For each contact period in contact_data
    for i = 1:c

        t_contact = contact_data(i,1);
        t_separation = contact_data(i,2);

        W = 1/pi * (HmHp_int(t_separation,m) - HmHp_int(t_contact,m));
        w = 1/pi * (Hp_int(t_separation,m) - Hp_int(t_contact,m));

        F = F + N0 * w + ky * W * Y;

        Kf = Kf + ky * W;

    end

end
```

APPENDIX E. ANSYS MACROS

```
MODAL DATA EXPORT

/PMACRO
/POST1
/OUTPUT, C:\MODALDATAEXPORT.TXT

*GET,Nnode,NODE,0,COUNT
*GET,Min_node,NODE,0,NUM,MIN
*GET,Max_node,NODE,0,NUM,MAX

! Get node numbers
*DIM, NodeNumber, ARRAY, Nnode

Ndof = Nnode*3

n = 1
*DO,k,Min_node,Max_node,1

sel = NSEL(k)
*IF,sel,EQ,1,THEN
NodeNumber(n) = k
n = n + 1
*ENDIF

*ENDDO

SET,FIRST
*GET,Nmodefirst,ACTIVE,0,SET,SBST
*GET,Ncycfirst,ACTIVE,0,SET,LSTP
SET,LAST
*GET,Nmodelast,ACTIVE,0,SET,SBST
*GET,Ncyclast,ACTIVE,0,SET,LSTP

Nmode = Nmodelast-Nmodefirst+1
Ncyclic = Ncyclast-Ncycfirst+1
NTmode = Nmode*Ncyclic

*DIM, Freq, ARRAY, NTmode , 3
*DIM, Modal, ARRAY, Ndof, NTmode

n = 1

*DO,cycno,Ncycfirst,Ncyclast,1
*DO,modeno,Nmodefirst,Nmodelast,1

SET,cycno,modeno

Freq(n,1) = cycno
Freq(n,2) = modeno
*GET,fff,ACTIVE,0,SET,FREQ
Freq(n,3) = fff

*DO,k,1,Nnode,1

nodeno = NodeNumber(k,1)
Modal( (k-1)*3+1 , n) = Ux(nodeno)
Modal( (k-1)*3+2 , n) = Uy(nodeno)
Modal( k*3 , n) = Uz(nodeno)

*ENDDO

n = n+1

*ENDDO
*ENDDO

*MWRITE, Freq, C:\FREQ.TXT
%I %I %20.13E
*MWRITE, Modal, C:\MODAL.TXT
(10000000000000000E22.13)
```

```
*MWRITE, NodeNumber, C:\NODENO.TXT
%I


/OUTPUT
```

```
IMPOSE MISTUNING ON BLADE MODULUS OF ELASTICITY

/PREP7
N = 36
Modulus = 207000
Density = 8.4E-006
Poisson = 0.3
*DIM, Mistuning, ARRAY, N , 1

*VREAD, Mistuning(1), D:\HQ\FEM\Projects\Ansys\macros\MistuningData.txt
(1F32.0)

*DO,sector,1,N,1

MP, EX , 2*sector-1 , Modulus
MP, PRXY , 2*sector-1 , Poisson
MP, DENS , 2*sector-1 , Density

MP, EX , 2*sector , Modulus*(1+Mistuning(sector))
MP, PRXY , 2*sector , Poisson
MP, DENS , 2*sector , Density

*ENDDO
```

APPENDIX F. PAPER

9th International Conference on Vibrations in Rotating Machinery

8-10 September 2008, Exeter, UK

Non-linear Periodic Response Analysis of Mistuned Bladed Disk Assemblies in Modal Domain

Günay Orbay and H. Nevzat Özgüven
Department of Mechanical Engineering
Middle East Technical University
Ankara 06531, TURKEY

1 SYNOPSIS

Mistuning phenomenon has been studied extensively for almost half a century, especially for bladed disk assemblies. However, the studies hitherto focus on either linear models with distributed parameter mistuning or nonlinear models with point mistuning. The former method is not realistic under significant non-linear effects. Whereas the latter method lacks accuracy since discrete mistuning elements distort the mode shapes unless their numbers are large. Therefore a model which includes both nonlinearities and distributed parameter mistuning is required. In this study, a formulation for the analysis of mistuned bladed disk assemblies under periodic loads in the presence of distributed parameter mistuning and nonlinearity is given. The proposed method combines the component mode synthesis based reduced order modeling approach with non-linear forced response analysis technique in modal space. The calculations are carried out in modal domain which reduces the computational effort considerably, especially for large size finite element (FE) models. The mistuning is imposed on individual blade natural frequencies, which is more realistic compared to adding discrete mistuning elements. A case study is presented to demonstrate the application of the method and the effect of macro-slip friction type nonlinearity on the dynamic analysis of a mistuned bladed disk assembly. It is concluded that considering non-linear effects in the dynamic analysis of mistuned bladed disks is crucial when there exists significant non-linearity, such as gaps and friction dampers in the system. It is believed that this is the first study in which non-linear dynamic analysis of bladed disk assemblies is carried out with distributed parameter mistuning.

2 INTRODUCTION

Forced response predictions of bladed disk assemblies have been the main focus of researchers for the last few decades. Due to their cyclic symmetric structure, slight differences in structural properties and geometry of blades in bladed disk assemblies may cause significant increases in vibration amplitudes. This weakens the robustness and durability of the structure. In order to predict such responses, mistuning can be imposed on FE models. But these models usually have large numbers of degrees of freedom (DOF) requiring enormous amount of computational time for response predictions. In addition, FE analyses can no longer use a single sector of the assembly for the dynamic analysis of the mistuned assembly, since mistuning destroys the cyclic symmetric property.

Studies hitherto can be grouped by the complexity of the models used, as several DOF per sector models [1-4] and FE models [5-17]. Studies using FE approach aim to construct reduced order models which provide faster results. In some studies, frequency response function (FRF) coupling or updating techniques were employed on the modal analysis results of the tuned FE model. Yang and Griffin [14] suggested coupling the tuned disk and mistuned blades via FRF coupling. A transformation which expresses the blade-disk interface motion by a number of translational and rotational rigid body modes is applied to reduce the number of connection DOF. Yet, the FRF matrix for each DOF on the blade should be calculated for each point in the frequency range.

Petrov et al. [17] proposed a frequency domain approach which is based on FRF updating. The mistuned FRF is determined by applying linear mistuning such as stiffness and point mass as a modification on a number of DOF of the FE model of a tuned assembly. In that study, keeping the modal vector data for the DOF at which the modification is applied will be sufficient. Consequently, if it is desired to apply distributed mistuning throughout the blade, each DOF in the blade should be kept. Such an approach will be computationally expensive when fine meshes are used.

In another group of studies, reduced order models in modal domain were introduced [5-11]. Óttarsson et al. [6] developed a model in which the mistuned mode shapes are represented as a combination of disk mode shapes and cantilevered blade mode shapes. Method proves to yield accurate results when the cantilevered blade natural frequencies are tuned to compensate the stiffening caused by the fixed boundary conditions. Bladh et al. [7] extended the formulation for shrouded blade disk assemblies. On the other hand, Yang and Griffin [11, 12] suggested reducing the mistuned system by using a subset of nominal modes (SNM) of the tuned system. Mistuning is applied as linear modification matrices which are transformed into the modal domain using the subset of selected modes. They also developed a formulation for transient response calculations using the reduced order model [13]. Later, Bladh [10] developed a formulation which combines a similar approach as SNM method with fixed interface coupling method which is called Craig-Bampton method [22]. Using this formulation, mistuning is applied on the cantilevered natural frequencies of the blades.

Non-linear response of bladed disk assemblies has been studied extensively in frequency domain [e.g. see 24-28]. Recently, Petrov [18] developed formulations for typical non-linear elements and used numerical path following methods to trace the solution in frequency domain where multi-harmonics were included. The model is reduced using Craig-Bampton method and non-linear elements are connected between statically condensed DOF. This reduction aims to represent the contact interface motion more accurately under non-linear loads since it may not be accurate enough when expressed by a combination of nominal modes of the system. On the other hand, Cigeroglu et al. [19] implemented a new two-dimensional micro-slip friction model to a bladed disk.

The objective of this study is to address the question of how non-linearity and mistuning affect the displacement and stress patterns in bladed disk assemblies. Proposed technique avoids using point mistuning elements since in order to apply mistuning throughout the blade, a large number of DOF should be kept in the model. Instead, it is suggest using a reduced order model. The mode shapes of the mistuned bladed disk are calculated by Craig-Bampton method as formulated by Bladh [21]. The non-linear periodic response is calculated in modal domain, by using the method suggested by Kuran and Özgüven [20]. Numerical path following approach based on Newton method is applied in the solution. The purpose of the proposed approach is to calculate non-linear response of mistuned bladed disk assemblies with mistuning applied on the individual blade natural frequencies. Since the response is calculated in modal domain, the size of the problem is reduced to the number of modes retained irrespective of the complexity of the FE model used.

3 THEORY

3.1 Reduced Order Model

It is a well known fact that mode shapes of a mistuned bladed disk assembly are closely related to the natural frequencies of individual blades attached to the disk. As long as the mistuning pattern, which is the set of deviations of natural frequencies of each blade from the ideally tuned case, is the same for different mistuning cases, the mode shapes of the mistuned bladed disks in each case will be similar. Therefore a formulation which is capable of mistuning individual blade natural frequencies rather than adding point mistuning elements is to be preferred.

In this study a component mode synthesis method, namely the Craig-Bampton method [22], is used for model reduction. Bladh [21] employed the Craig-Bampton method for mistuned bladed disk assemblies and obtained a reduced order model in which it is possible to impose mistuning on cantilevered natural frequencies of each blade in the assembly. The mass and stiffness matrices, $[M^{cb}]$ and $[K^{cb}]$, respectively, of the reduced order model are given below using the original notation used in [21]:

$$[M^{cb}]=\begin{bmatrix} [I] & [\tilde{\mu}_{dc}] & [0] \\ [\tilde{\mu}_{dc}]^T & [\tilde{\mu}_{cc,d}]+[I]\otimes[\mu_{cc,b}] & [\hat{F}]^T[I]\otimes[\mu_{tc}]^T] \\ [0] & [[I]\otimes[\mu_{tc}]][\hat{F}] & [I] \end{bmatrix} \tag{1}$$

$$[K^{cb}]=\begin{bmatrix} [\tilde{\Lambda}_d] & [0] & [0] \\ [0] & [\tilde{\kappa}_{cc,d}]+[I]\otimes[\kappa_{cc,b}] & [0] \\ [0] & [0] & [I]\otimes[\Lambda_b] \end{bmatrix} \tag{2}$$

Here $[I]$ is the identity matrix, $[0]$ is the zero matrix, $[\tilde{\Lambda}_d]$ is the modal stiffness matrix of the disk, $[\Lambda_b]$ is the modal stiffness matrix of a single cantilevered blade, $[\mu]$ and $[\kappa]$are the reduced mass and stiffness matrices, respectively, $[\hat{F}]$ is the transformation matrix from cyclic coordinates to physical coordinates, and $\otimes$ denotes the Kronecker product. Subscripts b, d and c represent the blade, the disk and the connection DOF, respectively.

Note that the lower-right element of the stiffness matrix is a diagonal matrix. It contains the modal stiffness values of each blade in the assembly, which makes modal stiffness mistuning possible. In order to impose mistuning, cantilevered blade modal stiffness values on the diagonal elements of $[I]\otimes[\Lambda_b]$ are perturbed as:

$$\underset{n=1,\ldots,N}{\text{Bdiag}}\left[\underset{m=1,\ldots,m_b}{\text{diag}}\left(1+\delta_n^k\right)[\Lambda_b]\right] \tag{3}$$

where $Bdiag[\bullet]$ denotes the block diagonal matrix, the argument being the n^{th} (n=1,2,…) diagonal block. The details of the formulation are given in reference [21].

3.2 Non-linear Forced Response in Modal Domain

The equation of motion of a non-linear system can be expressed as:

$$[M]\{\ddot{x}\}+[C]\{\dot{x}\}+[K]\{x\}+i[H]\{x\}+\{f_{NL}\}=\{f\} \tag{4}$$

where [*M*], [*K*], [*C*] and [*H*] are the mass, stiffness, viscous damping and structural damping matrices, $\{x\}$, $\{\dot{x}\}$ and $\{\ddot{x}\}$ are the vectors of physical displacements, velocities and accelerations, respectively. $\{f_{NL}\}$ is the vector of non-linear internal forces and $\{f\}$ is the vector of external forces. *i* is the unit imaginary number.

For a periodic excitation at fundamental frequency ω, the response can be assumed as a summation of harmonic responses at ω and its harmonics as:

$$\{x\} = \sum_{m=0}^{\infty} \{X\}_m e^{im\omega t} \tag{5}$$

Then the non-linear internal force due to non-linear elements can also be written as:

$$\{f_{NL}\} = \sum_{m=0}^{\infty} \{F_{NL}\}_m e^{im\omega t} \tag{6}$$

Knowing that the aerodynamic forces on blades may not be expressed by a single harmonic function only, the external forcing term can also be written as a summation of several harmonic functions as:

$$\{f\} = \sum_{m=0}^{\infty} \{F\}_m e^{im\omega t} \tag{7}$$

Substituting equations (5), (6) and (7) into the equation (4) we obtain:

$$[K]\{X\}_0 + \{F_{NL}\}_0 = \{F\}_0 \tag{8}$$

$$\left[-(m\omega)^2[M] + i(m\omega)[C] + [K] + i[H]\right]\{X\}_m + \{F_{NL}\}_m = \{F\}_m \text{ for m = 1, 2…} \tag{9}$$

Expressing the physical displacements as a linear combination of mode shapes as:

$$\{X\}_m = [\phi]\{p\}_m \tag{10}$$

and substituting equation (10) into equations (8) and (9) we obtain:

$$\left[\omega_r^2\right]\{p\}_0 + \{\overline{F}_{NL}\}_0 = \{\overline{F}\}_0 \tag{11}$$

$$\left[-(m\omega)^2[I] + i(m\omega)[\overline{C}] + [\omega_r^2] + i[\overline{H}]\right]\{p\}_m + \{\overline{F}_{NL}\}_m = \{\overline{F}\}_m \text{ for m = 1, 2…} \tag{12}$$

where

$$\{X\}_m = [\phi]\{p\}_m, \qquad [\overline{C}] = [\phi]^T[C][\phi], \qquad [\overline{H}] = [\phi]^T[H][\phi],$$

$$\{\overline{F}_{NL}\}_m = [\phi]^T\{F_{NL}\}_m, \quad \{\overline{F}\}_m = [\phi]^T\{F\}_m$$

It should be noted that non-linear forces occur only at DOF where non-linear elements are connected to, which will be referred to as "non-linear DOF". Therefore, in order to transform the non-linear forcing term $\{\overline{F}_{NL}\}_m$ into modal domain to obtain $\{F_{NL}\}_m$, only the mode shapes of the non-linear DOF are required. Thus, the internal non-linear forcing vector can be rewritten as:

$$\{\overline{F}_{NL}\}_m = [\phi_{NL}]^T\{F_{NL,NL}\}_m \tag{13}$$

where $\{F_{NL,NL}\}$ is the vector of internal non-linear forcing at non-linear DOF and $[\phi_{NL}]$ is the mode shape matrix which belongs to the non-linear DOF. In the original formulation of Kuran and Özgüven [20] the internal non-linear force vector is expressed as a matrix composed of describing functions representing nonlinearity, multiplied by the response vector. Then the response of the system is calculated by solving equations (11) and (12) iteratively. The details of the modal analysis of non-linear systems can be found in reference [20].

3.3 Numerical Solution with Path Following

In this study, the forced response of the system is calculated by using Newton solution procedure. Arranging the terms in the equations (11) and (12) we obtain:

$$\{R_0(\{p\}_0,\omega)\}=\left[\omega_r^2\right]\{p\}_0+\{\overline{F}_{NL}\}_0-\{\overline{F}\}_0=\{0\} \tag{14}$$

$$\{R_m(\{p\}_m,\omega)\}=\left[-(m\omega)^2[I]+i(m\omega)[\overline{C}]+\left[\omega_r^2\right]+i[\overline{H}]\right]\{p\}_m+\{\overline{F}_{NL}\}_m-\{\overline{F}\}_m=\{0\} \tag{15}$$

Combining the modal displacement vectors into a single vector as:

$$\{p\}=\left[\{p\}_0^T \quad \{p\}_1^T \quad \{p\}_2^T \quad \cdots\right]^T \tag{16}$$

and collecting the functions into a single function, we obtain:

$$\{R(\{p\},\omega)\}=\left[\{R_0(\{p\}_0,\omega)\}^T \quad \{R_1(\{p\}_1,\omega)\}^T \quad \{R_2(\{p\}_2,\omega)\}^T \quad \cdots\right]^T \tag{17}$$

Then a Newton solution procedure is applied to solve for the modal displacements. For each frequency, ω_k, iteration is applied as follows:

$$\{p\}_k^{i+1}=\{p\}_k^i-\left[\frac{\partial\{R(\{p\},\omega)\}}{\partial\{p\}}\right]^{-1}\Bigg|_{\{p\}_k^i,\omega_k}\left\{R\left(\{p\}_k^i,\omega_k\right)\right\} \tag{18}$$

where $\{p\}_k^i$ is the modal solution vector at k[th] frequency ω_k and at i[th] iteration, $\left[\frac{\partial\{R(\{p\},\omega)\}}{\partial\{p\}}\right]$ is the Jacobian matrix, and $\left\{R\left(\{p\}_k^i,\omega_k\right)\right\}$ is the function evaluated at $\{p\}_k^i$ and ω_k.

For non-linear systems, there may be multiple solutions for a single ω. In such cases, there will be some points on the solution curve at which the Jacobian matrix is singular [23]. Then a numerical continuation procedure is required to trace the solution, which can be achieved by introducing a new equation

$$\{\Delta q\}_k^{i\,T}\{\Delta q\}_k^i=s^2 \tag{19}$$

that makes the Jacobian matrix non-singular where

$$\{\Delta q\}_k^i=\left\{\{q\}_k^i-\{q\}_{k-1}\right\} \tag{20}$$

and

$$\{q\}=\begin{Bmatrix}\{p\}\\ \omega\end{Bmatrix} \tag{21}$$

Now here k represents a solution point on the curve. Equation (19) guarantees that the k[th] solution lies on a hyper-sphere centered at $\{q\}_{k-1}$ having a radius of *s*.

Arranging the terms in equation (19) to define a new function

$$\left\{g\left(\{p\}_k^i,\omega_k^i\right)\right\}=\{\Delta q\}_k^{iT}\{\Delta q\}_k^i-s^2=\{0\} \tag{22}$$

The Newton iteration becomes:

$$\{q\}_k^{i+1}=\{q\}_k^i-\left[\begin{matrix}\frac{\partial\{R(\{p\},\omega)\}}{\partial\{p\}} & \frac{\partial\{R(\{p\},\omega)\}}{\partial\omega}\\ \frac{\partial g(\{p\},\omega)}{\partial\{p\}} & \frac{\partial g(\{p\},\omega)}{\partial\omega}\end{matrix}\right]^{-1}\Bigg|_{\{p\}_k^i,\omega_k^i}\left\{\begin{matrix}\{R\left(\{p\}_k^i,\omega_k^i\right)\}\\ g\left(\{p\}_k^i,\omega_k^i\right)\end{matrix}\right\} \tag{23}$$

where $\left[\begin{matrix}\frac{\partial\{R(\{p\},\omega)\}}{\partial\{p\}} & \frac{\partial\{R(\{p\},\omega)\}}{\partial\omega}\\ \frac{\partial g(\{p\},\omega)}{\partial\{p\}} & \frac{\partial g(\{p\},\omega)}{\partial\omega}\end{matrix}\right]$ is the new Jacobian matrix which is not singular.

During the solution procedure, first order estimators, which are calculated by using the Jacobian inverse found at the previously converged solution, are used. The details of the numerical continuation methods can be found in reference [23].

4 CASE STUDY

In this section a case study is presented to demonstrate the application of the analysis method proposed. A bladed disk assembly which has 24 sectors with an angle of 15° per sector is used. The isometric view of the FE model of a single sector is given in Figure 1. The model is formed by eight node brick elements. The blades are of mid-shroud type. The disk is constrained at the nodes on the inner rim.

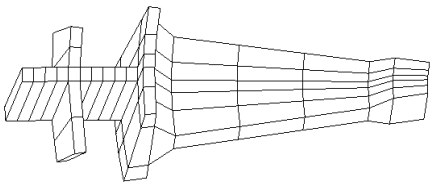

Fig 1 - FE model of a single sector

To construct the reduced order model, 20 modes for each blade and 260 modes (20 modes for each nodal diameter) for the disk is used. The resulting reduced order model has 1028 number of DOF. All finite element work is done in ANSYS.

As an example to non-linearity in the system, the friction between shrouds of adjacent blades is included into the analysis. The details of the formulation of the macro-slip friction element under constant normal load are given in reference [18]. Note that the dry friction between contact surfaces under changing normal loads can also be included into the analysis. The external forcing on the system is taken only in the axial direction of the disk. 3 engine-order (EO) single harmonic forcing is applied on all the nodes located at blade tips. The response is calculated using the first 20 modes.

The linear response of the tuned assembly in tangential direction at the tip of the first blade is given in Figure 2.

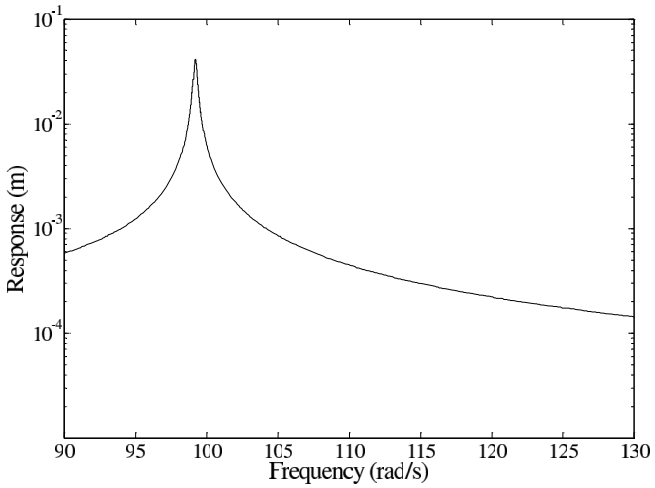

Fig 2 - Linear response of the tuned assembly in axial direction

To study the effect of mistuning, random deviations in the range of ± 5% are applied to the modal stiffness values of individual blades. The linear response of the mistuned assembly at the same DOF as above is given in Figure 3. Note that a number of new modes have appeared. This is due to the fact that a 3EO excitation can excite only 3 nodal diameter (ND) modes of a tuned assembly, whereas in a mistuned case this is not so, since the whole structure will loose its cyclic symmetry. Therefore, a 3EO excitation can excite all the modes in a mistuned assembly.

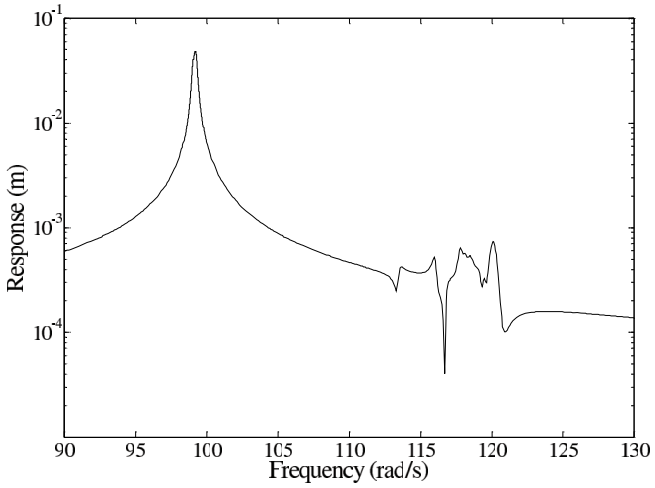

Fig 3 - Linear response of the mistuned assembly in axial direction

In order to consider the non-linearity in the system due to the friction between shrouds of adjacent blades, the relative motion between contact surfaces in normal direction is neglected and constant normal load assumption is made. Macro-slip friction elements with normal load values between 1N and 100N are used. Then both tuned and mistuned responses of the same blade are calculated. The

mistuning pattern used in linear case is also employed here. The non-linear responses of tuned and mistuned bladed disk assemblies are given in Figures 4 and 5, respectively.

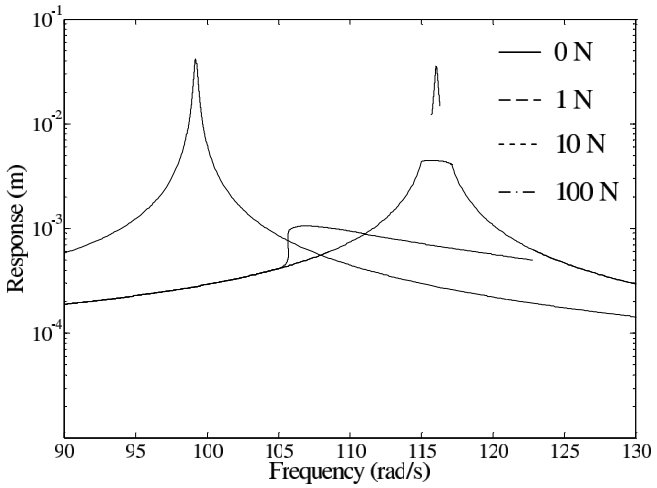

Fig 4 - Non-linear response of the tuned assembly in axial direction
for various normal load values

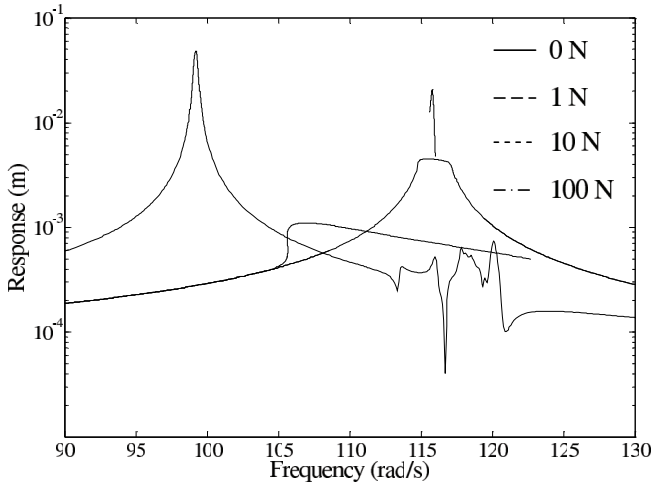

Fig 5 - Non-linear response of the mistuned assembly in axial direction
for various normal load values

As demonstrated above, friction type nonlinearity can alter the forced response of both tuned and mistuned bladed disk assemblies significantly both in peak magnitudes and resonant frequencies.

5 CONCLUSION

In this study, a new approach is suggested for the dynamic analysis of bladed disk assemblies under periodic loads in the presence of distributed parameter mistuning and nonlinearity. To the best of our

knowledge, this is the first study which uses distributed parameter mistuning in non-linear dynamic analysis. The method proposed combines the component mode synthesis based reduced order modeling approach with non-linear forced response analysis technique in modal space. Mistuning is imposed on individual blade natural frequencies of the reduced order model. Path following approach based on Newton method is employed in numerical solutions.

In the case study presented, a mistuned bladed disk assembly with friction type non-linearity between shrouds of adjacent blades is considered. Both linear and non-linear analyses of the system are carried out, and the forced responses of a mistuned blade under periodic loads are calculated. In both analyses several normal load values for macro-slip friction are employed. By comparing the linear and non-linear forced responses obtained in the case study, it is demonstrated that non-linearity can change the response of the system considerably.

Note that the current state-of-the-art suggests either adding point mistuning elements to FE model of the system or using modal synthesis and perturbing individual blade natural frequencies for the dynamic analysis of mistuned bladed disk assemblies. In the former method, in order to have realistic models, fine meshing is required and mistuning should be applied on a large number of DOF. The latter method has been applied only for linear systems. The method proposed in this study has the advantage of making non-linear analysis while keeping the benefits of using modal synthesis and thus applying distributed parameter mistuning. Making the non-linear solution in modal domain reduces computational time drastically.

6 REFERENCES

[1] G. Óttarsson, 1994, "Dynamic Modeling and Vibration Analysis of Mistuned Bladed Disks", PhD Thesis, The University of Michigan, Ann Arbor, MI.

[2] C.-C. Lin, M.P. Mignolet, 1997, "An Adaptive Perturbation Scheme for the Analysis of Mistuned Bladed Disks", *Journal of Engineering for Gas Turbines and Power,* Vol. 119, pp. 153-160.

[3] M. P. Mignolet, Chung-Chih Lin, "Identification of Structural Parameters in Mistuned Bladed Disks", *Transactions of the ASME Journal of Vibration and Acoustics,* Vol. 119, pp. 428-438.

[4] D. Cha, A. Sinha, 2002, "Effects of the Nature of Excitation on the Response of a Mistuned Bladed Disk Assembly", *Transactions of the ASME Journal of Turbomachinery,* Vol. 124, pp. 588-596.

[5] Lim, S.-H., Castanier, M. P., and Pierre, C., "Predicting Mistuned Blade Amplitude Bounds and Stress Increases from Energy Formulations," *Proceedings of the 9th National Turbine Engine High Cycle Fatigue Conference* (published on CD-ROM), Pinehurst, NC, March 2004.

[6] Castanier, M. P., Óttarsson, G., Pierre, C., 1997, "A Reduced Order Modeling Technique for Mistuned Bladed Disks", *Transactions of the ASME Journal of Vibration and Acoustics,* Vol. 119, pp. 439-447.

[7] Bladh, R., Castanier, M. P., and Pierre, C., 1999, "Reduced Order Modeling and Vibration Analysis of Mistuned Bladed Disk Assemblies with Shrouds," *Journal of Engineering for Gas Turbines and Power*, Vol. 121, pp. 515-522.

[8] Lim, S.-H., Pierre, C., and Castanier, M. P., "Mistuning Identification and Reduced-Order Model Updating for Bladed Disks Based on a Component Mode Mistuning Technique," *Proceedings of the 9th National Turbine Engine High Cycle Fatigue Conference* (published on CD-ROM), Pinehurst, NC, March 2004.

[9] Lim, S.-H., Castanier, M. P., and Pierre, C., "Predicting Mistuned Blade Amplitude Bounds and Stress Increases from Energy Formulations," *Proceedings of the 9th National Turbine Engine High Cycle Fatigue Conference* (published on CD-ROM), Pinehurst, NC, March 2004.

[10] Bladh, R., Castanier, M. P., and Pierre, C., 2001, "Component-Mode-Based Reduced Order Modeling Techniques for Mistuned Bladed Disks - Part I: Theoretical Models," *Journal of Engineering for Gas Turbines and Power*, Vol. 123, pp. 89-99.

[11] Yang, M.-T., Griffin, J. H., 2001, "A Reduced-Order Model of Mistuning Using a Subset of Nominal System Modes", *Transactions of the ASME Journal of Engineering for Gas Turbines and Power,* Vol. 123, pp. 893-900.

[12] Feiner, D. M., Griffin, J. H., 2002, "A Fundamental Model of Mistuning for a Single Family of Modes", *Transaction of the ASME Journal of Turbomachinery,* Vol. 124, pp. 597-605.

[13] Ayers, J. P., Feiner, D. M., Griffin, J. H., "A Reduced-Order Model for Transient Analysis of Bladed Disk Forced Response", *Transactions of the ASME Journal of Turbomachinery,* Vol. 128, pp. 466-473.

[14] Yang, M.-T., Griffin, J. H., 1997, "A Reduced Order Approach for the Vibration of Mistuned Bladed Disk Assembly", *Transactions of the ASME Journal of Engineering for Gas Turbines and Power,* Vol. 119, pp. 161-167

[15] Petrov, E. P., Ewins, D. J., 2003, "Analysis of the Worst Mistuning Patterns in Bladed Disk Assemblies", *Transaction of the ASME Journal of Turbomachinery,* Vol. 125, pp. 623-631.

[16] Petrov, E. P., Ewins, D. J., 2005, "Method for Analysis of Nonlinear Multiharmonic Vibrations of Mistuned Bladed Disks With Scatter of Contact Interface Characteristics", *Transaction of the ASME Journal of Turbomachinery,* Vol. 127, pp. 128-136.

[17] Petrov, E. P., Sanliturk, K. Y., Ewins, D. J., 2002, "A New Method for Dynamic Analysis of Mistuned Bladed Disks Based on the Exact Relationship Between Tuned and Mistuned Systems", *Transactions of the ASMA Journal of Engineering Gas Turbines and Power,* Vol. 122, pp. 586-597.

[18] Petrov, E. P., Ewins, D. J., 2003, "Analytical Formulation of Friction Interface Elements for Analysis of Nonlinear Multi-Harmonic Vibrations of Bladed Disks", *Transactions of the ASME Journal of Turbomachinery,* Vol. 125, pp. 364-371.

[19] Cigeroglu, E., An, N., Menq, C.-H., 2007, "A Microslip Friction Model With Normal Load Variation Induced by Normal Motion", *Nonlinear Dynamics,* Vol. 50, pp. 609-626.

[20] Kuran, B., Özgüven, H. N., 1996, "A Modal Superposition Method for Non-linear Structures", *Journal of Sound and Vibration,* Vol. 189, pp. 315-339.

[21] Bladh, J. R., 2001, "Efficient Predictions of the Vibratory Response of Mistuned Bladed Disks by Reduced Order Modeling", PhD Thesis, The University of Michigan, Ann Arbor, MI.

[22] Craig, R. R., Jr., and Bampton, M. C. C., 1968, "Coupling of Substructures for Dynamic Analysis", AIAA J., **6**(7), pp. 1313-1319.

[23] Allgower, E. L., and Georg, K., 1990, *Introduction to numerical continuation methods*, Springer-Verlag, Berlin.

[24] Sanliturk, K. Y., Imregun, M., Ewins, D. J., 1997, "Harmonic Balance Vibration Analysis of Turbine Blades With Friction Dampers", *Transactions of the ASME Journal of Vibration and Acoustics,* Vol. 119, pp. 96-103.

[25] Yang, B.-D., Menq, C.-H., 1997, "Modeling of Friction Contact and Its Application to the Design of Shroud Contact", *Transaction of the ASME Journal of Engineering for Gas Turbines and Power,* Vol. 119, pp. 958-963.

[26] Cigeroglu, E., Özgüven, H. N., 2006, "Nonlinear Vibration Analysis of Bladed Disk With Dry Friction Dampers", *Journal of Sound and Vibration,* Vol. 295, pp. 1028-1043.

[27] Yang, M.-T., Griffin, J. H., 1995, "Exploring How Shroud Constraint Can Affect Vibratory Response in Turbomachinery", *Transactions of the ASME Journal of Engineering for Gas Turbines and Power,* Vol. 117, pp. 198-206.

[28] Berthillier, M., Dupont, C., Mondal, R., Barrau, J. J., "Blades Forced Response Analysis With Friction Dampers", *Transactions of the ASME Journal of Vibration and Acoustics,* Vol. 120, pp. 468-474.